The Energy Implications of Air-Side Fouling in Constant Air Volume HVAC Systems

by

Eric J.H. Wilson

B.S., University of Illinois at Urbana-Champaign, 2006

A thesis submitted to the

Faculty of the Graduate School of the

University of Colorado in partial fulfillment

of the requirements for the degree of

Masters of Science

Department of Civil, Environmental and Architectural Engineering

2011

This thesis entitled:
The Energy Implications of Air-Side Fouling in Constant Air Volume HVAC Systems
written by Eric J.H. Wilson
has been approved for the Department of Civil, Environmental and Architectural Engineering

Zhiqiang (John) Zhai, PhD

Moncef Krarti, PhD, P.E.

Michael Brandemuehl, PhD, P.E.

Date

The final copy of this thesis has been examined by the signatories, and we find that both the content and the form meet acceptable presentation standards of scholarly work in the above mentioned discipline.

Wilson, Eric J.H. (M.S.)

The Energy Implications of Air-Side Fouling in Constant Air Volume HVAC Systems

Thesis directed by Prof. Zhiqiang (John) Zhai, PhD

This thesis examines the effect of air-side fouling on the energy consumption of constant air volume (CAV) heating, ventilating, and air conditioning (HVAC) systems in residential and small commercial buildings. There is a particular focus on evaluating the potential energy savings that may result from the remediation of such fouling from coils, filters, and other air system components.

A computer model was constructed to simulate the behavior of a building and its duct system under various levels of fouling. The model was verified through laboratory and field testing and then used to run parametric simulations to examine the range of energy impacts for various climates and duct system characteristics. A sensitivity analysis was conducted to determine the impact of parameters like duct insulation, duct leakage, duct location, and duct design on savings potential.

Duct system pressures, temperatures, and energy consumption for two houses were monitored for one month. The houses' duct systems, which were both in conditioned space, were given a full cleaning, and were then monitored for another month. The flow rates at the houses improved by 10% and 6%. The improvements were primarily due to installing a new filter, as both houses had only light coil fouling. The results indicate that there was negligible change in heating energy efficiency due to the system cleaning.

The parametric simulation results are in agreement with the field experiment: for systems in all eight climates, with flowrates degraded by 20% or less, if ducts are located within the thermal zone, HVAC source energy savings from cleaning are negligible or even slightly negative. However, if ducts are outside the thermal zone, savings are in the 1 to 5% range. For systems with flowrates degraded by 40%, if ducts are within the thermal zone, savings from cleaning occurs only for air conditioning energy, up to 8% in climates like Miami, FL. If ducts are outside the thermal zone, savings occurs with both heating and cooling energy, and ranges from 7% in Los Angeles, CA to 13% in Fairbanks, AK. These results assume a leaky and uninsulated duct system. The potential for savings from cleaning decreases if duct insulation is in place or sealing has been performed. The potential for energy savings is directly related to the distribution system's

thermal efficiency, with air conditioner performance also playing a minor role.

Results for small commercial buildings with constant air volume HVAC systems and leaky and uninsulated duct systems span a wider range: from -12% in Miami, FL to 30% in Minneapolis, MN. However, for improved ducts or ducts in the conditioned space, small commercial HVAC source energy savings is always negative (down to -17%) for flowrates degradation in the 0-40% range.

The sensitivity of these results to duct characteristics (location, leakage, and insulation) and the after-cleaning flowrate, as it varies from an ideal flowrate, was also evaluated. Energy savings can reach up to 80% for some scenarios where clean airflow is severely restricted down to 20% of ideal by poor duct layout or other obstructions not removable by cleaning.

In addition, a simplified spreadsheet tool was developed for technicians to use in the field to estimate potential savings resulting from a system cleaning. Measuring the temperature rise across the furnace was found to give less uncertainty than measuring the pressure rise and assuming a fan curve. Despite the uncertainty, the tool can give a general idea of the range of savings possible under various conditions.

Acknowledgements

The author would like to thank: the National Air Duct Cleaners Association (NADCA) for providing the funding for this research; Bill Lundquist, the NADCA member in charge of the project, for his guidance and feedback; Monster Vac Inc., for donating their HVAC system cleaning services for the field testing; Mari and Karl Linden and Xiang Liu, for their time and willingness to participate in the field testing; Zhiqiang (John) Zhai, PhD, Moncef Krarti, PhD, P.E., and Michael J. Brandemuehl, PhD, P.E. for their advice and patience throughout the process; James McNeill for his previous work on the project, and his advice to me as a new researcher early in the project; Stephen Johnson for his work on the laboratory testing portion of the project and help preparing for the field testing; Donghyun Seo for generating custom solar data and lastly, Julie Zielinski, for her constant support, understanding, and encouragement throughout this journey.

Contents

Chapter

Tables

Table

Figures

Figure

Chapter 1

Introduction

1.1 Motivation

Space heating and air conditioning accounts for 26% of all electricity consumption and 69% of all natural gas consumption in U.S. residential buildings. In the U.S., ductwork is the most common method of delivering conditioned air to building occupants: 62% of home space heating is done with a central warm-air furnace and 72% of space cooling is done with a central air-conditioning system [1]. Therefore, an efficient distribution system is essential to minimizing space conditioning energy consumption in North American buildings.

It is often recommended that furnace or air conditioning filters are replaced every 1-3 months to prevent damage to equipment and save energy[2]. It is well understood that regularly changing filters saves energy in large commercial buildings [3], but it is not known exactly how much energy this saves in residential and smaller commercial systems, if any. Because HVAC equipment is often out of sight, out of mind, many filters are changed much less frequently than recommended, leading to greater accumulation of dust. In addition to filters, particle accumulation occurs on all part of a duct system, including heat exchanger coils, fans, supply diffusers, return registers, and the ductwork itself. Incorrectly installed or damaged filters can cause filter bypass, which exacerbates dust loading on system components. Dust loading on system components increases the system pressure drop, which, for the constant air volume systems most common to residential and smaller commercial buildings, corresponds to a decrease in system air flow rate. Particle accumulation on the heat exchanger coils found in air conditioners and heat pumps can also degrade the

heat transfer effectiveness of the coils.

Duct cleaning services aim to remove the dust and debris that accumulates in duct systems. Although cleaning ductwork will not have a significant effect on system flow rate or efficiency, some duct cleaners also clean cooling coils, fans, and heat exchangers, which may have an effect on system efficiency [4][5]. Little research has been done on the impact of cleaning these components on heating and cooling energy consumption in residential and small commercial buildings. Quantifying this impact is the focus of this thesis.

1.2 Questions to be Answered

(1) What is the energy impact of cleaning coils, filters, and other components that contribute to HVAC system pressure drop?

(2) While low airflow is known to result in degraded air conditioner performance, the effect on heating system efficiency has largely been ignored. This prompts the question: do low airflow rates significantly affect forced-air heating energy use?

(3) How does the energy impact change for different system parameters, including climate, duct location, duct insulation, and duct leakage?

(4) Can a simplified tool be used to estimate potential savings resulting from system cleaning?

1.3 Thesis Organization

This thesis presents a review of the research on the energy implications of system fouling, organized chronologically. Chapter 3 presents the details of the simulation model development, including the two custom components that were developed, the fan curve models, and the pressure drop models used. The field testing experiment is described next, in Chapter 4. This includes the equipment used to collect data and the methods used to analyze the collected data and determine results. Chapter 5 explains how the simulation model was verified through laboratory and field testing, as well as how a simulation model of one of the field testing houses was developed and calibrated in order to verify the model and help explain the field testing

results. Next, the design of the parametric simulation analysis was presented. The parametric analysis was divided into three sections: pressure drop, building, and duct system characteristics. Chapter 7 covers the spreadsheet tool developed for technicians to use in the field to estimate the potential savings resulting from a system cleaning. The uncertainty associated with the fan curves used by the tool to estimate flowrate is also presented. Next, the results of the field testing and parametric simulations are presented along with a discussion. The sensitivity of the results to the various parameters (fan curve, duct location, duct insulation, duct leakage, after-cleaning flowrate) is also covered. Finally, Chapter 9 summarizes the conclusions from the research and suggests future areas of research.

Chapter 2

Literature Review

This chapter presents a review of the literature relevant to the research conducted in this thesis, organized chronologically. There have been relatively few studies of the impact of air-side fouling on HVAC system energy consumption.

The works of Krafthefer and Bonne [6] and Krafthefer et al. [7] are the first studies concerning the energy impact of air-side fouling of HVAC systems. They conducted lab tests to determine coil fouling rates as a function of the particle concentration in the air stream. They define "significant" coil fouling as a doubling of the pressure drop across the coil. This definition has been adopted by most subsequent studies of coil fouling. Their lab tests showed that pressure drop across the coils doubles in 4 to 7 years. They then used a first principles approach to relate coil fouling to heat pump performance in a residential building. This was used in conjunction with the coil fouling rates to evaluate the energy implications of coil fouling. This was accomplished with an annual analysis using seasonal average values for heat pump capacity and COP, seasonal operating hours, and building load (in heating degree days / cooling compressor hours). They found that maintaining coil cleanliness, either with a regiment of frequent coil cleanings or using a high-efficiency electronic air cleaner, saves 10-25% on operating costs, averaged over 15 years of operation in a residential scenario. The savings are 25-55% for the dirtiest year of fouling (15 years of particle accumulation). However, Siegel et al. [8] suggest that these studies might be an "overestimate of the impacts of fouling because their analysis used indoor particle concentrations which are considerably larger than suggested by more recent literature." Additionally, these studies are limited in that they assume a constant system operating time, ignore distribution system losses, and do not address the effect of low airflow due to coil fouling on heating

with forced-air furnaces.

Rossi and Braun (1996) [9] determined an optimal cost schedule for coil cleaning, based on simulations. They did not quantify the savings to be achieved from coil cleaning because their reference case involved coil cleaning whenever comfort criteria was not met.

Fisk et al. (2002) conducted a life cycle cost analysis of filtration in large commercial buildings with VAV systems (simulated) and found that, as expected, more frequent filter changes can save energy. They did not find a strong relationship between filter efficiency and energy costs [3]. None of the existing literature specifically addresses the energy implications of air-side fouling in small commercial buildings with constant air volume (CAV) HVAC systems. These buildings required outside ventilation air, making them unique from the residential case.

In 2002, Siegel et al. [8] conducted an evaluation of the energy implications of coil fouling. They developed a model for predicting particle deposition on the coil as a function of the particle concentration in the air stream, filter efficiency, filter bypass, coil bypass, fin spacing, duct complexity, and operating mode (cycling or continuous). Their experimental results show that for typical coils, the coil pressure drop doubles (at a constant flow rate) after about 7.5 years of fouling. The study considered three different fan curves, all of which were linear in the range of flows considered. The corresponding flow rate reductions were 5-7%. They assumed constant values for fan efficiency, which resulted in a 1-10% increase in fan power with fouling. Based on the work of Parker et al. [10] and Palani et al. [11] (experiments), they conclude that the 5-7% flow rate reduction would cause a 2-4% decrease in EER, capacity, and power draw of a "properly tuned air conditioner," but that the effect could be 10-20% or greater for a system that already had insufficient air flow or low refrigerant charge [8]. They did not look at seasonal performance, changes in system run time, heating mode effects, or changes in distribution losses.

Yang et al. (2004) performed a series of laboratory experiments that evaluated the impact of filter and coil fouling on the performance of air conditioners [12][13][14]. They evaluated several different filter and coil combinations, but only looked at fouling with up to one year's worth of dust (600 g). The average reduction in air flow rate was 8%. However, only one duct configuration was used: a length of straight ductwork. More complex duct systems would moderate the effect of the increased pressure drop and result

in smaller reductions in flow rate. The researchers found that the impact of fouling on coil air-side effective heat transfer coefficient was relatively small, ranging from -14% to 4%. At some smaller amounts of fouling, they found that heat transfer could actually be enhanced, likely due to increased turbulence caused by the dust accumulation. They conclude that the reduction in flow rate due to fouling pressure drop affects air conditioner performance more than the effect of fouling on air-side effective heat transfer coefficient. The studies found that a year of fouling can degrade air conditioner EER by 2-10%, depending on the filter-coil combination and system size. They did not look at seasonal performance, changes in system run time, heating mode effects, or changes in distribution losses.

The Yang et al. studies used fan curves that result in increased fan power with fouling (up to 40%), which would not be the case with forward-curved blade fan curves, for which fan power typically decreases with decreasing flow rate [15]. Because evaporator fan power and heat both affect air conditioner EER, this choice of fan curve significantly affects the results of the study. If forward-curved fan curves were used, the decrease in EER and capacity due to fouling would be smaller. To explore the effect of fan efficiency curves, the authors consider cases with constant fan efficiency, but, just as in the Siegel et al. study, this results in fan power curves with which fan power increases with decreased flow rate [12].

A recent field experiment study by Stephens et al. evaluates the energy implications of choosing a high-efficiency HVAC filter versus a low-efficiency filter [16]. Although this study does not specifically address the effects of fouling, filter choice affects the system pressure drop in much the same way as filter fouling. This is the first study of residential HVAC systems that looks at the impact of pressure drop on system run time rather than just instantaneous air conditioner or heat pump performance. The statistical analysis of the field study of 17 residential and light commercial systems found that a doubling of the filter pressure drop (due to fouling or use of a higher-efficiency filter) would likely result in a 7 to 10% decrease in cooling-mode flow rate, a 4 to 6% decrease in cooling-mode fan power draw, a 10 to 15% decrease in supply- and return-side leakage flow rates, and a 7 to 25% reduction in latent capacity of the air conditioner. The analysis detected no significant changes in sensible or total capacity. In terms of seasonal energy consumption, switching from a low-MERV filter to a high-MERV filter increased energy consumption at some of the sites and decreased energy consumption at some of the sites. The authors attribute the changes primarily to

climatic and behavioral factors and conclude that the energy impact of filter efficiency in smaller forced-air cooling systems is small compared to the effects of thermostat settings, climatic conditions, refrigerant charge, and duct leakage. A companion study by Stephens et al., which used an unoccupied test house for the experiment and thus was able to better control for climate and behavioral factors, found that daily energy consumption did not significantly differ based on filter MERV rating [17]. These studies focus on cooling system performance and the authors note that with the exception of heat pumps, "flow has never been shown to affect heating capacity." However, flow rate does affect the supply temperature, which can affect thermal losses associated with ducts located in un- or semi-conditioned spaces. Evaluating the significance of this effect is one aim of this thesis.

Chapter 3

Simulation Model Development

The TRNSYS 16 software was used as the engine for the simulation model. TRNSYS was chosen because of its modular design which makes it easy to add custom components. Two custom components were developed to model the complexities of the fan-duct system behavior:

Fan curve and system pressure curve model: This component calculates the pressure drop across each component in the duct system (filter, coil, supply duct, return duct) and determines the operating point of the fan.

Duct model: This component models duct system effects, including supply leakage (out), return leakage (in), and duct surface heat transfer.

3.1 Fan Curve and System Pressure Curve Model

3.1.1 Fan Curve

The relationship between the flow rate provided by a fan and the static pressure rise it generates is known as its fan curve. The shape of a fan curve determines how much the flow rate changes as a result of increased pressure drop in the system. Also necessary is either a fan power curve or fan efficiency curve, which describe the relationship between flow rate and fan shaft power or efficiency.

Some manufacturers of HVAC furnaces or air handlers provide information about their equipment's fan curve, usually in the form of ten static pressures and ten corresponding flow rates. There are three problems with using manufacturer fan curve data:

(1) Static pressures are typically *external static pressure*, which means that filter pressure drop is already included. This means that if a filter's actual pressure drop is different than what the manufacturer assumed, either because it is fouled or is a different type of filter, the manufacturer fan curve will be inaccurate. Ideally, a fan curve would specify fan pressure rise as *total static pressure*.

(2) The manufacturer fan curve is typically only given for a very small range of flow rates—the range over which that fan is designed to operate. The fouling effects that are of interest to this thesis correspond to flowrates much lower than the selection range. Extrapolating outside of this range can give erroneous results.

(3) Because of the "system effect," the actual performance of installed fans is often considerably different from performance data provided by manufacturers or from laboratory measurements [18]. Thus, two identical fans installed in two different buildings will have significantly different operational fan curves.[1] Therefore, caution must be used when using any fan curve that was not measured *in situ*.

To address the first problem, several fan curves were found that use total static pressure. The first set of fan curves was developed for a generic furnace model for a Technical Support Document for the U.S. Department of Energy [19]. The document describes how four blowers were chosen from Lau Industries, a manufacturer that supplies blowers to the furnace industry. Pressure and shaft power curves for the four blowers are available in Lau Industries' fan selection software. Polynomial equations were fit to the curves so that they could be used in the Department's generic furnace models, after accounting for other factors like motor slip and system effect. The four curves, hereafter referred to as the "DOE generic fan curves" are shown in Figure 3.1.

For the simulation model, in order to address the three problems discussed above, a variety of fan curves, including those measured for the field testing experiment, was used to examine the range of flowrate reductions possible for a given increase in system pressure drop (see Figure 7.4).

However, for the simplified field tool discussed in Chapter 7, it is desirable to get a close approximation

[1] For example, Stephens et al. found that two identical air handlers, one in an upflow configuration, and one in a downflow configuration, had different ranges of operating flowrates and had fan power and efficiency curves that were of different shapes [17].

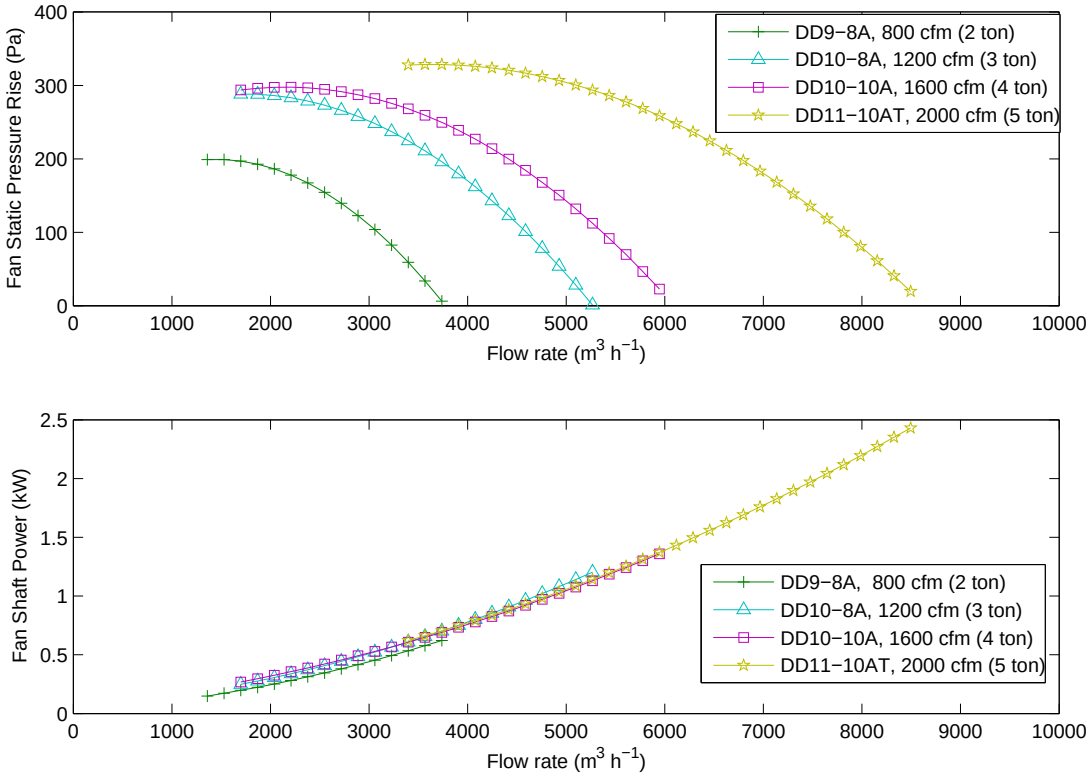

Figure 3.1: DOE Generic Fan Curves: Pressure (top) and Fan Power (bottom)

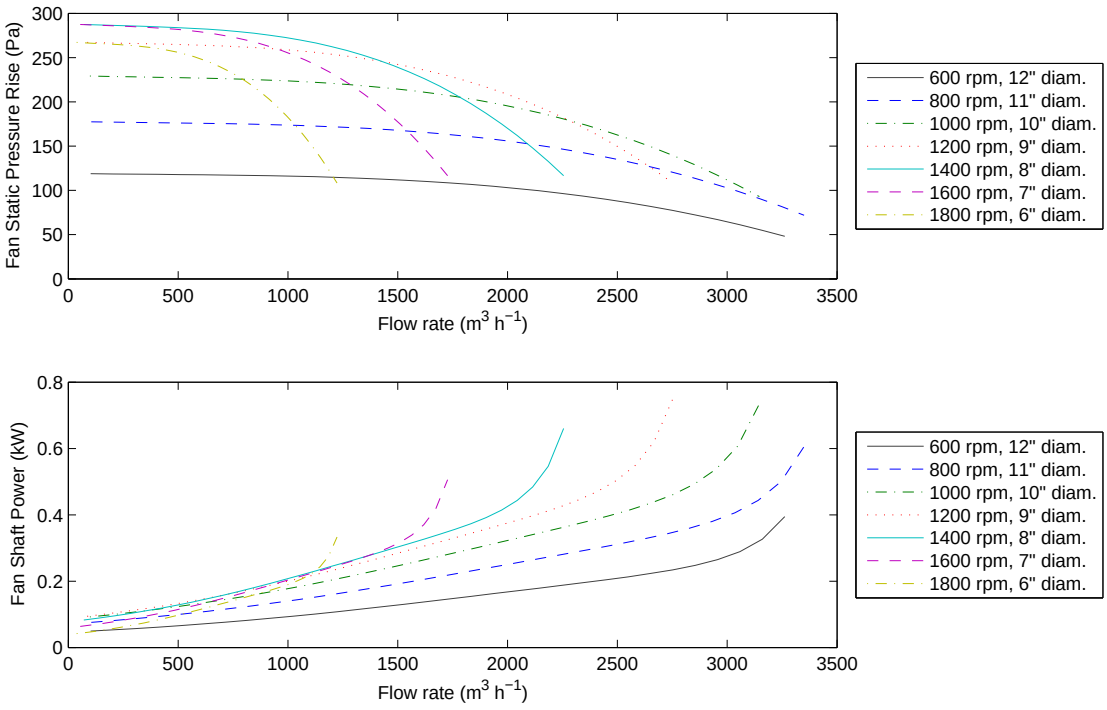

Figure 3.2: Dimensionless Fan Model Curves: Pressure (top) and Fan Power (bottom)

of the fan curve for the building at hand. For this reason, a dimensionless fan curve model was used. Brandemuehl and Wassmer developed the model from manufacturer data for a line of packaged rooftop equipment, with nominal cooling capacities of 3, 4, 5, and 6 tons and forward-curved fan blades [20]. They converted from external static pressure to total static pressure using estimates for internal pressure drop. Given a blower diameter and rotational speed, the dimensionless model can be used to generate pressure vs. flow rate and efficiency vs. flow rate curves. An array of example fan curves generated with this dimensionless mode is shown in Figure 3.2.

3.1.2 Pressure Drop Models

Just as fan curves relate a fan's flow rate to the pressure rise, a system curve relates a duct system's total pressure drop to the fan's flow rate. From the ASHRAE Handbook of Fundamentals, Chapter 35: Duct Design, the total system pressure change caused by friction, fittings, and equipment is calculated by the equation:

$$\Delta P_{total} = \Delta P_{return} + \Delta P_{filter} + \Delta P_{coil} + \Delta P_{supply} \tag{3.1}$$

where
ΔP_{total} = total system pressure drop, Pa
ΔP_{return} = effective pressure drop for return duct system, including friction, fitting, and register losses, Pa
ΔP_{filter} = pressure loss due to filter, Pa
ΔP_{coil} = pressure loss due to evaporator coil, Pa
ΔP_{supply} = effective pressure drop for supply duct system, including friction, fitting, and diffuser losses, Pa

For the purposes of this study, pressure losses due to friction and fittings are lumped together, along with thermal gravity (stack) effects. Pressure drop models are needed to relate the pressure drop across a filter, coil, or duct, to the air flow rate or velocity at that component. This relationship is given by:

$$\Delta P = aV^b \tag{3.2}$$

where ΔP is pressure drop, V is air velocity, a is the power law coefficient, and b is the power law exponent. This relationship can be used for all duct system components, including coils, filters, and ducts.

It is generally assumed that $b = 2$ for ductwork (completely laminar flow) [15] but laboratory experiments showed that b has a wider range (1 to 3) when measured for real duct systems (see Table 5.1). Therefore, the duct pressure drop model was coded to accept a variety of values for b, and the parametric simulations will include it as a variable.

3.1.2.1 Coil Pressure Drop

Yang et al. derived a and b for four different coils, each at seven different fouling levels (clean, fouled with one year's worth of dust with five different filters, and fouled with no filter in place) [12]. The pressure drop versus coil air velocity curves are shown in Figure 3.3

Although the pressure drop coefficients measured by Yang et al. are representative of only one year of fouling under typical conditions (600 grams of dust), the case where the coil was fouled with no filter in place fits the definition of "significant fouling" (see Chapter 2) because, for the 2-row and 4-row coils (3- and 5-ton systems), it corresponds to a more than doubling of coil pressure drop. Thus, the coefficients presented by Yang et al. are sufficient to be used for an evaluation of the impact of significant fouling on HVAC systems. The 8-row coils did not experience a doubling of pressure drop, but these larger coils are only found on larger equipment (e.g., 35 ton) which is not a focus of this study.

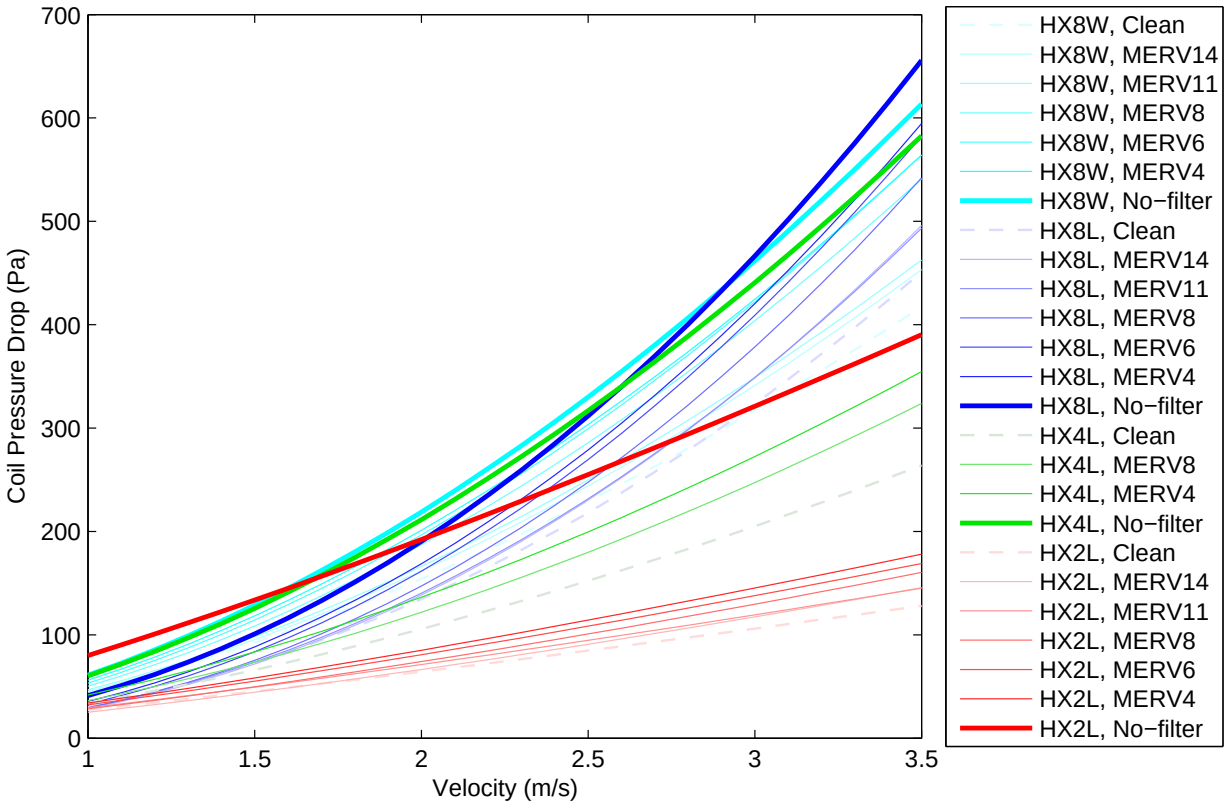

Figure 3.3: Coil Pressure Drop Curves

3.1.2.2 Filter Pressure Drop

Liu et al. (2003) used measurements taken by Murphy and Rivers (1996) to develop a filter pressure drop model that can simulate dynamic fouling [21] [22]. The model is a more complex version of the power law relationship given in Equation 3.2. In simplified form, it is:

$$\Delta P = \Delta P_0 \left(\frac{\Delta P_e}{\Delta P_0} \right)^{\dot{\tau}} \left(\frac{m}{m_0} \right)^{b} \tag{3.3}$$

where

ΔP = filter pressure drop, Pa

ΔP_0 = filter pressure drop at initial or clean state, Pa

ΔP_e = filter pressure drop at end of lifetime, Pa

$\dot{\tau}$ = dimensionless time: 0 = initial, 1 = final; dimensionless

m = mass flow rate of air, kg s^{-1}

m_0 = mass flow rate of air at initial or clean state, corresponding to ΔP_0, kg s^{-1}

b = power law exponent, dimensionless

This model assumes that the power law exponent is independent of the amount of accumulated dust. This assumption is experimentally verified by Liu et al. The model also assumes that the amount of accumulated dust is proportional to the operating time since filter replacement [21]. The model requires an end-of-lifetime filter pressure drop, ΔP_e to be specified. Because the model uses dimensionless time, it does not assume a certain rate of fouling.

3.2 Duct Model

A custom TRNSYS component was developed to model duct effects, including duct surface heat transfer and duct leakage.

3.2.1 Duct Surface Heat Transfer Model

The component uses the duct surface heat transfer model developed by Wray (2003) [23], which uses heat exchanger effectiveness methods, and accounts for conduction through the duct wall (and any insulation) and convection at the inner and outer surfaces. Radiation between the duct and its surroundings is ignored for simplicity.

$$q = \varepsilon \cdot C_{min} \cdot (T_{exterior} - T_{interior}) \tag{3.4}$$

where

ε = heat exchanger effectiveness: the dimensionless ratio of actual heat transfer rate to maximum possible heat transfer rate
C_{min} = heat capacity rate: the product of the air mass flow rate in the duct and the air's specific heat ($c_{p,air}$), W/°C
$T_{exterior}$ = temperature of air surrounding duct exterior,°C
$T_{interior}$ = temperature of air entering duct,°C

Assuming $T_{exterior}$ is constant along the length of the duct, the heat exchanger effectiveness is given by:

$$\varepsilon = 1 - \mathrm{e}^{(-UA/C_{min})} \tag{3.5}$$

where, UA, the overall duct heat transfer coefficient (neglecting radiation) is:

$$UA_{duct} = \frac{1}{R_{conv,interior}} + \frac{1}{R_{cond}} + \frac{1}{R_{conv,exterior}} \tag{3.6}$$

The interior and exterior convection resistances are given by:

$$R_{conv,interior} = \frac{1}{h_{conv,interior} \cdot A_{duct}} \quad \text{and} \quad R_{conv,exterior} = \frac{1}{h_{conv,exterior} \cdot A_{duct}} \tag{3.7}$$

Assuming turbulent forced convection inside the duct, the convection coefficient can be calculated using the empirical expression [15]:

$$h_{conv,interior} = 0.023 \cdot \frac{k_{air}}{D_h} \cdot \mathrm{Re}^{0.8} \cdot \mathrm{Pr}^{0.4} \tag{3.8}$$

where

A_{duct} = duct surface area, m^2
k_{air} = thermal conductivity of air, W/(m·°C)
D_h = duct hydraulic diameter, m
Re = Reynolds number ($\mathrm{Re} = \rho_{air} \cdot V_{duct} \cdot D_h/\mu_{air}$), dimensionless
Pr = Prandtl number ($\mathrm{Pr} = \mu_{air} \cdot c_{p,air}/k_{air}$), dimensionless
ρ_{air} = air density inside duct, $\mathrm{kg/m}^3$
V_{duct} = bulk air velocity through duct, m/s
μ_{air} = air viscosity in duct, $\mathrm{N{\cdot}s/m}^2$

Convection on the exterior duct surface has both a forced and natural component, which are combined using a correlation:

$$h_{conv,exterior} = \left(h^3_{natural,exterior} + h^3_{forced,exterior}\right)^{1/3} \tag{3.9}$$

The forced and natural convection coefficient can be expressed by these two empirical correlations:

$$h_{forced,exterior} = \left[18.192 - 0.0378 \cdot \left(\frac{T_{duct,surface} + T_{exterior}}{2}\right)\right] \cdot V^0_{exterior}.8 \tag{3.10}$$

$$h_{natural,exterior} = 3.2 \cdot |T_{duct,surface} - T_{exterior}|^{1/3} \tag{3.11}$$

where

$T_{duct,surface}$ = average temperature of duct exterior surface, °C
$V_{exterior}$ = bulk air velocity across duct exterior, m/s

and

$$T_{duct,surface} = T_{exterior} - \left(\frac{q}{h_{conv,exterior} \cdot A_{duct}} \right) \tag{3.12}$$

$T_{duct,surface}, q$, and UA_{duct} must be solved for iteratively [23].

3.2.2 Duct Leakage Model

Most building energy modeling programs that can model duct leakage, including DOE-2 and Energy Plus, require it to be input as a percentage of system air flow. Similarly, the Building America Research Benchmark Definition specifies duct leakage as a percentage of air flow. However, duct leakage is dependent on the pressure differential across the leak in the duct wall, and will change if duct pressures change due to fouling or cleaning. This relationship was documented through testing by AISI/SMACNA (1972), ASHRAE/SMACNA/TIMA (1985), and Swim and Griggs (1995), and is detailed in the Duct Design Chapter of the ASHRAE Handbook of Fundamentals (2009) [15]:

$$Q = C\Delta P_s^N \tag{3.13}$$

where

Q = duct leakage rate, cfm (l/s)
C = constant reflecting area characteristics of leakage path
ΔP_s = static pressure differential from duct interior to exterior, in. W.C.
N = exponent relating turbulent or laminar flow in leakage path

The concept of *duct leakage class* was introduced to categorize duct construction based on leakage rate. It is defined:

$$C_L = Q/\Delta P_s^{0.65} \tag{3.14}$$

where

Q = duct leakage rate per unit area, cfm/100 ft^2
C_L = leakage class, cfm per 100 ft duct surface at 1 in. of water static pressure

Table 3.1 lists allowable leakage rates for different duct types [15]. This leakage class model is used to model duct leakage so that it responds to changes in supply or return duct pressures.

Table 3.1: AISI/ASHRAE/SMACNA/TIMA Duct Leakage Classification[a]

	Predicted Leakage Class C_L [Eq. 3.14]	
Duct Type	Sealed [b, c]	Unsealed [c]
Metal (flexible excluded)		
Round and flat oval	3	30 (6 to 70)
Rectangular	6	48 (12 to 110)
Flexible		
Metal, aluminum	8	30 (12 to 54)
Nonmetal	12	30 (4 to 54)
Fibrous glass		
Round	3	NA
Rectangular	6	NA

[a] Leakage classes here are averages based on tests conducted by AISI/SMACNA (1972), ASHRAE/SMACNA/TIMA (1985), and Swim and Griggs (1995).

[b] Sealed leakage classes assume that, for metal ducts, all transverse joints, seams, and openings in duct wall are sealed.

[c] Leakage classes anticipate about 25 joints per 100 linear feet of duct. For systems with a high fitting-to-straight-duct ratio, greater leakage occurs in both sealed and unsealed conditions.

3.3 Building Models

3.3.1 Residential Model

The building model used for the residential simulations is based on the Building America Research Benchmark Definition [24]. The basic characteristics are shown in Table 3.2. Heating and cooling systems are sized based on design day simulations. The heating setpoint is 21°C and the cooling setpoint is 24.5 °C.

Table 3.2: Residential Building Model Parameters

Parameter	Value[a]	Units	Value	Units
Conditioned Floor Area	173	m^2	1,857[b]	ft^2
Volume	466	m^3	16,448	ft^3
Floor to Ceiling height	2.7	m		
Basement floor area	13.9	m^2		
Capacitance	1100	kJ/K		
Wall Areas				
North	30.7	m^2	331	ft^2
East	20.5	m^2	220	ft^2
South	30.7	m^2	331	ft^2
West	20.5	m^2	220	ft^2
Total one story	102.4	m^2	1,102	ft^2
Two stories	204.8	m^2	2,204	ft^2
Window Areas				
North	8.2	m^2	88	ft^2
East	8.2	m^2	88	ft^2
South	8.2	m^2	88	ft^2
West	8.2	m^2	88	ft^2
Total	32.8	m^2	353	ft^2
U-value	2.83	W/mK	0.498	Btu/°F-ft^2-h
Solar Heat Gain Coefficient	0.755			
Wall R-value	3.3	m^2 K/W	19	h ft^2 °F/Btu
Basement wall R-value	0.5	m^2 K/W	2.6	h ft^2 °F/Btu
Attic floor R-value	6.7	m^2 K/W	38	h ft^2 °F/Btu
Exterior doors area (facing north)	3.7	m^2	40	ft^2
Door R-value	0.9	m^2 K/W	5	h ft^2 °F/Btu
Exterior walls solar absorptivity	0.50			
Roof solar absorptivity	0.75			
Total emittance of exterior surfaces	0.90			
Infiltration	0.50	ACH annual average (Sherman-Grimsrud)		

[a] All values from the Building America Research Benchmark Definition [24] unless otherwise specified.
[b] National average for detached, single-family homes, EIA 2008 [25]

3.3.2 Small Commercial Model

A small office building (511 m^2 / 5,500 ft^2) was used for the small commercial building simulations. The model was based on the DOE Commercial Building Benchmark Model developed by NREL [26]. The building is served by a constant air volume (CAV) packaged single-zone rooftop unit. The primary difference from the residential model is the requirement for ventilation air, which means that the fan runs almost constantly; the fan is off only during unoccupied hours with no demand for heating or cooling). For the residential case, fan energy increases slightly with cleaning, due to the greater fan power. For the commercial case, this increase is even greater because the of the fan's almost constant operation (i.e., the number of fan runtime hours does not decrease as it does in the residential case). There is another effect of reduced flow rates on commercial CAV systems that bring in outside air for ventilation: if the outside air damper stays in the set position, then the volume of outside air introduced into the building decreases. This reduces the energy used to condition outside air, but also results in less fresh air, possibly degrading the indoor air quality. Thus, there is a non-energy benefit (and additional energy penalty) to remedying fouled commercial CAV systems. The internal loads, schedules, and geometry are the other differences between the residential and commercial models. The specifications of the small office building model are including in Appendix D.

Chapter 4

Field Testing Experiment

4.1 Methodology

Field testing was conducted on two single-family-detached houses in the Boulder, Colorado area, during winter and spring months, to test the effect of system cleaning on heating energy use. HVAC system energy consumption, pressures, temperatures, and humidities were monitored for 4-6 weeks. Then an Air Systems Cleaning Specialist (ASCS), certified by the National Air Duct Cleaners Association (NADCA), performed a thorough HVAC system cleaning, which included cleaning the evaporator coil, furnace, and blower, in addition to the ductwork. The furnace filters were also replaced with identical clean filters at the time of system cleaning. The houses were then monitored for an additional 4-6 weeks. The collected data was then analyzed to determine the change in HVAC energy consumption, if any.

4.1.1 Site Selection and Descriptions

A contact at NADCA attempted to find customers who had a significantly fouled duct system and who would be willing to participate in the study. However, no willing customers were found, so volunteers for the study were solicited from staff, faculty, and graduate students of the University of Colorado at Boulder, Department of Civil, Environmental, and Architectural Engineering. Of the 11 responses, five were eliminated because the houses did not have air conditioning, and therefore, a coil that could be fouled. Duct systems at six of the houses were inspected and two that had older systems and expected to have a higher degree of evaporator coil fouling were selected for the study. Figure 4.11 shows photographs of the two selected houses and Table 4.1 shows basic characteristics of the two houses.

(a) House #1 (b) House #2

Figure 4.1: Photographs of the field test houses

Table 4.1: Field Test House Characteristics

Characteristic	House #1	House #2
Location	Boulder, Colorado	Superior, Colorado
Year Built	1988	1993
Conditioned Floor Area	3,800 ft^2 (357 m^2)	2,000 ft^2 (186 m^2)
Estimated Winter Monthly Energy Cost	$300	$100
Estimated Summer Monthly Energy Cost	N/A	$50
Furnace Output Capacity	72,000 Btu/hr (21.1 kW)	80,000 Btu/hr (23.5 kW)
Air Conditioner Output Capacity	36,000 Btu/hr (10.55 kW)	36,000 Btu/hr (10.55 kW)

4.1.2 Testing and Monitoring Equipment

All testing equipment is listed, along with their measurement accuracies, in Table 4.2. Energy consumption of the furnace fan motors was measured with Continental Control Systems (CCS) WattNode AC true power meters connected to Magnelab 0-20A split-core AC current transformers and wall voltage. The power meters were connected to an Onset H22 HOBO Energy Logger Pro via Onset Electronic Switch Pulse Input Adapters. Pressure differences were measured with Setra Model 265 pressure transducers using static pressure probes inserted into holes drilled in the ductwork. The transducers were connected to the Onset data logger via Onset FlexSmart Analog Modules. Temperature and relative humidity measurements were taken with Onset U12 HOBO data loggers.

Pressure differences were measured in four locations (refer to Figure 4.2): across the evaporator coil (ΔP_{coil}), across the fan (ΔP_{fan}), across the filter (ΔP_{filter}), and between the return plenum and the ambient air (P_{return}). Given those measurements, the supply plenum pressure (P_{supply}) can be calculated, although with less accuracy than the direct measurements. Temperature and relative humidity measurements were taken in three locations: in the return air stream before the furnace, in the supply air stream after the furnace, and in the conditioned zone placed near the thermostat.

Volumetric air flow rate measurements were taken periodically throughout each testing period. Using a Fluke 922 Airflow Meter/Micromanometer, a pitot tube traverse with 15 measurement points was conducted for each flow rate measurement in accordance with ISO 3966 standards [27]. Due to the duct system configurations, it was not possible conduct the pitot tube traverse with ten straight duct diameters upstream and three straight duct diameters downstream. The measurement location was chosen in the straightest section of duct available, and each flow rate measurement was taken three times and averaged in an attempt to even out fluctuations in flow. The uncertainty of the flow rate measurements is calculated as follows:

The instrument uncertainty of the digital manometer (published as $dP = \pm 1.0\% + 0.001$ in w.c.) is propagated through to flow rate:

From Bernoulli's equation:

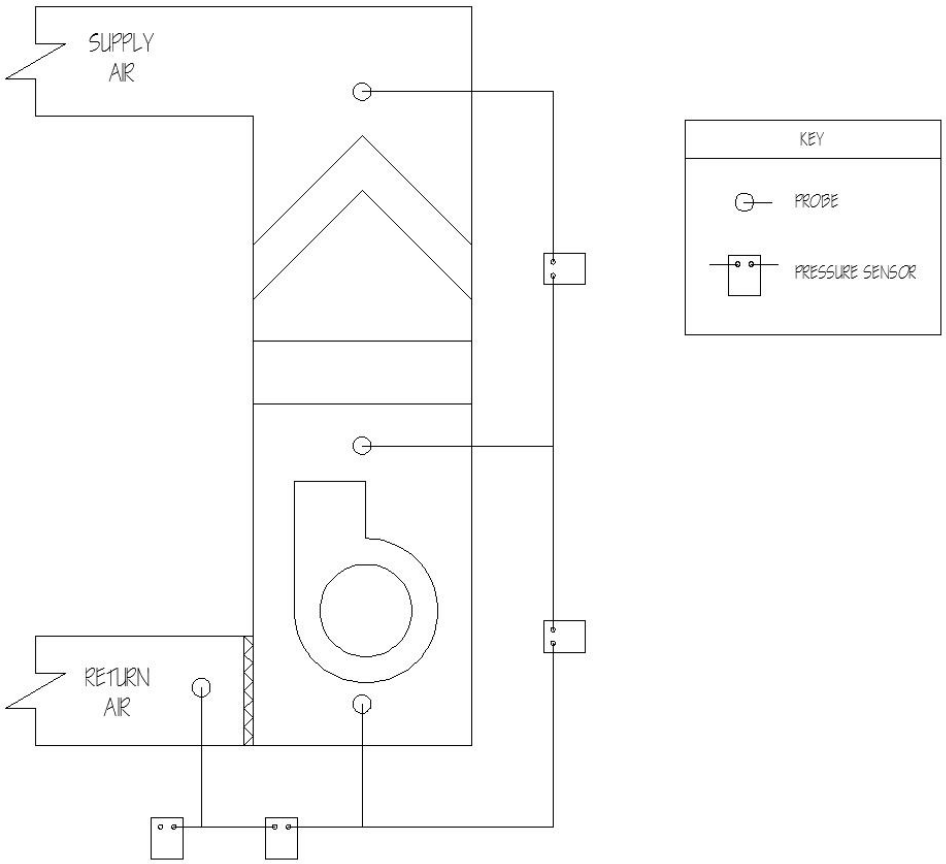

Figure 4.2: Pressure Measurement Locations

Table 4.2: Field Test Equipment

Measurement	Units	Equipment	Accuracy
Logged Measurements			
Pressure	Pa (in. w.c.)	Setra Model 265 Pressure Transducer 0-0.5", 0-2.5", and 0-5.0" range	± 1.0% FS
Amperage	A	Magnelab 0-20A Current Transformer	±1% at 10% to 130% of rated current
Energy Consumption	kWh	CCS WattNode kWh Transducer	±1.2%[a]
Temperature	°C (°F)	Onset U12 HOBO	±0.35°C from 0°to 50°C (±0.63°F from 32°to 122°F)
Relative Humidity	%	Onset U12 HOBO	±3.5% from 10% to 90%
Periodic Measurements			
Pressure	Pa (in. w.c.)	Fluke 922 Airflow Meter/ Micromanometer	±1.0% + 1 Pa (±1.0% + 0.001 in w.c.)
Volumetric Airflow Rate	$m^3\ h^{-1}$ ($ft^3\ min^{-1}$)	Fluke 922 Airflow Meter/ Micromanometer	±2.5% of reading at 10 m s^{-1} (2000 ft min^{-1})[b]

[a] ±1% for CT and ±0.5% for WattNode added in quadrature

[b] Each recorded flow rate was an average of three pitot tube traverses, each of which was an average of 15 points.

$$V = \sqrt{\frac{2gP_V}{\rho}} = \sqrt{\frac{2(115,831\ [\text{ft min}^{-2}])P_V}{0.0627\ [\text{lb}_\text{f}\ \text{ft}^{-3}]}}$$
$$= 4384\ [\text{ft min}^{-1}\ \text{inw.c.}^{-0.5}]\sqrt{P_V}$$

$$\frac{dV}{dP_V} = \frac{(4384\ [\text{ft min}^{-1}\ \text{inw.c.}^{-0.5}])^2}{2V}$$
$$dV = (0.01P_V + 0.001\ [\text{inw.c.}]) \cdot \frac{(4384\ [\text{ft min}^{-1}\ \text{inw.c.}^{-0.5}])^2}{2V}$$
$$dV(V) = \left[0.01\left(\frac{V}{4384\ [\text{ft min}^{-1}\ \text{inw.c.}^{-0.5}]}\right)^2 + 0.001\ [\text{inw.c.}]\right] \cdot \frac{(4384\ [\text{ft min}^{-1}\ \text{inw.c.}^{-0.5}])^2}{2V}$$
$$dV(V) = 0.005V + \frac{9611}{V}\ [\text{ft min}^{-1}]^2$$

where

$V =$ velocity, ft min^{-1}
$g =$ gravitational constant, 115,831 ft min^{-2}
$P_V =$ velocity pressure, in w.c.
$\rho =$ density of air at 5,400 ft = 0.0627 lb_f ft^{-3}
$dV =$ uncertainty in velocity measurement, ft min^{-1}
$dP_V =$ uncertainty in pressure measurement, in w.c.

This gives the velocity measurement uncertainty as a function of velocity, which is converted to flow rate using the duct dimensions. In addition, the sampling uncertainty must be accounted for. The 95% confidence interval is calculated as follows:

$$\Delta = \pm\frac{t\sigma}{\sqrt{n}}$$

where

$\Delta =$ 95% confidence interval
$t = t$-distribution value, in this case: $t_{(0.05,n-1)} = 4.303$
$\sigma =$ standard deviation of 3 samples for each flow rate measured
$n =$ sample size = 3

The instrument uncertainty and sampling uncertainty values are added in quadrature to determine the

overall uncertainty for each measurement point. These are shown as the horizontal error bars in Figures 4.3 and 4.4.

4.1.3 Fan Curve Measurement

At each of the field test houses, fan pressure and power curves were measured in both heating-mode (low speed) and cooling-mode (higher speed). Volumetric air flow rate, fan static pressure rise, and fan motor power measurements were taken over a range of flow rates. These flow rates were achieved by introducing obstructions, such as sheet metal or cardboard, in locations such as the filter slot, supply plenum, return registers, and supply diffusers, to cause the system to run at a variety of operating points on the fan curve. In order to achieve a flow rate greater than the normal operating point, the filter was removed. Measured fan pressure and power curves are shown in Figures 4.3 and 4.4. The duct configuration in House #2 made it difficult to obstruct the flow enough to achieve flow rates lower than 1100 m^3 h^{-1}. Vertical error bars indicate measurement uncertainty for the pressure transducers and the WattNode. Horizontal error bars indicate the overall measurement uncertainty for the air flow measurements, as calculated above.

4.1.4 Calculation of Energy Consequences

In order to detect any change in heating system distribution effectiveness, energy consumption for the before and after cleaning periods was normalized with respect to weather and compared. There were two components of heating energy consumption: natural gas used by the furnace and electricity used for the fan motor. The respective run-times of the furnace burner and fan motor were similar but not the same; the burner fires for a short amount of time before the fan starts, and the fan runs for a short time after the burner stops firing. The fan motor energy consumption was measured directly, but the burner gas consumption had to be calculated indirectly. The response time of the temperature sensors, 6 minutes, was too long to be used to determine burner runtime. Instead, the blower run time was calculated by adding 84 seconds to the beginning of each blower cycle, and subtracting 94 seconds from the end of each blower cycle.[1] The furnace gas consumption was then calculated as follows:

[1] Times indicated are for House #1.

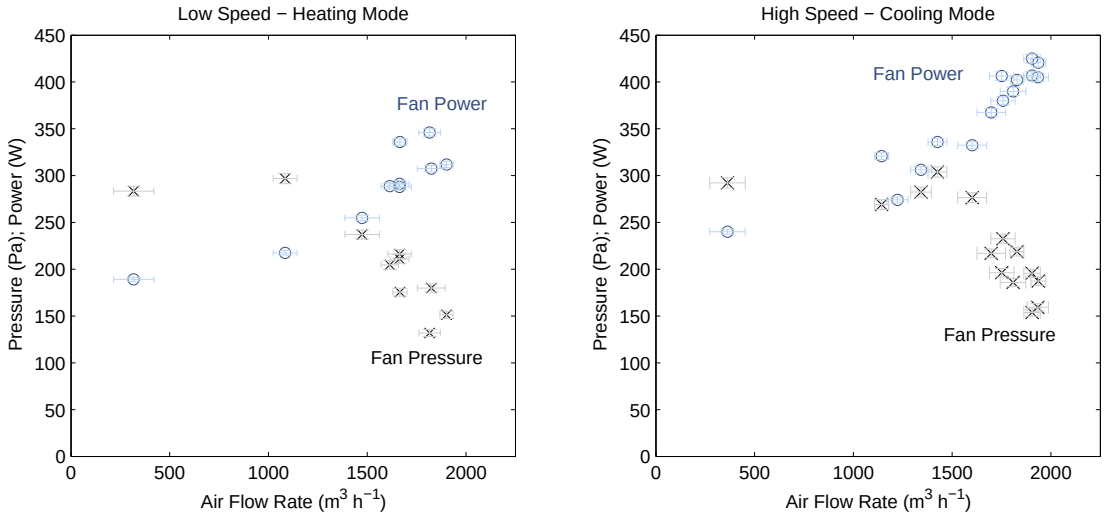

Figure 4.3: Measured Fan Pressure and Power Curves - House #1

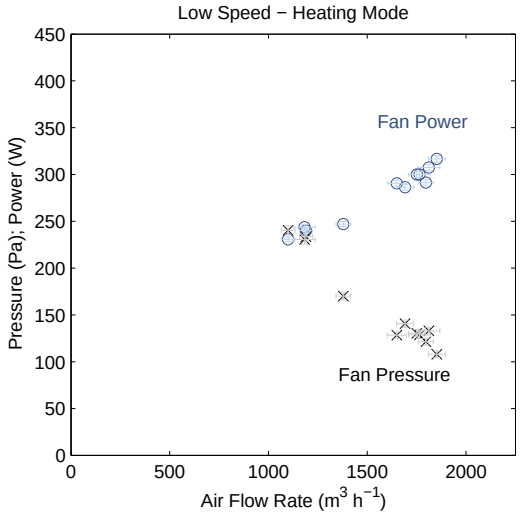

Figure 4.4: Measured Fan Pressure and Power Curves - House #2

$$E_{furnace} = W_{furn,cap,in} \cdot \int t_{\text{burner on}} \tag{4.1}$$

where

$E_{furnace} =$ furnace natural gas consumption, kWh
$W_{furn,cap,in} =$ furnace input capacity, kW
$t_{\text{burner on}} =$ time that burner is firing, hours

4.1.4.1 Weather Normalization

A variable base degree day (VBDD) method was used to quantify heating energy demand for the before and after cleaning periods. It was necessary to account for changing thermostat setpoints in the calculation of degree days. House #1 used a setpoint schedule as shown in Figure 4.5. To account for internal gains, an offset was added to the setpoint temperature: $T_{balance} = T_{set} + T_{offset}$. To determine the offset temperature that best represents average internal gains of the house, daily furnace energy consumption was plotted against degree days calculated with a variety of different values for T_{offset}. For House #1, it was found that an offset temperature of 1.5°C provides the best fit because at this value, the linear relationship has a y-intercept closest to zero. This regression is plotted in Figure 4.6. One can see that the coefficient of correlation of the linear regression does not change dramatically with different values of T_{offset}) The variable base degree days were then calculated as:

$$VBDD = \sum_{t} [(T_{set} - 1.5°\text{C}) - T_{amb}] \cdot \frac{1 \text{ day}}{24 \text{ hours}} \tag{4.2}$$

where

$VBDD =$ variable base degree days (heating), $°\text{C} \cdot \text{days}$
$T_{set} =$ thermostat setpoint temperature in heating mode, °C
$T_{amb} =$ ambient outdoor temperature, °C

The weather-normalized energy consumption can then be calculated (Eq. 4.3):

$$\bar{E} = \frac{E_{furnace} + E_{fan}}{VBDD} \tag{4.3}$$

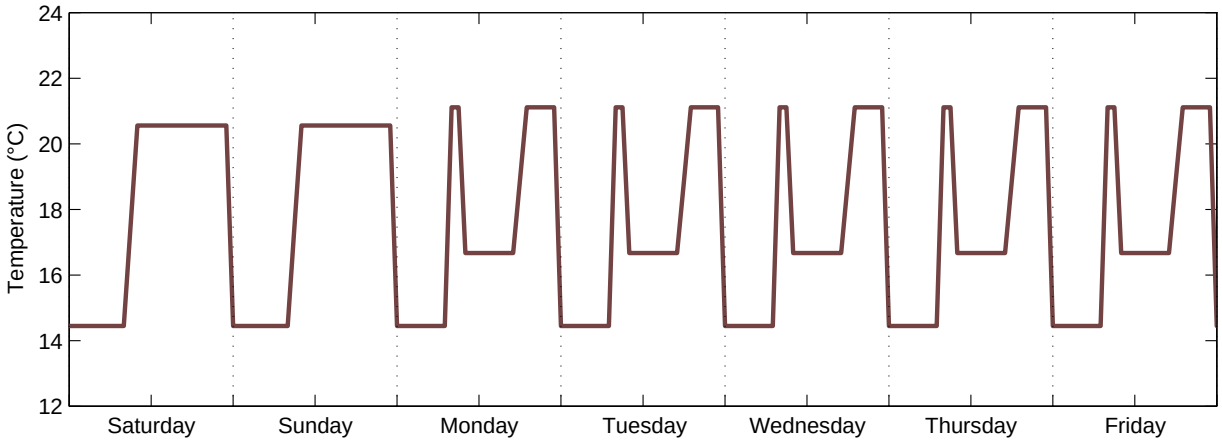

Figure 4.5: Thermostat Setpoint Schedule for House #1

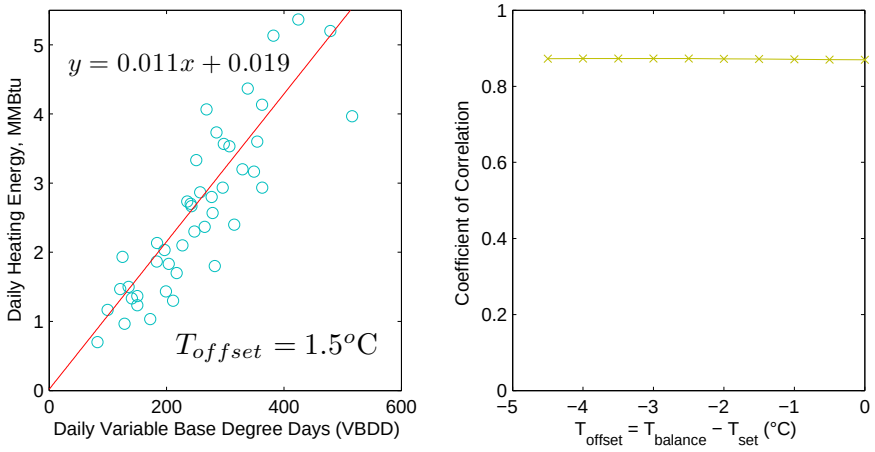

Figure 4.6: Determination of Balance Temperature

where

$\bar{E}$ = weather-normalized energy consumption, kWh per $^{\circ}\mathrm{C} \cdot$ day
E_{fan} = energy consumption of furnace fan motor, kWh

One concern with this method is that thermal mass and solar gain effects could distort the results. For example, a house with sufficient thermal mass will use less heating energy over a two week period of diurnal temperature swings than over a period with equal degree days, but including a week of cold weather followed by a week of warm weather. In addition, the shape of the thermostat schedule, with the morning spike in temperature, could further distort the degree day calculation.

4.2 Field Testing Results

Field test houses #1 and #2 were monitored for 72 days and 71 days, respectively, in winter and spring 2010. The timing of the test periods meant that the after cleaning period had fewer cold days, and therefore less demand for heating, than the before cleaning period. This reduced the amount of data available for comparison. In fact, the testing at House #2 did not yield usable energy results because there was only one day that required heating after the cleaning was done (see Figure 4.8). This was due to a combination of low thermostat setpoint, mild weather, and large internal gains. However, the House #2 data is still valuable in terms of studying the change in pressures and air flow rate with cleaning. Figure 4.7 shows the measured zone and ambient temperatures for house #1. Note the four-day period of low zone temperature after cleaning (hours 700 to 780), when the occupants were on vacation and the thermostat was set back. This period immediately following the cleaning was removed from the analysis.

4.2.1 System Cleaning Effects

Several changes in system operation were observed after an Air Systems Cleaning Specialist cleaned the ductwork, evaporator coil, blower, and furnace, and the filter was replaced with a clean one. These changes are summarized in Table 4.3. At the time of cleaning, a clean pleated filter identical to the existing dirty filter (Figure 4.11(a)) was not available. An inexpensive spun fiberglass filter with much lower pressure drop was installed temporarily until a clean pleated filter could be installed a few days later. Thus, the data

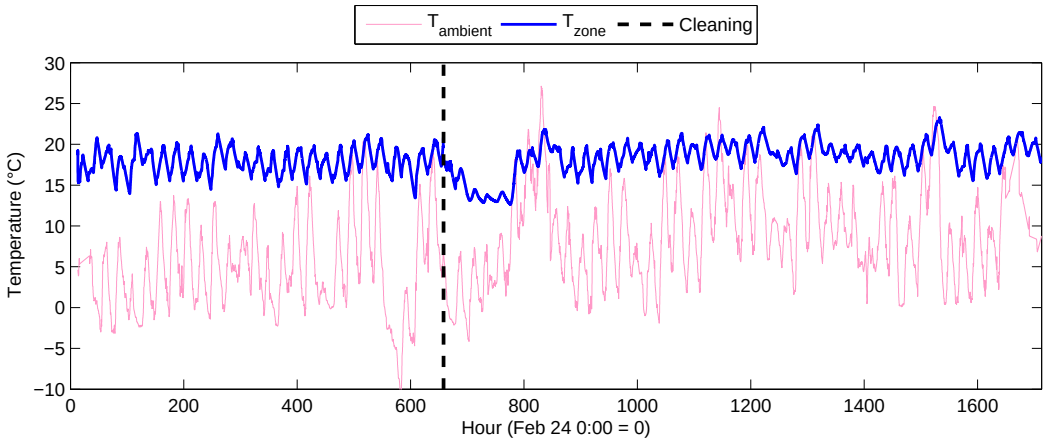

Figure 4.7: House #1 Temperature Measurements

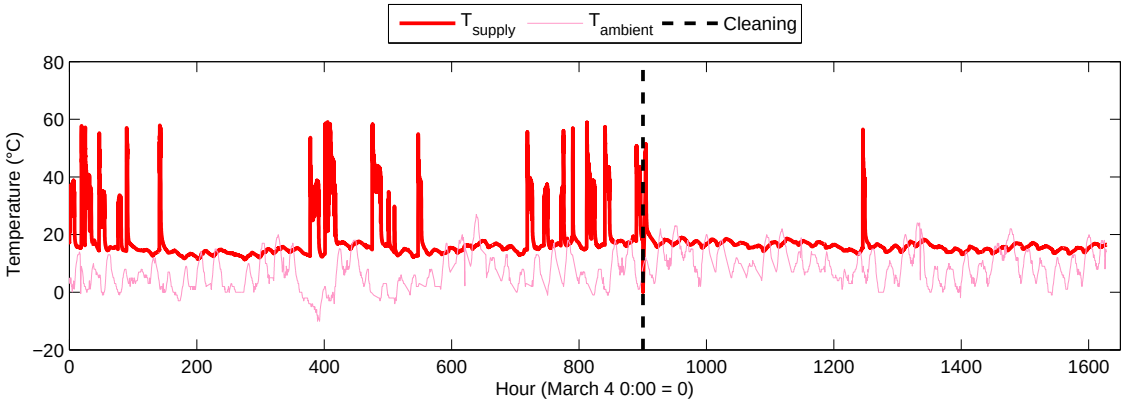

Figure 4.8: House #2 Supply Temperature Measurements

from hours 700 to 780 was erroneous and not included in the analysis.

For House #1, the coil pressure drop decreased 6%, the filter pressure drop decreased 34%, the supply ductwork pressure drop increased 10%, and the return ductwork pressure drop increased 4% after cleaning. The resulting decrease in fan pressure rise was 15%. The heating-mode air flow rate increased 10%, to 1823 m^3h^{-1} (1073 ft^3min^{-1}). The fan power draw increased 5%, to 308 W.

The cleaning effects at House #2 were less pronounced; the coil pressure drop decreased 2%, the filter pressure drop decreased 26%, the supply ductwork pressure drop decreased 17%, and the return ductwork pressure drop decreased 3% after cleaning. The resulting decrease in fan pressure rise was 14%. The heating-mode air flow rate increased 6%, to 1796 m^3h^{-1} (1057 ft^3min^{-1}). The fan power draw increased 2%, to 291 W. Note that the supply and return plenum pressures increased for one duct system and decreased for the other. Because duct leakage is a function of these pressures, a duct system cleaning will not definitively increase or decrease duct leakage; the change depends on the characteristics of each duct system.

The before- and after-cleaning static pressure distribution profiles are shown in Figures 4.9 and 4.10. For both test houses, it is apparent that the greatest change in pressure drop was that of the filter. Figure 4.11(c) confirms this by showing that there is very little dust build up visible on the evaporator coil at House #2. House #1 had a similarly low level of visible coil fouling.

The 10% increase in flow rate is evident in the measurement of furnace temperature rise ($T_{supply} - T_{return}$). Figure 4.12 shows how the temperature rise is around 3°C greater with the lower, before cleaning, flow rate. The low temperature rise during hours 700 to 780 is a result of the even higher flow rate during that period, due to the spun fiberglass filter mentioned above.

4.2.2 Impact on Energy Use

Figure 4.13 compares the cumulative furnace energy consumption and variable base heating degree days for the before and after cleaning periods (650 hours each) at House #1. Several periods with high ambient temperatures were removed in an attempt to reduce the possibility of skewing the degree day calculations [28]. Based on this cumulative comparison, the heating energy used per degree day decreased

Table 4.3: System Cleaning Effects

		House #1			House #2		
Measurement	Units	Before	After	% Change	Before	After	% Change
Coil Pressure Drop	Pa	28	26	-6%	26.4	25.9	-2%
Filter Pressure Drop	Pa	102	67	-34%	49	36	-26%
Supply Plenum Pressure	Pa	55	61	+10%	32	26	-17%
Return Plenum Pressure	Pa	-24	-25	+4%	-34	-33	-3%
Fan Pressure Rise	Pa	212	179	-15%	141	121	-14%
Air Flow Rate	$m^3\ h^{-1}$	1663	1823	+10%	1691	1796	+6%
Fan Power	W	292	308	+5%	286	291	+2%

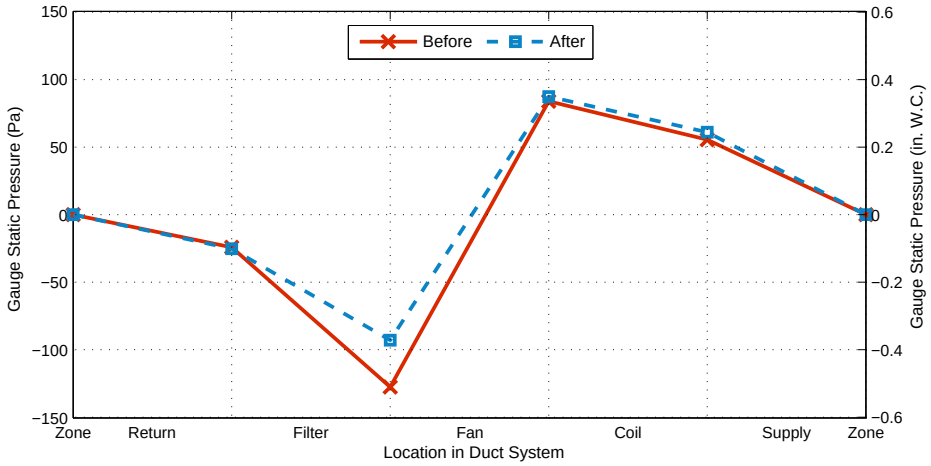

Figure 4.9: Static Pressure Distribution Profiles - House #1

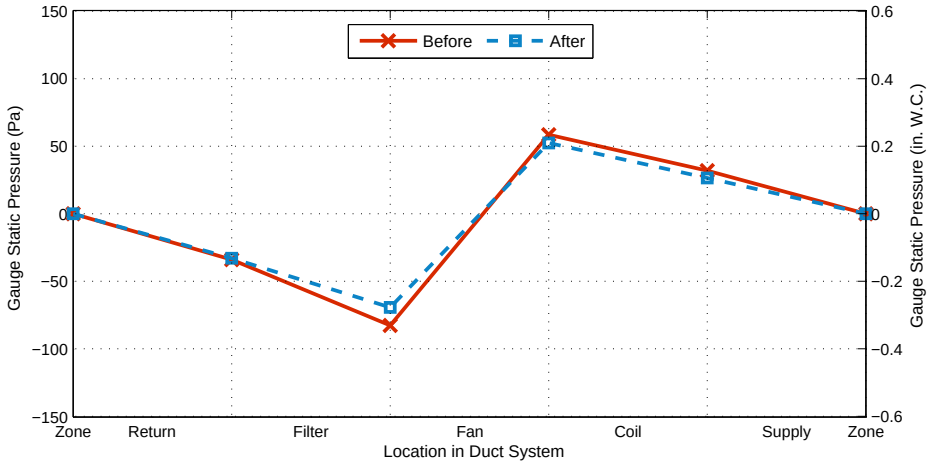

Figure 4.10: Static Pressure Distribution Profiles - House #2

(a) House #1 - Dirty Filter (b) House #2 - Dirty Filter (c) House #2 - Dirty Coil

Figure 4.11: Photographs of Fouled Components

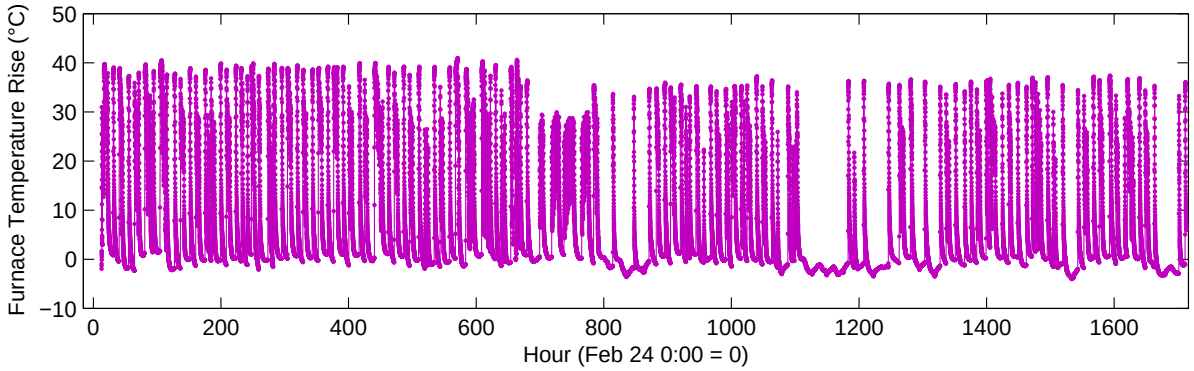

Figure 4.12: Measured Furnace Temperature Rise - House #1

by 11% after cleaning (see Table 4.4).

Because of the difference in weather between the before- and after-cleaning periods, additional methods were used to verify the results. Figure 4.14 plots the daily furnace energy against the daily heating degree days (variable base). One can see that the before cleaning period has more cold days than the after cleaning period. To account for this in calculating the impact of cleaning, only the days within a common range of weather conditions were considered (between 5 and 12 degree days). Using this method, the average heating energy used per degree day decreased by 10%, although there is considerable spread in the results.

Figure 4.15 presents another approach, for which the testing periods were further subdivided into periods with similar mean ambient temperatures. The cumulative heating energy used per degree day for each period was then plotted for comparison. Periods with outlying mean ambient temperatures (shown in lighter shades) were removed. The skewing effect of these periods is obvious, and it raises concerns about the weather normalization method in general. The cumulative before and after heating use intensities were then compared. The result shows a 8% decrease in heating energy use per degree day. The validity of the weather normalization and the field test results is discussed further in Section 5.2.2

Table 4.4: Energy Effects - House #1

	Units	Before Cleaning	After Cleaning	% Change
Entire Test Period Total (Fig. 4.13)				
Furnace Energy	kWh	1541	1102	
Fan Energy	kWh	17	13	
Degree Days	°C day	209	167	
HVAC Energy per DD	kWh (°C day)$^{-1}$	7.5	6.7	-11%
Mean Daily Energy (Fig. 4.14)				
HVAC Energy per DD	kWh (°C day)$^{-1}$	8.1	7.2	-10%
Similar Weather Period Total (Fig. 4.15)				
HVAC Energy per DD	kWh (°C day)$^{-1}$	7.3	6.7	-8%

4.3 House #3

One limitation of the field testing results is that the evaporator coils were only minimally fouled. In order to evaluate a case with more significant fouling, a NADCA representative collected information and

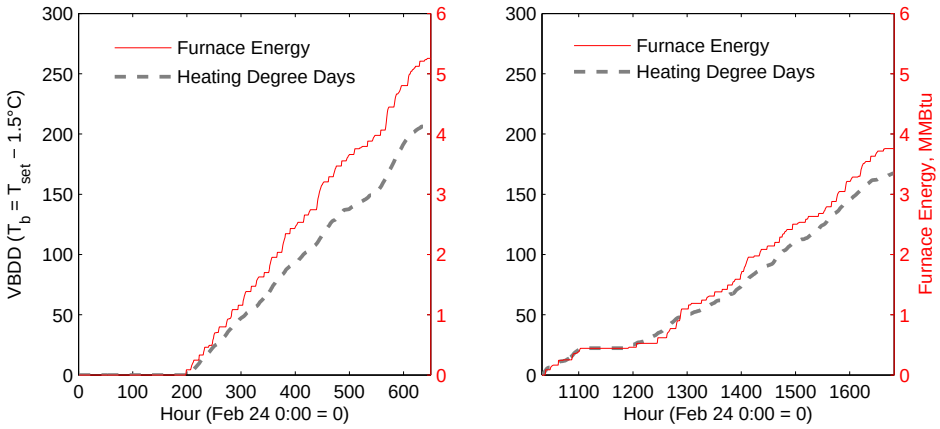

Figure 4.13: House #1 Results - Cumulative Totals

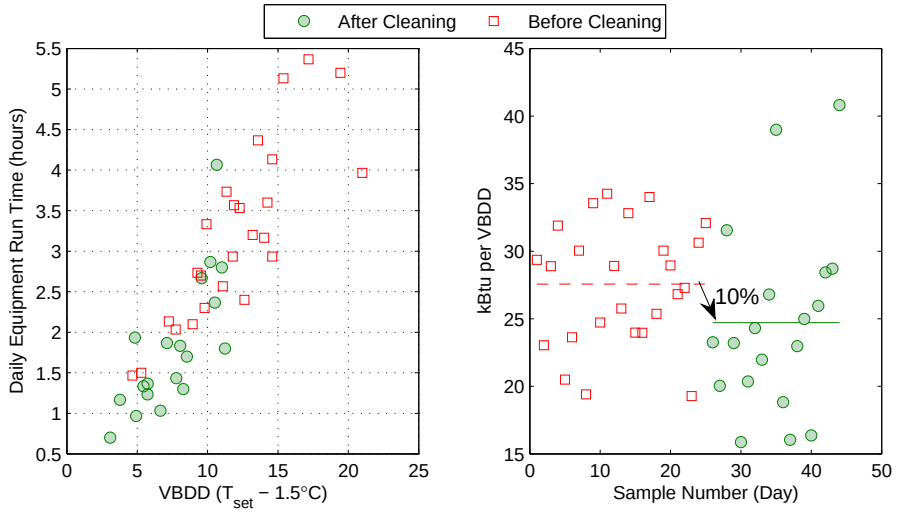

Figure 4.14: House #1 Results - Daily Comparison

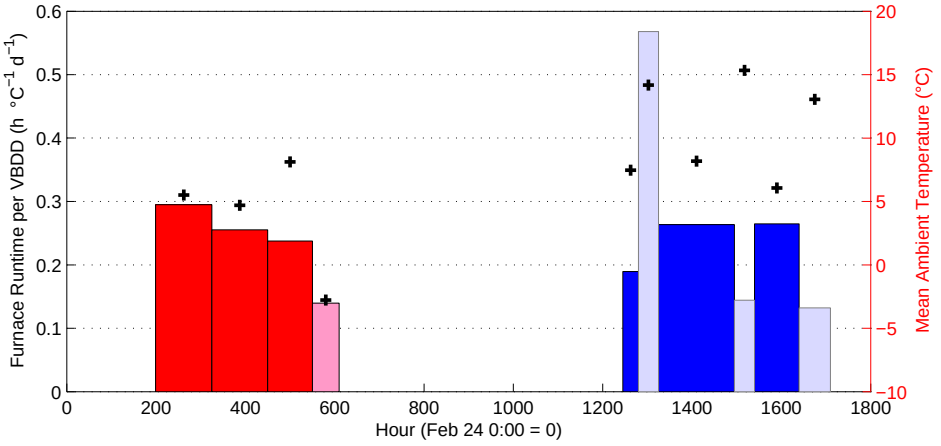

Figure 4.15: House #1 Results - Isolating Similar Weather Periods

measurements for a house that had significant fouling. The characteristics of this house, hereafter referred to as "House #3," are shown in Table 4.5. The pressure and fan motor current measurements taken before and after cleaning are shown in Table 4.6. The data form used to record these measurements is included in Appendix A. Unfortunately, detailed measurements like flow rate could not be taken at this house, but it can still be used as a case study of a system with more significant fouling. Note that the pressure drop across the coil has doubled with fouling, so this case satisfies the Krafthefer-Bonne definition of significant coil fouling [6][7].

Table 4.5: House #3 Characteristics

Characteristic	House #3
Location	Lakewood, Colorado
Conditioned Floor Area	1980 ft^2 (184 m^2)
Stories	2
Heating Fuel	Natural Gas
Blower Wheel Diameter	9 inches
Motor Speed - Heating	925 RPM
Motor Speed - Cooling	1050 RPM
Furnace Output Capacity	72,000 Btu/h (21.1 kW)
Furnace Nominal Efficiency	80%
Air Conditioner Output Capacity	36,000 Btu/h (10.55 kW)
Evaporator Coil Fouling	Heavy (visual inspection)
Duct Location	Conditioned basement
# return registers	2
Duct insulation	none
Duct sealing	none
Duct shape	rectangular

Table 4.6: House #3 Measurements

Measurement[a]	Before Cleaning	After Cleaning	% Change
ΔP across fan	169 Pa 0.68 in w.c.	137 Pa 0.55 in w.c.	-19%
ΔP across coil	37 Pa 0.15 in w.c.	17 Pa 0.07 in w.c.	-53%
P_{gauge} in supply plenum	62 Pa 0.25 in w.c.	47 Pa 0.19 in w.c.	-24%
P_{gauge} in return plenum	67 Pa 0.27 in w.c.	62 Pa 0.25 in w.c.	-7%
Fan Motor Current	3.2 A	3.8 A	+19%

[a] All measurements made in "fan-only" mode, which is the same motor speed as cooling mode.

Chapter 5

Simulation Model Verification

5.1 Verification with Laboratory Testing

In addition to the computer simulation and field testing discussed in this thesis, laboratory testing was conducted as part of the research project. One goal of the lab testing was to verify the accuracy of the pressure drop and fan models used in simulations. The lab testing was conducted at the HVAC Larson Laboratory located in the Engineering Center on the campus of the University of Colorado at Boulder. The lab includes an air handling unit that supplies conditioned air to two full size experiment zones, which are well insulated in order to make them thermally isolated, and two zone simulators, which are heating and cooling coils that can simulate building heating and cooling loads. A full description of the Larson Lab and the equipment used in the experiment is included in Appendix C.

The first step in the verification process was to measure the fan curve for the Larson Lab's supply fan, along with the coefficient and power law exponent (see Eq. 3.2) for each of the distribution system components contributing to pressure drop: return ductwork, filter, cooling coil, heating coil, supply ductwork, and zone simulator. The fan pressure and power curves are show in Figure 5.1. The measured coefficients and exponents are listed in Table 5.1.

The next step is to input the fan curve and pressure drop coefficients into the TRNSYS model, run the model, and compare the resulting calculated pressure drops, air flow, and fan power with those measured in the lab. This comparison is shown in Figure 5.2 and in Table 5.2. To further verify the ability of the simulation model to determine the operating point of the fan, a 'fouled' state was simulated in the lab by

obstructing the flow with a piece of plywood.[1] New coefficients were found for this fouled state, and the model was used to determine the new operating flow rate and pressures. The results of this comparison are shown in Figure 5.3 and Table 5.2. In both cases, the errors are small, and can be attributed to instrumentation uncertainty.

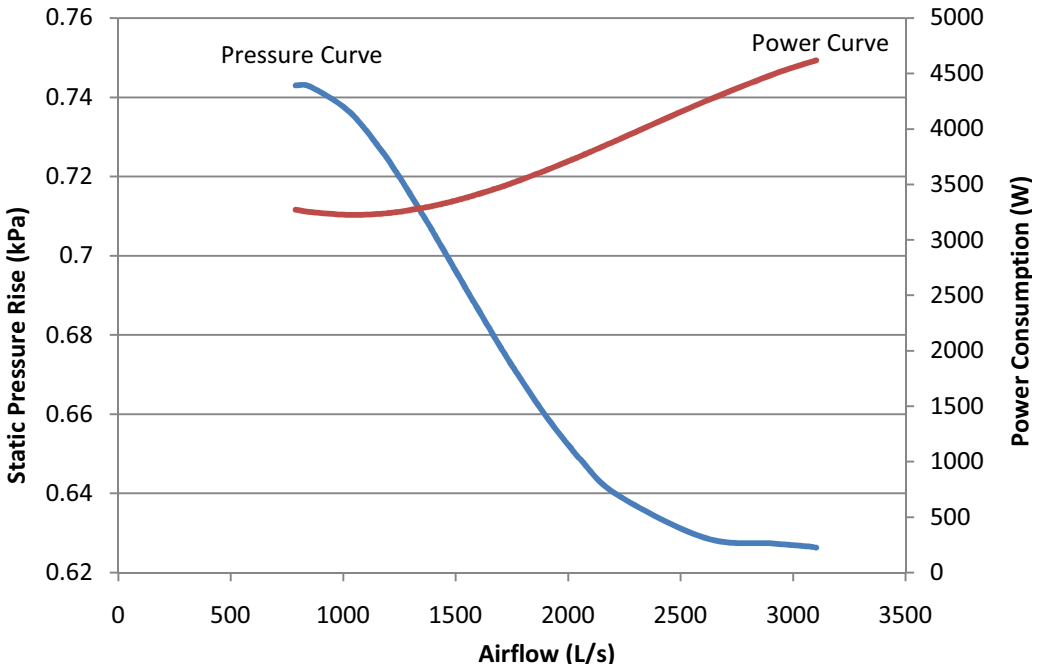

Figure 5.1: Larson Lab Supply Fan - Pressure and Power Curves

5.2 Verification with Field Testing

The field testing experiment described in Chapter 4 was also used to verify the simulation model. While the laboratory experiment was used to verify that the model is able to simulate the operation of the fan, the field testing experiment is used to verify the building and furnace models.

To conduct this verification, a detailed model of field test House #1 was constructed in the TRNSYS environment (see Section 4.1.1 for a description of the house). A detailed energy audit was conducted in

[1] Note that the difference in flow rate between the clean and fouled states is not simply due to the simulated fouling; the fouled state experiment bypassed the zone simulator and sent the air through one of the lab zones.

Table 5.1: Larson Lab Pressure Drop Coefficients

Component	a	b
Filter, Clean	12.061	1.551
Filter, Fouled	312.436	1.956
Cooling Coil	12.541	1.473
Heating Coil	4.360	1.421
Supply Duct	5.937	3.015
Zone Simulator	15.924	1.792
Return Duct	55.353	1.147

Table 5.2: Verification of Pressure Drop and Fan Curve Models

		Air Flow Rate (m^3h^{-1})	Power (W)
Clean	Lab	7,225	3,740
	Simulation	7,240	3,742
	Error	0.2%	0.1%
Fouled	Lab	5,332	3,527
	Simulation	5,386	3,355
	Error	1.0%	-4.9%

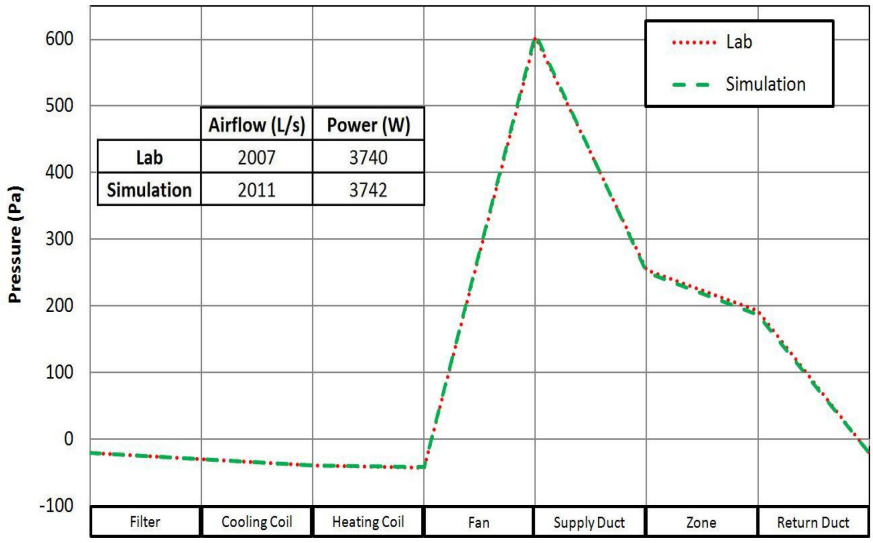

Figure 5.2: Verification of Pressure Drop and Fan Curve Models - Clean

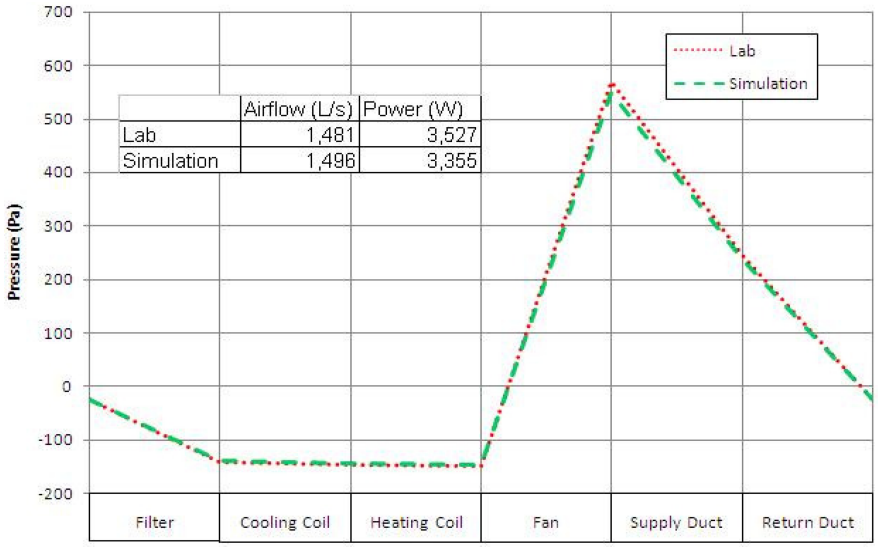

Figure 5.3: Verification of Pressure Drop and Fan Curve Models - Fouled

order to collect the information needed for the model. This included a blower door test that determined that the house has an equivalent leakage area (ELA) of 775 cm^2 (120 in^2). The Sherman-Grimsrud infiltration model was implemented in TRNSYS [29]. The model results in an average annual natural infiltration rate of 0.24 ACH.

5.2.1 Model Calibration

The model was calibrated by adjusting the lighting schedule, equipment schedule, and thermal mass so that the model output matched the temperatures and energy use measured in the field. Figure 5.4 shows the match between modeled and measured furnace energy for the before cleaning period. Figure 5.5 shows an excerpt of the measured and modeled zone and ambient temperature profiles.

5.2.1.1 Weather Data

One of the difficulties in calibrating a building energy model to measured data is weather data. While measured temperature, humidity, atmospheric pressure, wind speed, and cloud cover are commonly available from NOAA (National Oceanic and Atmospheric Administration) and other sources, recent solar radiation measurements are difficult to attain. Because of the detailed level of calibration necessary for this model, solar radiation data is important.

To address this, solar radiation data for the field test period was generated using a solar model developed by Seo [30]. The predicted solar radiation data was checked against solar radiation data for Golden, CO, measured in 2010. The prediction error is estimated to be around 10% and the prediction bias is 0.97 [31]. This accuracy is considered precise enough for building energy modeling.

5.2.1.2 Thermal Mass Calibration

Figure 5.5 (*top*) shows a modeled zone temperature that fluctuates much more quickly than the measured zone temperature. In an attempt to match the warm-up and cool-down pattern of the measured zone temperature, thermal mass was added to the model. However, this resulted in an unrealistic amount of thermal mass: 41,100 kJ K^{-1} (not including the mass of wall and floor components), which corresponds to

59,000 kg of concrete. The fact that so much mass is needed to match zone temperatures can be explained because the TRNSYS model uses a single zone for the first and second floors of the house and assumes perfect and immediate mixing of air in the zone. This hypothesis was confirmed by creating a multi-zone model with only 10% of the supply air directed to the zone with the thermostat (Figure 5.5 *bottom*). With a more realistic amount of mass, 3,000 kJ K^{-1}, the modeled furnace energy consumption matches the measured value well (Figure 5.4).

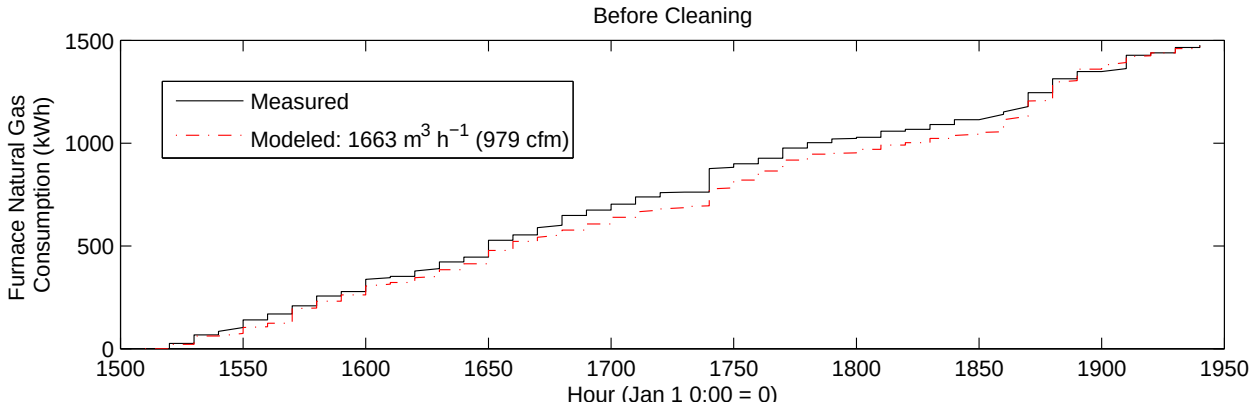

Figure 5.4: Model Calibration - House #1 Energy

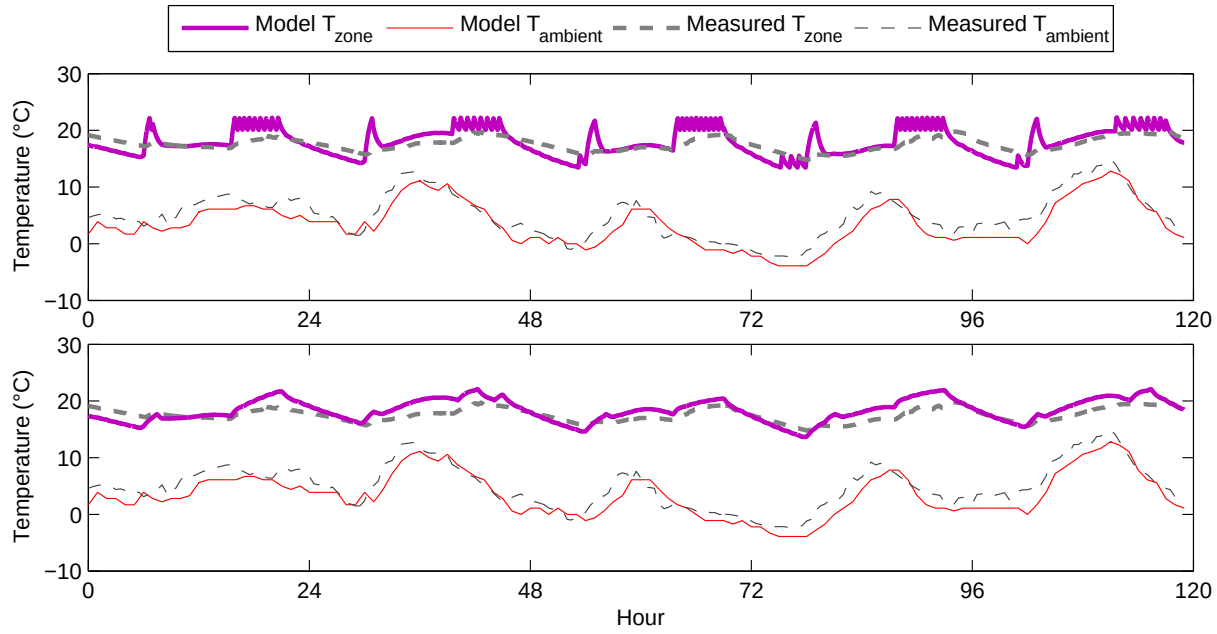

Figure 5.5: Model Calibration - House #1 Temperatures - zone temperature fluctuations due to immediate mixing (top) and multi-zone model without fluctuations (bottom)

5.2.2 Reconciliation of Model with Field Test Results

Because this field test was for heating only, the decrease in weather-normalized heating energy consumption that was observed in the field test data can only be attributed to three possible effects:

(1) The greater flow rate results in a lower supply temperature, which translates to greater thermal distribution efficiency.

(2) The change in duct pressures causes a decrease in duct leakage.

(3) The greater fan power adds more heat to the building, which decreases heating energy consumption.

However, the first two effects would be expected to be minimal for a duct system located entirely in conditioned space; losses due to leakage and duct surface heat transfer would simply enter the conditioned zone and not be lost. Since the ductwork runs through ceilings, floors, and walls, and is enclosed in gypsum wallboard, there is the possibility of some of the thermal losses leaving the conditioned space via exfiltration pathways, such as interior wall cavities that lead to the attic. However, this would not be able to account for the 8-10% decrease in weather-normalized energy consumption. The fan heat effect is also negligible and could not account for a 8-10% change. Thus, there is still the concern that the results are distorted because of the weather differences between the before- and after-cleaning periods.

In an attempt to explain the 8-10% decrease in weather-normalized energy consumption and address the concern about complications in degree day calculations, the simulation model described in Chapters 3 and 5 was used. The model was changed in order to reflect the building and HVAC system characteristics of field test House #1 (see Section 4.1.1 for a description of the house). The model was calibrated to match the temperatures and energy use measured in the before-cleaning portion of the field experiment (see Figure 5.6, *top*). Section 5.2 describes the details of the model calibration process. After this calibration, a simulation was run with the flowrate changed to the after-cleaning value (1823 m^3 h^{-1}). The change in energy consumption was less than 1% (see Figure 5.6, *bottom*). Additionally, if the simulation is run for the after-cleaning period, the energy consumption matches the field measured consumption within 1% (using either the before-cleaning or after-cleaning values for flowrate). In fact, reducing the flow rate by 50% only

increases the energy consumption by 3-5%. These simulation results (summarized in Table 5.3) confirm that the results of the weather normalization method discussed above cannot be trusted, and that the system cleaning had a negligible impact on the house's heating energy efficiency. This agrees with the expectation that there would be negligible savings because the ducts are all located within the thermal zone. Although the effect on cooling energy consumption was not a part of the field experiment, this effect has been well studied; for the 10% change in flow rate, one would expect an increase in sensible EER on the order of 2% to 10% [8][10][11][32]. Using the relationship between EER and SEER given in Brandemuehl and Wassmer (2009), this translates to a decrease in annual cooling energy in the range of 3-12% [20].

Table 5.3: Simulation of System Cleaning Effects- House #1

Air Flow Rate	Before Cleaning Period (kWh)	Relative to Measured	After Cleaning Period (kWh)	Relative to Measured
Field Test Measurement	1477	100.0%	820	100.0%
Model: 1663 m^3 h^{-1} (before cleaning)	1471	99.6%	822	100.3%
Model: 1823 m^3 h^{-1} (after cleaning)	1463	99.0%	820	100.0%
Model: 1154 m^3 h^{-1} (50% of original)	1525	103.3%	859	104.7%

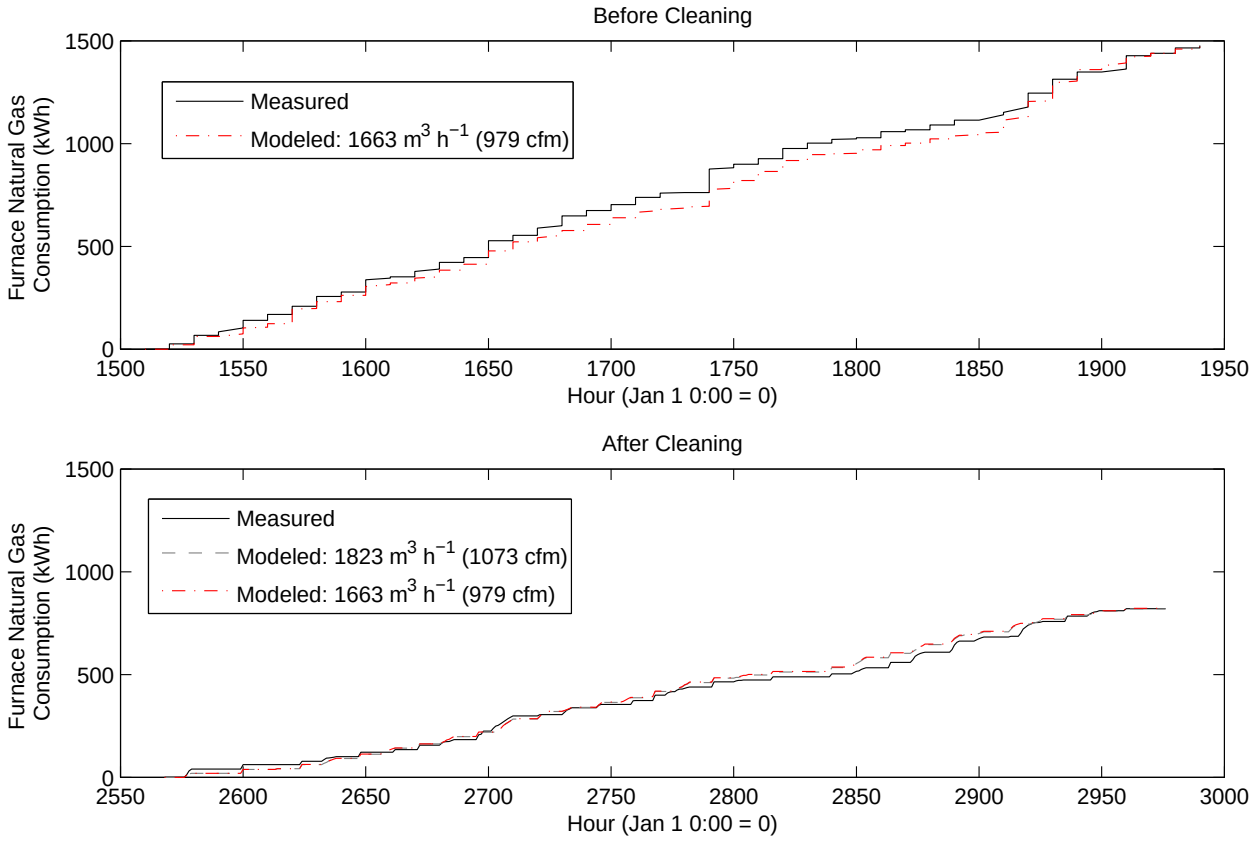

Figure 5.6: Simulation of House #1 - Energy Consumption

Chapter 6

Parametric Simulation Design

This chapter details the design of the parametric simulation analysis that was conducted in order to determine the range of possible effects of cleaning a fouled HVAC system. The parametric analysis was divided into two segments to make the simulation run time reasonable. The first parametric simulation runs all combinations of filter, coil, and duct pressure drop coefficients to determine the range of changes in system flowrate possible with system cleaning. The second parametric analysis determines the range of energy effects possible with this change in flowrate.

6.1 Pressure Drop Parametric Analysis

This analysis aimed to determine the largest possible increase in system flow rate that might result from a system cleaning. Twenty combinations of filters, coils, and duct coefficients from the literature were simulated with eight different size fans, for a total of 160 simulations (see Table 6.1). For all size fans, the greatest change in flow rate occurred with an existing dirty system as follows:

Coil: 2-row DX coil, fouled with one years worth of dust with no filter in place (380 g)
Filter: a clean MERV14 cartridge filter[1]

which was replaced with the following clean system:

Coil: 2-row DX coil, clean
Filter: clean MERV1-MERV4 cartridge filter.[2]

This "worst-case scenario" occurs with a system with simple ductwork that has low resistance to flow (25 Pa at 1870 m^3 h^{-1}), which translates into a smaller negative feedback on an increasing system pressure drop.

[1] MERV14 corresponds to a dust-spot efficiency of 90-95%.
[2] MERV1-MERV4 filters have a dust-spot efficiency of <20%.

This fouling scenario represents a 200% increase in coil pressure drop and a 600% increase in filter pressure drop, resulting in a 23% to 39% decrease in air flow rate, depending on the blower size. Figure 6.1 shows this maximum flow rate reduction for the eight different fan sizes. To illustrate how much the system would have to be fouled to experience this change in flow rate, consider that for the field test, this level of reduction in flow rate was only achievable by completely blocking the entire return path with cardboard or sheet metal (see Section 4.1.3). The decrease in supply plenum pressurization and return plenum depressurization resulting from cleaning ranged from 41% to 63% (shown in Figure 6.1). This will decrease the amount of duct leakage, although previous studies have shown that the percent leakage tends to stay the same even if the magnitude changes [33].

Table 6.1: Pressure Drop Parametric Table

Parameter	Values	Number of Options
Fan Blower Diameter	6, 8, 10, 12, 14, 16, 18, 20 (in)	8
Filter Coefficients	highest, lowest values from literature	2
Evaporator Coil Coefficients	highest, lowest values from literature	2
Ductwork Friction Coefficients	0.25, 0.5, 1, 2, 4 times field test value	5
	Total Combinations:	160

6.2 Building Parametric Analysis

Once the range of possible flow rate and duct pressurization changes was known, this range was applied to an assortment of building models to determine the impact of the changes on building HVAC energy consumption. Table 6.2 shows the building characteristics simulated in the parametric analysis. A variety of duct system characteristics were then applied to the simulation results (see Table 6.3). The results of these parametric analyses are presented and discussed in Chapter 8.

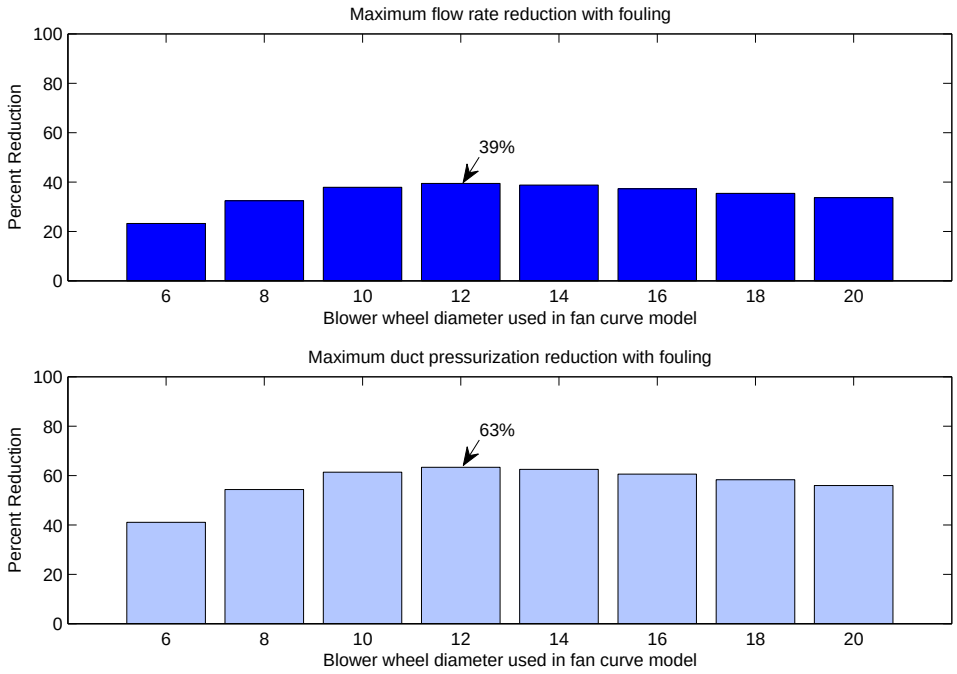

Figure 6.1: Pressure Drop Parametric Results - Maximum Decrease due to Fouling vs. Blower Diameter

Table 6.2: Building Characteristic Parametric Table

Parameter	Values	Number of Options
Climate Zone	Miami, FL; Houston, TX; Los Angeles, CA; New York, NY; Denver, CO; Minneapolis, MN; Anchorage, AK; Fairbanks, AK	8
Building Type	Residential (single family detached; Small Commercial (constant air volume HVAC system)	2
Flow rate	Depends on system capacity	11
	Total Combinations:	176

Table 6.3: Duct System Parametric Table

Parameter	Values	Number of Options
Duct Location	Conditioned zone, unconditioned basement, crawlspace, attic	4
Duct Leakage Class	3, 6, 12, 30, 48 (cfm per 100 ft^2 duct surface area at 1 in. W.C.)	5
Duct Insulation	R-0, R-3, R-6, R-9, R-12, R-15	6
	Total Combinations:	120

Chapter 7

Savings Estimation Tool

A simplified method of estimating potential savings resulting from a system cleaning was developed and incorporated into a savings estimation spreadsheet tool that can be used by field technicians. The tool makes use of correlations derived from parametric simulations of the TRNSYS model. The interface for inputting information is shown in Figure 7.1. Sample output is shown in Figure 7.2. A paper data form that mirrored the input page of the spreadsheet tool was developed to facilitate collection of information in the field. A sample completed form is included in Appendix A. The simplified spreadsheet tool will hereafter be referred to as HVAC-COST, the HVAC Cleaning Operational Savings Tool.

7.1 Assumptions and Limitations

7.1.1 Input Limitations

Because this tool needs to be used by technicians in the field, there is a restriction on the the time and equipment required to collect input information. One particular area of difficulty is flow rate. It would have been ideal for technicians to measure the before- and after-cleaning flow rates in the field, because these values have the greatest impact on energy use. However, it can be difficult to accurately measure air flow rate without certain equipment [34][35]. It would be convenient for technicians to use equipment that they already commonly carry with them, such as digital manometers. However, the field technicians do not have enough time to conduct pitot tube traverses in the field. This limited the available inputs to several pressure differentials. This strategy does not avoid the uncertainty of flow rate measurement, but instead relocates the uncertainty to the fan curve, which is discussed below.

HVAC Cleaning Operational Savings Tool (HVAC-COST)

Building Information:

State: COLORADO | City: DENVER | Climate Zone used: 5

Conditioned floor area: 1,980 sf | Number of stories: 2

Does the building have?

(•) Both forced-air heating and central A/C ( ) Just forced-air heating ( ) Just central A/C

Electricity cost: $0.10 per kWh

Heating Fuel: (•) Natural Gas ( ) Propane ( ) Oil ( ) Electricity

Natural Gas cost: $1.00 per therm

HVAC Information

Blower Wheel Diameter: 9 in.

Motor speed: Heating: 925 RPM (•) Direct Drive

Cooling: 1050 RPM ( ) Belt Driven { Motor sheave diameter: 3 / Fan sheave diameter: 4

Furnace Input Capacity: 90,000 Btu/hr

Output Capacity: 72,000 Btu/hr

A/C ( ) Tons | (•) Volts: 240.0 Amps: 20.0 ≈ 2.8 tons [ ] 3-Phase

SEER: 8.7 or Age: 1986

Ducts	Supply Ducts	Return Ducts
Where are the majority of the ducts located?	[ ] attic [ ] garage [ ] basement [ ] crawlspace [ ] living area	[ ] attic [ ] garage [ ] basement [ ] crawlspace [ ] living area
Is that space conditioned?	(•) Conditioned ( ) Uncond.	(•) Conditioned ( ) Uncond.

Number of return registers: 2

Duct Insulation thickness... on Supply duct: 0 in. ...on Return duct: 0 in.

Duct Sealing: [ ] All transverse joints and openings sealed

Duct shape: (•) Rectangular ( ) Round ( ) Flexible

Measurements (take all measurements in "Fan-On" thermostat mode)

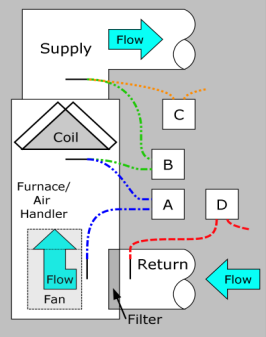

Measure static pressure differences to two decimal places.
Measure amps to two decimal places.
Measure watts or volts to nearest whole number.

	Before cleaning:		After cleaning:	
A) ΔP across fan:	0.68	in w.c.	0.55	in w.c.
B) ΔP across coil:	0.15	in w.c.	0.07	in w.c.
C) Gauge P in supply plenum:	0.25	in w.c.	0.19	in w.c.
D) Gauge P in return plenum:	0.27	in w.c.	0.25	in w.c.
Fan: ( ) watts		watts		watts
(•) amps/volts	3.2	Amp.	3.8	Amp.
	121	Voltage	121	Voltage

Calculate Savings

Figure 7.1: Savings Estimation Tool - Sample Input from House #3

Annual Energy Savings Resulting from System Cleaning

Climate Zone used for calculation: 5

	Site Energy	Energy Cost Savings
Fan energy savings:	**-92** kWh per year	**-$9** per year
Cooling energy savings:	**112** kWh per year	**$11** per year
Heating energy savings:	**4,732** kBtu per year	**$139** per year
Total energy savings:	**4,800** kBtu per year	**$141** per year
	Percent energy cost savings:	**6%**

Back to Input Form

Figure 7.2: Savings Estimation Tool - Sample Output from House #3, if ducts were in unconditioned attic and not insulated or sealed

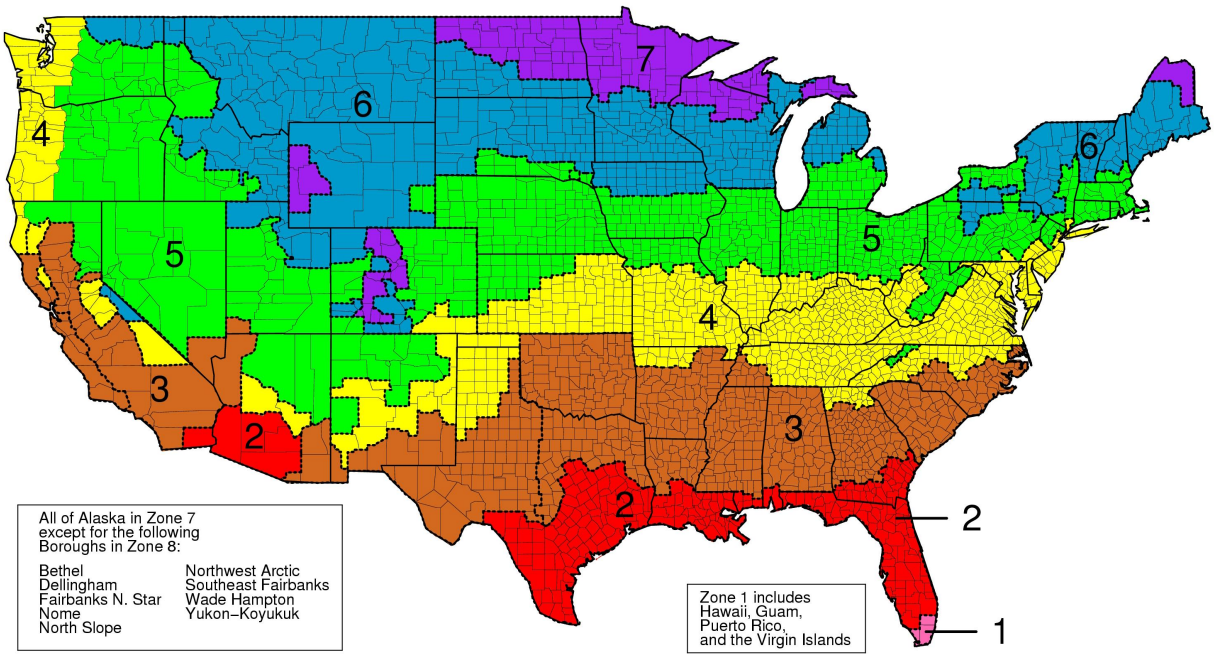

Figure 7.3: Map of ASHRAE Climate Zones

7.1.2 Climate

HVAC-COST is based on correlations derived from TRNSYS simulations for eight different locations, one for each ASHRAE Climate Zone found in the U.S. The eight locations are listed in Table 7.1, along with their respective heating and cooling degree days. A map showing how the eight zones are distributed across the U.S. is in Figure 7.3. Obviously, heating and cooling demand varies within each climate zone: Seattle, Albuquerque, and Washington D.C. have very different climates, yet are all located in climate zone 4. Simulation runtime limits the number of climates that can be used; therefore, HVAC-COST is meant to give a general idea of the possible range of savings that might be achieved in a particular building.

Table 7.1: HVAC-COST Climate Locations [15]

Zone #	Selected Representative Location		Annual Degree Days, Base 65°F (°F days)	
	City	State	Heating	Cooling
1	Miami	Florida	130	4458
2	Houston	Texas	1414	3001
3	Los Angeles	California	1284	617
4	New York City	New York	4603	1210
5	Denver	Colorado	5920	685
6	Minneapolis	Minnesota	7464	632
7	Anchorage	Alaska	10360	11
8	Fairbanks	Alaska	13528	71

7.2 Overall Structure

There are only three ways in which pressure drop affects building energy consumption:

(1) Change in flow rate

(2) Change in duct leakage

(3) Change in fan heat

Many different pressure distributions can result in the same change in system flow rate, with the same end effect on building HVAC energy consumption. This makes it computationally advantageous to split the simulation into two segments: one which determines flow rate, duct leakage, and fan power from the pressure measurements, and passes these values to the main simulation to determine energy consumption.

Another simplification made to reduce simulation runtime was the choice to deal with distribution system effectiveness (i.e., duct leakage and duct surface heat transfer) outside of the main TRNSYS simulation. Instead of using the duct model discussed in Chapter 3, ASHRAE Standard 152-2004a was used to calculate seasonal distribution system effectiveness for the before- and after-cleaning scenarios, which are then incorporated into the savings estimation [36]. A spreadsheet-based model of the distribution system efficiency method of ASHRAE Standard 152 is available from U.S. DOE [37]. This spreadsheet was adapted and incorporated into HVAC-COST.

7.3 Fan Curve Uncertainty

The before- and after-cleaning flow rates are not measured and have to be determined from pressure drop measurements using a fan curve. Fan curve shapes can vary greatly depending on the installation; two identical air handlers could have differently shaped fan curves because of the system effect factor [17]. This uncertainty can be a source of error in the savings predicted by HVAC-COST. Figure 7.4 shows how five different fan curves can give a wide range of values for the increase in flow rate resulting from the improvement in pressure drop measured at House #3. Because flow rates were not measured, there is no way to know the accuracy of the predictions. This uncertainty has a huge effect on the predicted reduction in HVAC source energy, as will be shown by the results in Chapter 8. This demonstrates the difficulty of accurately predicting energy savings based on pressure drop alone.

An alternate method of determining system flow rate was explored: measuring the temperature rise across the furnace. This method has drawbacks, but the uncertainty is less than that when assuming a fan curve. Thus, while both input methods are available in the tool, it is recommended that the temperature rise method be used whenever possible. If greater accuracy for the tool is desired, it is recommended that flow rate is measured directly; a flow-plate type device that fits into the filter slot, such as the one described by Francisco and Palmiter [35], would be able to quickly and accurately take the necessary flow rate measurements.

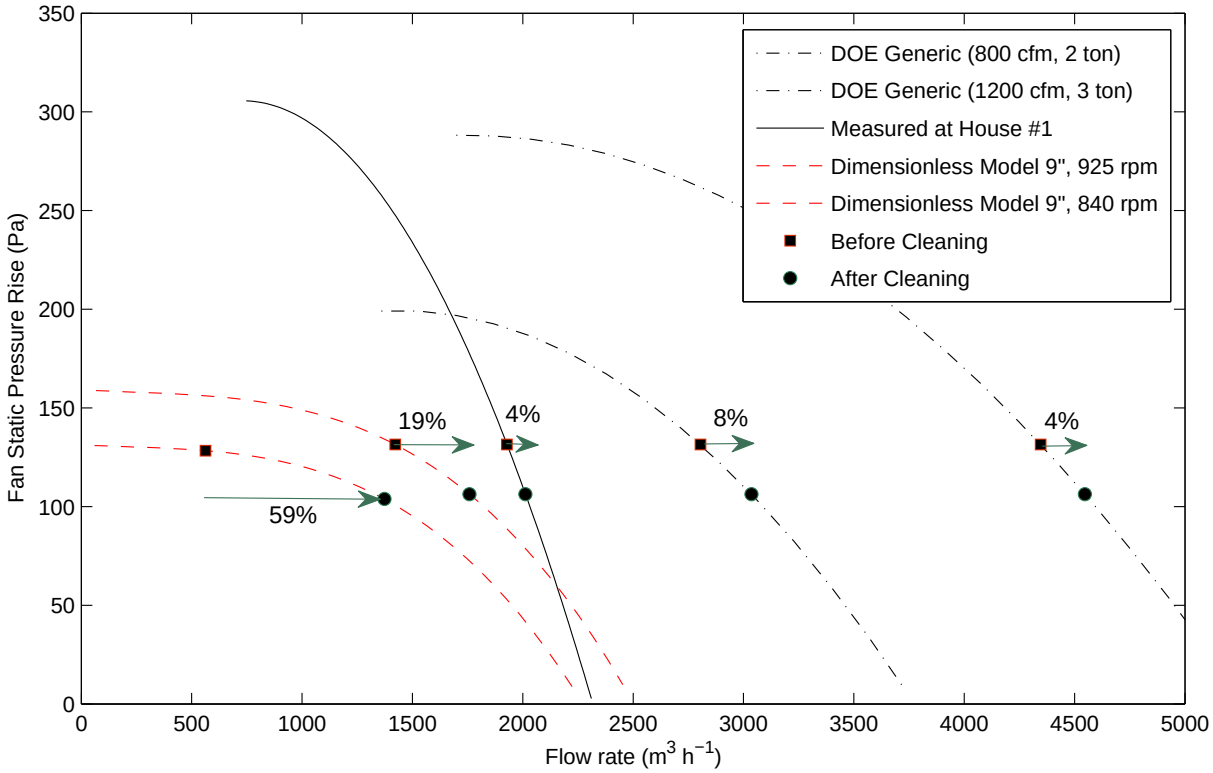

Figure 7.4: The same before- and after- cleaning pressure measurements can give a wide variety of increases in flowrate depending on the fan curve used

Chapter 8

Results and Discussion

8.1 Field Testing

As presented in Section 5.2.2, the field testing experiment found that system cleaning had a negligible impact on the heating energy efficiency of house #1 (house #2 did not yield useful energy results). This agrees with the expectation that there would be negligible savings because the ducts are all located within the thermal zone. Although the effect on cooling energy consumption was not a part of the field experiment, this effect has been well studied; for the 10% change in flow rate, one would expect an increase in sensible EER on the order of 2% to 10% [8][10][11][32]. Using the relationship between EER and SEER given in Brandemuehl and Wassmer (2009), this translates to a decrease in annual cooling energy in the range of 3-12% [20].

In order to have some data for a case with more significant fouling, a NADCA technician took pressure measurements at a house that that was found to have significant fouling (the coil pressure drop had doubled). Section 4.3 gives more details on this House #3.

8.2 Parametric Simulation

8.2.1 Sensitivity to Fan Curve

In order to apply the results of the parametric simulation, the information and measurements for House #3 were entered into the HVAC-COST spreadsheet. Because flow rates were not measured at this house, the tool's fan curve model is used to determine the before and after cleaning operating points based

on the pressure measurements. As discussed in Chapter 7, the largest uncertainty in the tool arises from the fan curve. Using the dimensionless fan curve model built into the tool, the 19% decrease in fan pressure rise after cleaning corresponded to a 19% increase in flowrate, as a percentage of normal, clean flowrate. In other words, the fouling caused the flow rate to decrease 19%, from 1996 m^3 h^{-1} to 1616 m^3 h^{-1} (1175 cfm to 951 cfm). To explore the sensitivity of this change in flow rate to the fan curve shape, different RPM values can be used in the fan curve model, to generate fan curves of different shapes. Figure 8.1 shows how this increase in flowrate changes as the RPM used in the fan curve model is varied from the 925 RPM listed on the motor nameplate. This increase in flowrate ranges from more than 60% at 840 RPM down to 3% at 1425 RPM. This shows the importance of using the correct RPM in the fan curve model; even being off by 85 RPM can drastically change the results. It is apparent that there is greater sensitivity at lower flow rates because the fan curve is less steep (see Figure 3.2). The 60% decrease in flowrate due to fouling is quite unrealistic considering that the pressure drop parametric showed a maximum decrease of 39% for the most extreme case (discussed in Section 6.1). However, this means that the parametric analysis covers a sufficient range of flowrate changes.

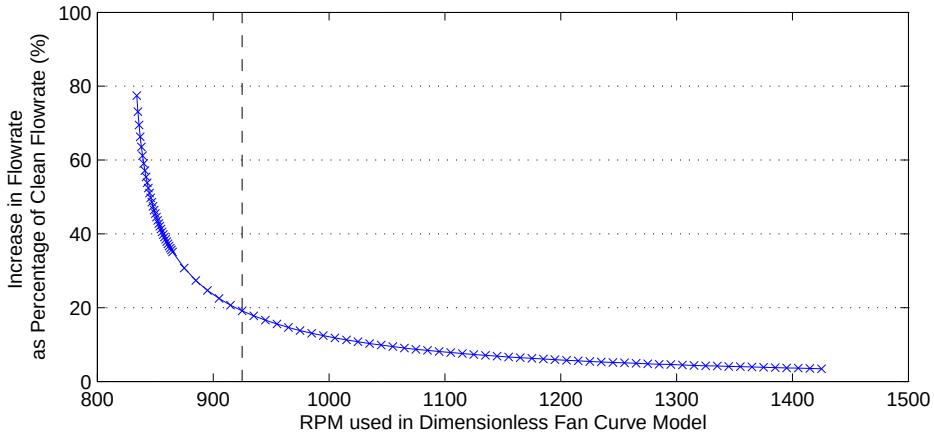

Figure 8.1: Sensitivity of Increase in Flow Rate to RPM used in Fan Curve Model. Based on House #3 pressure measurements.

In order to see how the energy savings results vary for different levels of improvement in system flowrate, it is useful to define a variable, ΔQ, as the increase in flowrate due to a system cleaning, relative to the flowrate under clean conditions. Figure 8.2 shows the results of the parametric simulations, for both

the residential and small commercial analyses, in terms of energy savings due to cleaning (i.e., the percent reduction in HVAC source energy[1]) vs. ΔQ.

8.2.2 Single Family Detached Residential Results

The results for the residential building case show that there is only savings if the increase in flowrate due to cleaning is greater than 20% (relative to normal), or if the ducts are located outside the thermal envelope and are uninsulated and poorly sealed. Otherwise, the change in HVAC source energy resulting from cleaning will be negligible or slightly negative. At 20% increase in flowrate relative to normal, ranges from 1% in the hotter climates, to 3-5% in the colder climates.

For more extreme increases in flowrate, if the ducts are inside the conditioned zone or outside but well sealed and insulated, the only savings is for climates with air conditioning demand. This is because there are no longer any distribution losses, the only savings is due to improving air conditioner performance by having a flow rate closer to the ideal 595-765 m^3 h^{-1} (350-450 cfm/ton). Thus, even cleaning a system for which fouling caused a 60% decrease in flowrate, the model shows that there is absolutely no savings for heating-only climates like Anchorage and Fairbanks. This highlights the assumption of the model that when ducts are in the conditioned zone, 100% of the distribution losses (duct surface heat transfer and leakage) make it to the zone as useful conditioned air. This ignores the possibility that ducts are enclosed in drywall, making the losses less useful and possibly even allowing them to leak to the exterior. A common example of this in commercial buildings is when a ceiling plenum is used for return air instead of using a ducted return, allowing a link between return leakage and infiltration [38].

At a 39% increase in flowrate corresponding to the extreme fouling scenario discussed above, savings ranges from -4% (Anchorage) to 8% (Miami) if ducts are inside the conditioned zone, 0% (Anchorage) to 9% (Miami) if ducts are in an unconditioned attic but are sealed and insulated, or 7% (Los Angeles) to 13% (Fairbanks) if the ducts are in an unconditioned attic and are poorly sealed and not insulated.

[1] For the site-to-source conversion factor, the U.S. national average of 3.34 kWh_{source}/kWh_{site} was used.

8.2.3 Small Commercial Results

In general, the results from the small office building parametric simulation show less potential for savings than the residential case (shown in Figure 8.2). If ducts are inside the conditioned zone or are outside but are sealed and insulated, then the savings is negative for all climates, for the realistic range of flow degradation (0-40%). When the ducts are located in an unconditioned attic, with no duct insulation and typical leakage (10% supply, 5% return), there will be positive savings for heating-dominated climates. At 20% increase in flowrate, savings with cleaning ranges from -8% in Miami to 5% in Minneapolis. At 40% increase in flowrate, savings with cleaning ranges from -13% in Miami to 30% in Minneapolis.

The major difference between commercial and residential buildings is that bringing in outside air for ventilation is required in commercial buildings. This difference explains the predominance of negative savings for the small commercial case; when a system cleaning increases the flowrate in a small commercial CAV system, more outside air will be brought in (assuming the OA damper position remains the same). This is beneficial (typically) from an indoor air quality perspective, but leads to an increase in heating energy in all eight climate locations. The increase in outside air actually decreases cooling energy in all climates except for Miami and Houston, because it increases the potential for free cooling in the climates that can take advantage of it. However, this effect would be negated if air-side economizers were installed.

Because of the need for ventilation, commercial building air handler fans run for many more hours than in residential buildings. This gives greater weight to the increase in fan power that results from cleaning constant air volume systems, which also contributes to the predominance of negative savings.

Another effect of the ventilation requirements of commercial buildings is that the increased run time of the fan and the increased particulate matter brought in with outside air results in faster fouling times. This is not reflected in these results because they are presented in terms of increase in flowrate, but should be kept in mind.

8.2.4 Sensitivity to Duct Location

Figure 8.3 shows the effect of duct location on the energy savings due to cleaning for the residential model in eight different climate zone locations. The results are presented for two cases: one where flowrate

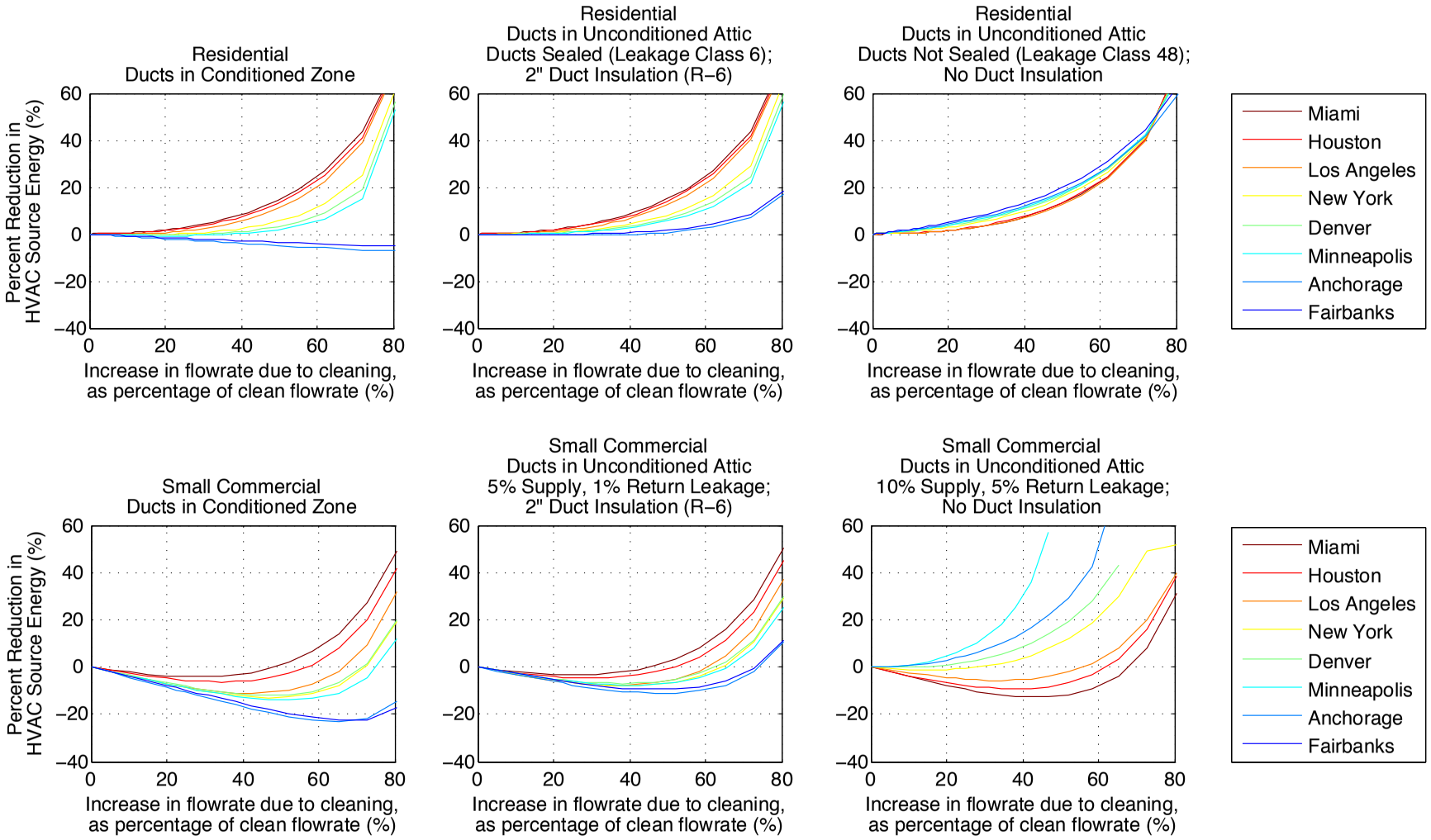

Figure 8.2: Percent reduction in HVAC source energy vs. the increase in flowrate due to cleaning: Three residential cases and three small office cases

was degraded by 19% by fouling and a second where flowrate was degraded by 39% because of fouling. For the 19% case, with ducts located within the conditioned envelope, the change in HVAC energy is not significant (ranges from 0.90% in Miami to -1.4% in Anchorage). The negative values are due to the increase in fan energy. The four scenarios with ducts located in unconditioned areas all show positive savings. The basement and crawlspace results were virtually identical and smaller than the savings in the garage and attic scenarios. All of these scenarios assume no duct insulation and no duct sealing (leakage class 48), unless otherwise specified.

8.2.5 Sensitivity to Duct Insulation and Leakage Class

Figures 8.4 and 8.5 examine the sensitivity of the residential simulation results to the level of duct insulation and leakage class, with the ducts located in an unconditioned attic. Like those presented above, these results are based on the pressure measurements taken at House #3. Figure 8.4 uses the original 925 RPM in the fan curve model, which gives a 19% increase in flow rate relative to clean. Figure 8.5 presents the more extreme case of a 39% increase in flowrate relative to normal. Note the difference in scales between the two figures.

Five different leakage classes were considered: 3, 6, 12, 30, and 48 (cfm per 100 ft^2 duct surface at 1 in w.c.). See Table 3.1 for examples of the different classes. The duct insulation ranged from 0 to 5 inches (0 to 127 mm) thick. The corresponding insulation value ranged from RSI 0 to RSI 2.6 m^2K/W (R-0 to R-15 ft^2 h ^oF /Btu). Sheet metal ducts were used for this parametric study, which add RSI 0.3 m^2K/W (R-1.67 ft^2 h ^oF /Btu) to the thermal resistance [15].

The Miami, FL case shows that cooling energy savings is much more sensitive to duct leakage than it is to duct insulation. The Denver and Fairbanks cases show that the first inch of insulation (R-3) is most significant. With more insulation than that, duct leakage becomes more significant than surface heat transfer. These conclusions hold true for both the 19% case and the 39% case. The 39% case highlights another finding: in Fairbanks, where there is no cooling load, decent duct insulation and sealing reduces the savings to less than 5%. However, in Miami, and to a lesser extent in Denver, there is savings even with virtually no distribution losses. This savings is due to improving air conditioner performance by having a

flow rate closer to the ideal 595-765 m^3 h^{-1} (350-450 cfm/ton).

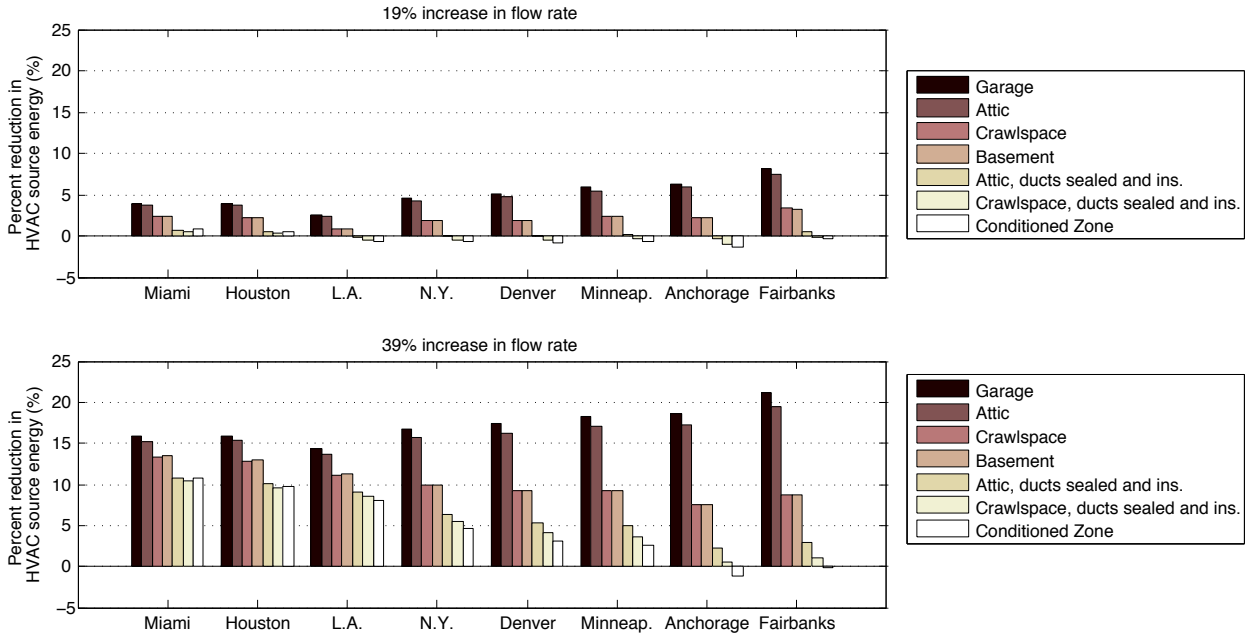

Figure 8.3: Reduction in HVAC Source Energy due to System Cleaning vs. Duct Location, House #3, 925 RPM

8.2.6 Sensitivity to Clean Flowrate

The results presented above assume that the flowrate after cleaning is ideal for optimum system performance: 595-765 m^3 h^{-1} (350-450 cfm/ton) for cooling mode. Because of poor duct system layout, high-resistance flex duct, fan undersizing, or closed supply registers, the after-cleaning flowrate is often lower than the ideal flowrate. The results presented in this section demonstrate the sensitivity of the results to the after-cleaning flowrate, shown as a percentage of ideal system flowrate. Sensitivity to clean flowrate for each of the three duct scenarios is presented in Figures 8.6-8.8 (residential) and 8.9-8.11 (small office).

In general, for the same percentage increase in flowrate (relative to clean), systems with clean flowrates lower than ideal have greater savings than when the clean flowrate is closer to ideal. This is because the relationship between energy consumption and flowrate is non-linear; improvement is more dramatic for systems that have low or very low flowrates. This is apparent from the plot of air conditioner performance vs. flow rate shown in Figure 8.14. Note that when ducts are located inside the conditioned zone (distribution

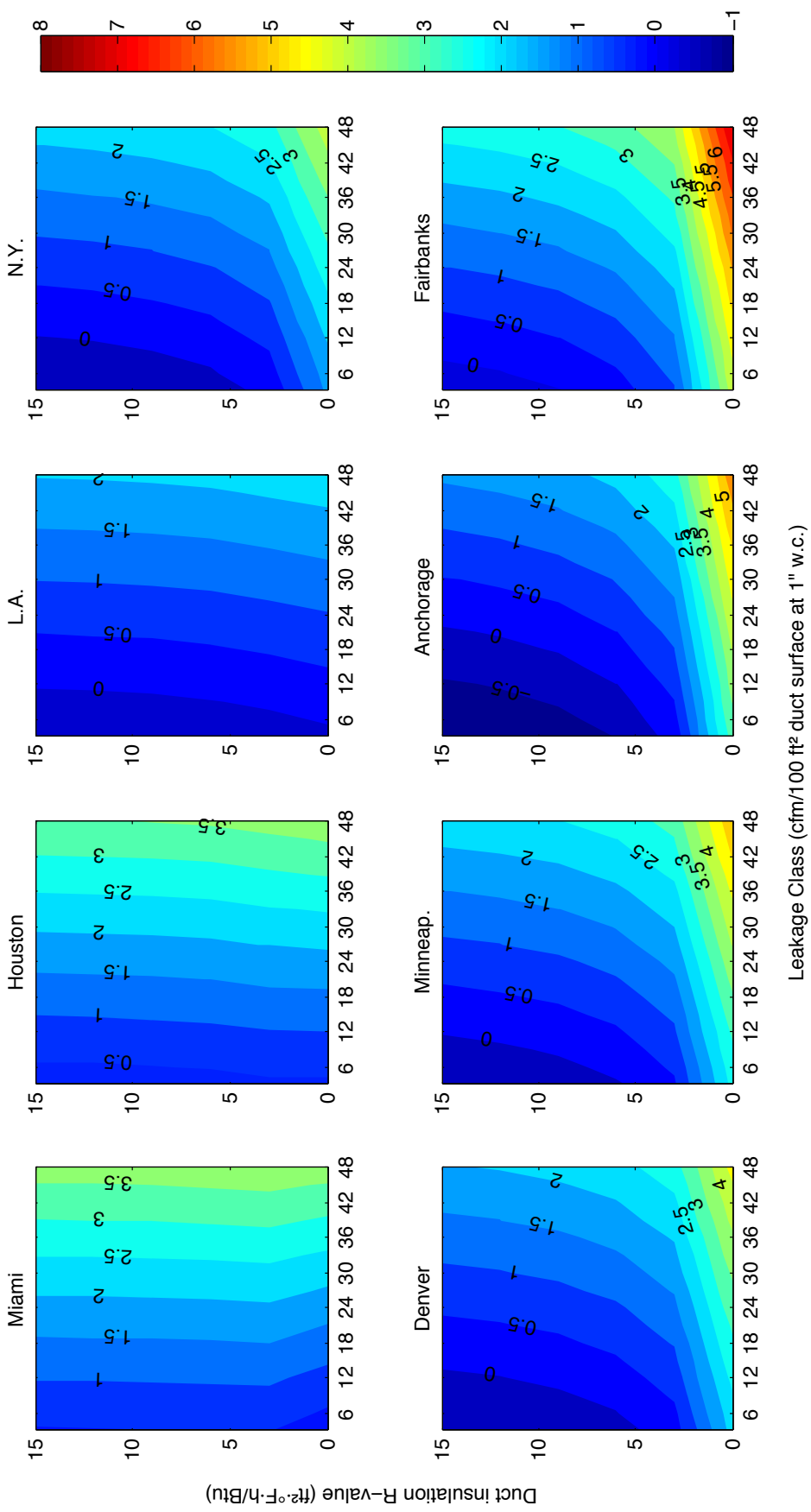

Figure 8.4: Sensitivity of cleaning energy savings to ductwork characteristics, all ducts in unconditioned attic. Based on House #3 pressure measurements. Using 925 rpm fan curve, cleaning increased flowrate from 81% to 100% of clean condition.

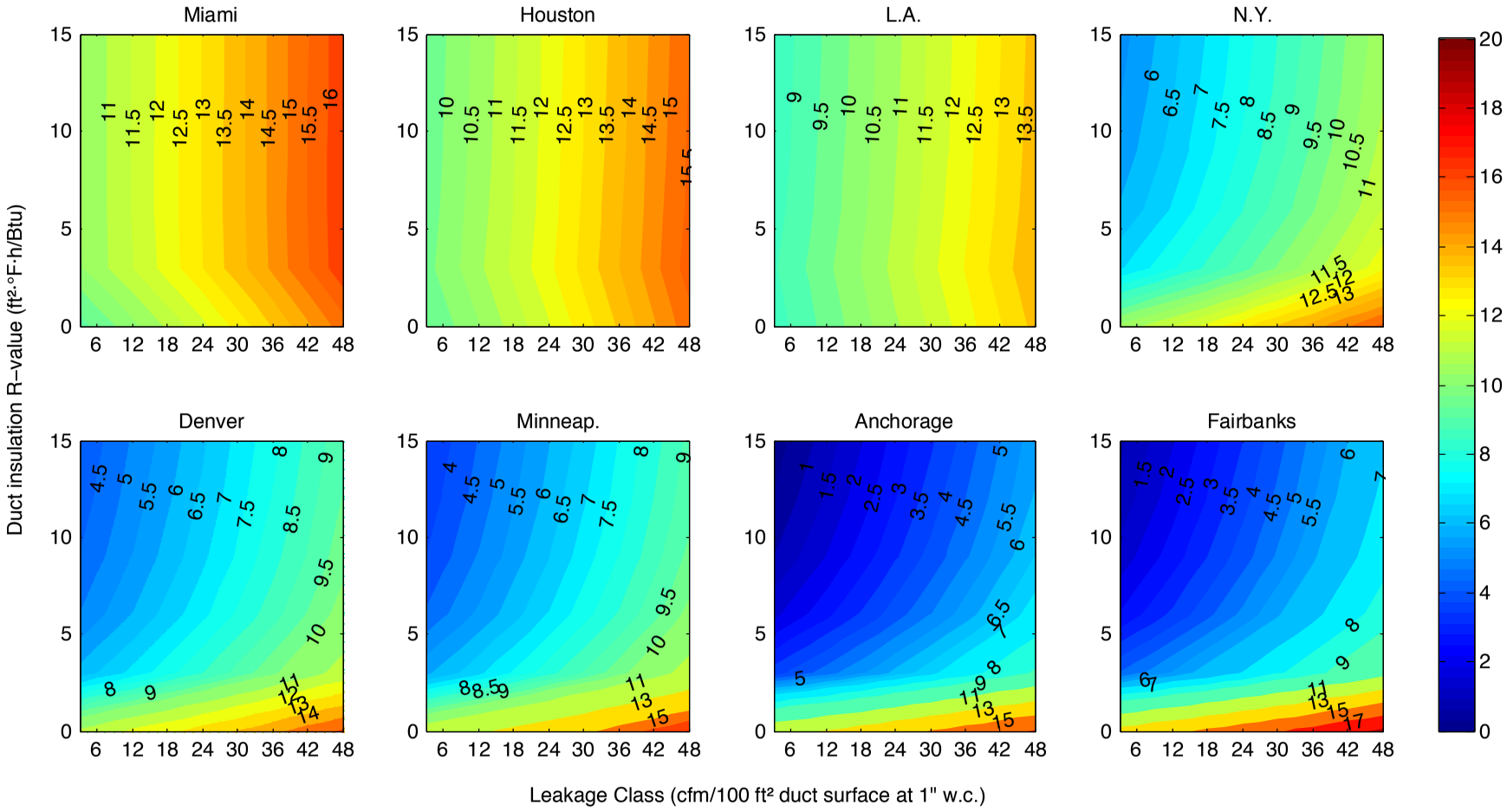

Figure 8.5: Sensitivity of cleaning energy savings to ductwork characteristics, all ducts in unconditioned attic. Based on House #3 pressure measurements. Using 859 rpm fan curve, cleaning increased flowrate from 61% to 100% of clean condition.

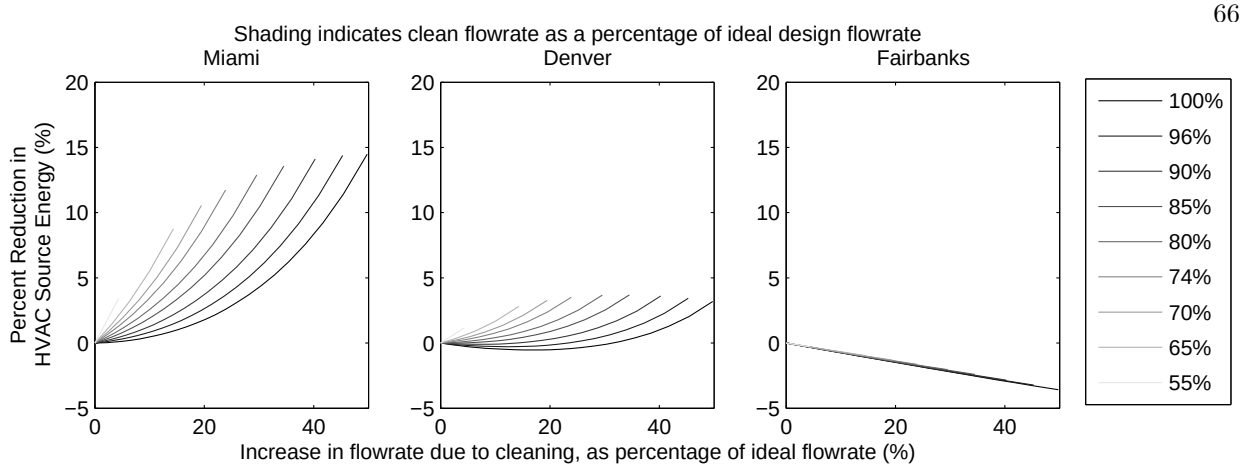

Figure 8.6: Sensitivity of energy savings to clean flowrate as a percentage of ideal flowrate (residential), ducts in conditioned zone.

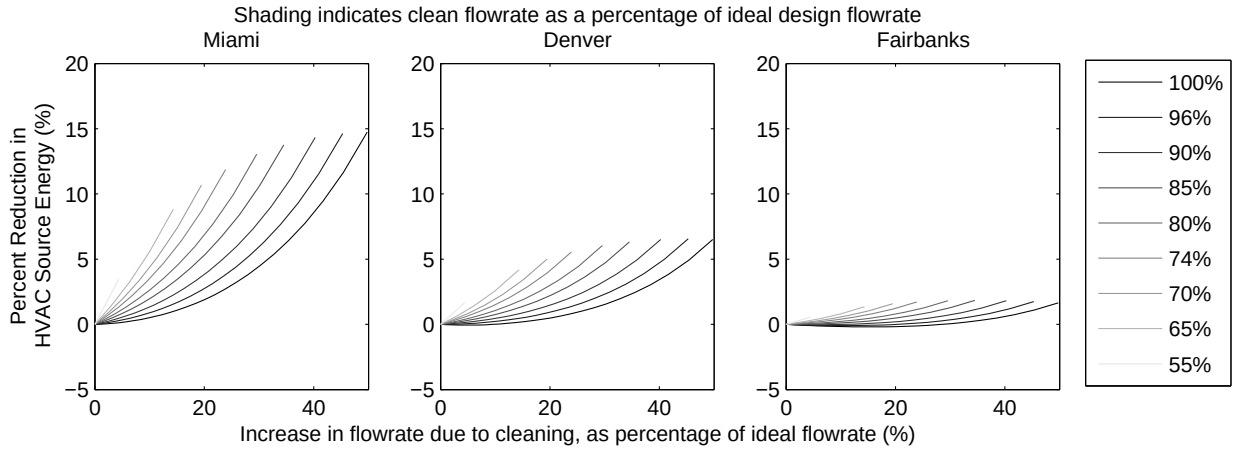

Figure 8.7: Sensitivity of energy savings to clean flowrate as a percentage of ideal flowrate (residential), insulated sealed ducts in unconditioned attic.

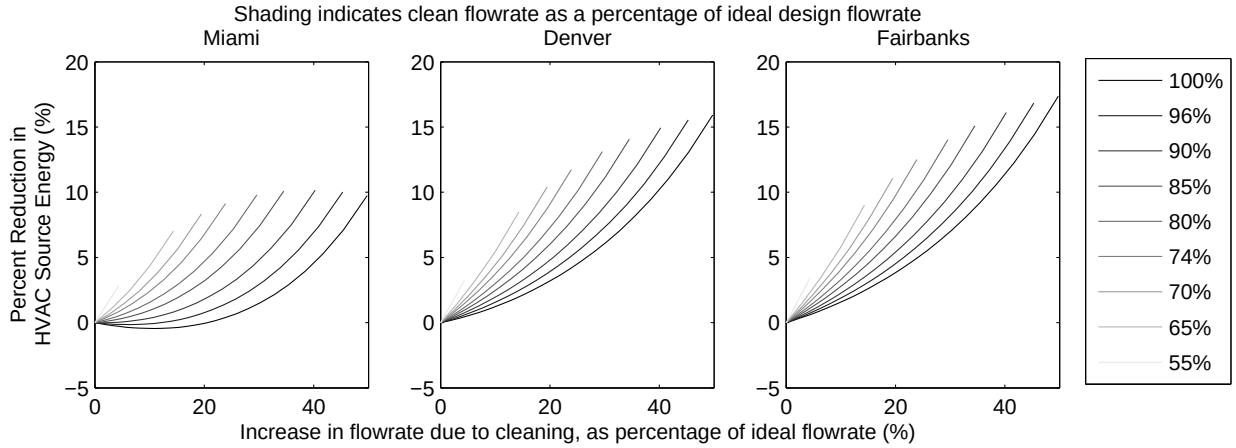

Figure 8.8: Sensitivity of energy savings to clean flowrate as a percentage of ideal flowrate (residential), uninsulated leaky ducts in unconditioned attic.

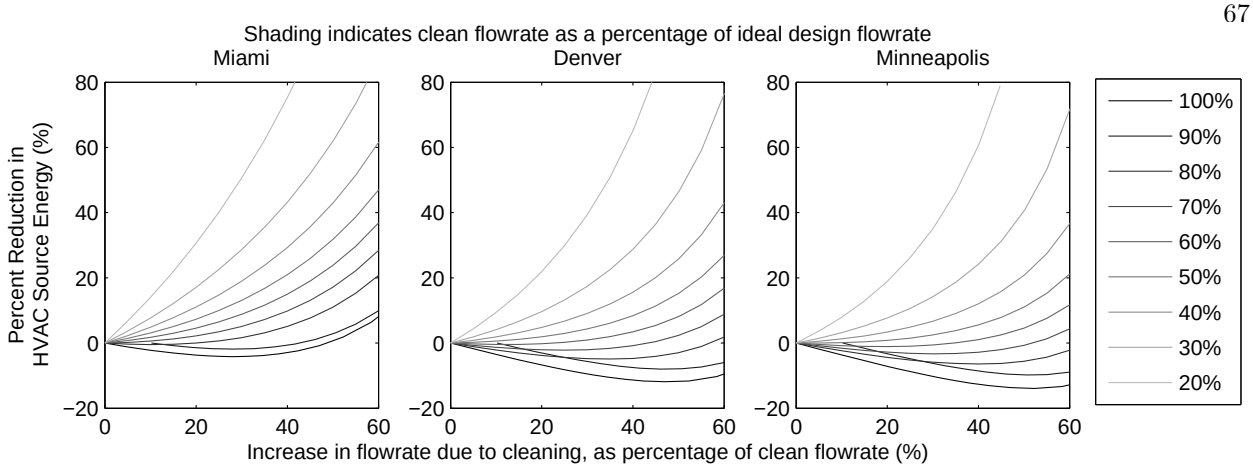

Figure 8.9: Sensitivity of energy savings to clean flowrate as a percentage of ideal flowrate (small commercial), ducts in conditioned zone.

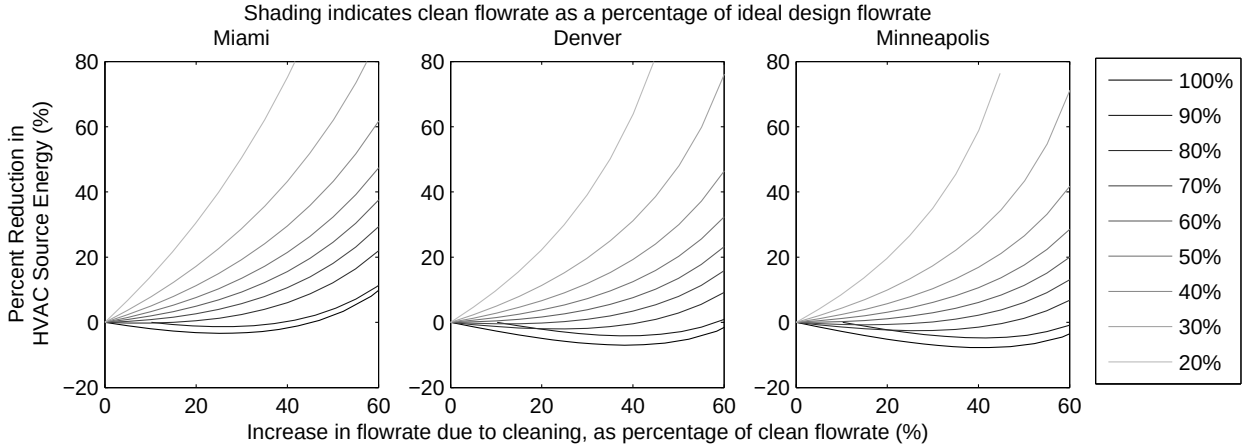

Figure 8.10: Sensitivity of energy savings to clean flowrate as a percentage of ideal flowrate (small commercial), insulated sealed ducts in unconditioned attic.

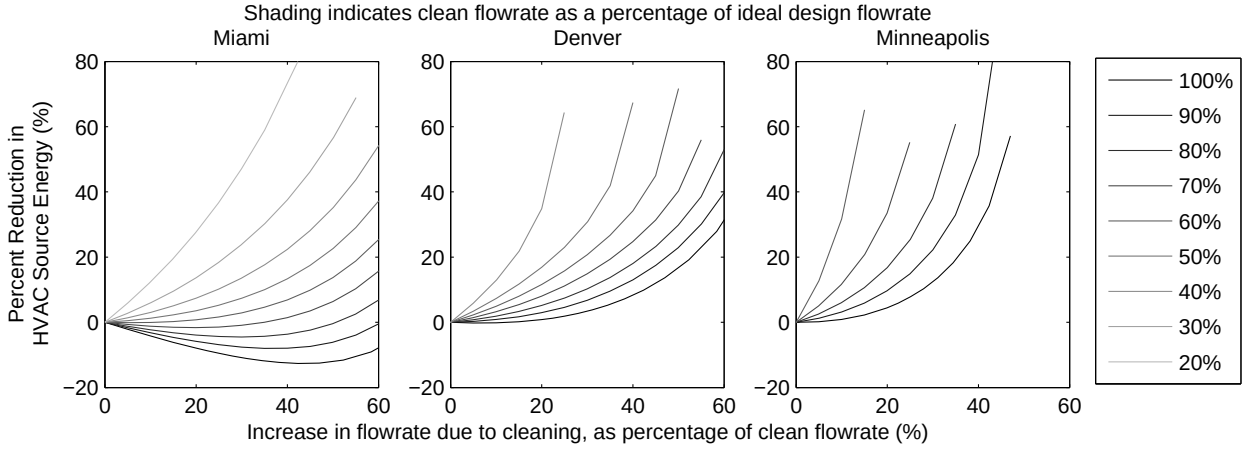

Figure 8.11: Sensitivity of energy savings to clean flowrate as a percentage of ideal flowrate (small commercial), uninsulated leaky ducts in unconditioned attic.

efficiency is 100%), then there are only increased savings at lower flowrates for buildings that have cooling demand (see Figure 8.6c). Note that some climates and flowrate combinations resulted in errors due to the distribution system efficiency being calculated as negative. Therefore, for the commercial case, Minneapolis is presented instead of Fairbanks, and some cases have a limited range of flowrates for which there is valid results.

8.2.7 Impact of Cleaning on Unmet Load Hours

In order to compare the before and after cleaning energy consumption, one must take into account occupant comfort. The analysis uses the number of hours during which the thermostat set point is not met (unmet load hours) as a simple analog for comfort. If the number of unmet load hours is significantly higher before cleaning, it can be concluded that the system cleaning provided a non-energy benefit. The number of unmet load hours for the residential scenario with ducts located inside the conditioned zone is shown in Figure 8.12. For both heating and cooling, the number of unmet load hours is small, even at 25% of ideal flow rate. This indicates that comparing the energy use before and after cleaning is a fair comparison in this case. However, the results presented are for a house with ducts inside the conditioned zone and properly sized heating and cooling capacities. The impact of cleaning on unmet load hours may be different for different duct locations and for under-sized or over-sized systems.

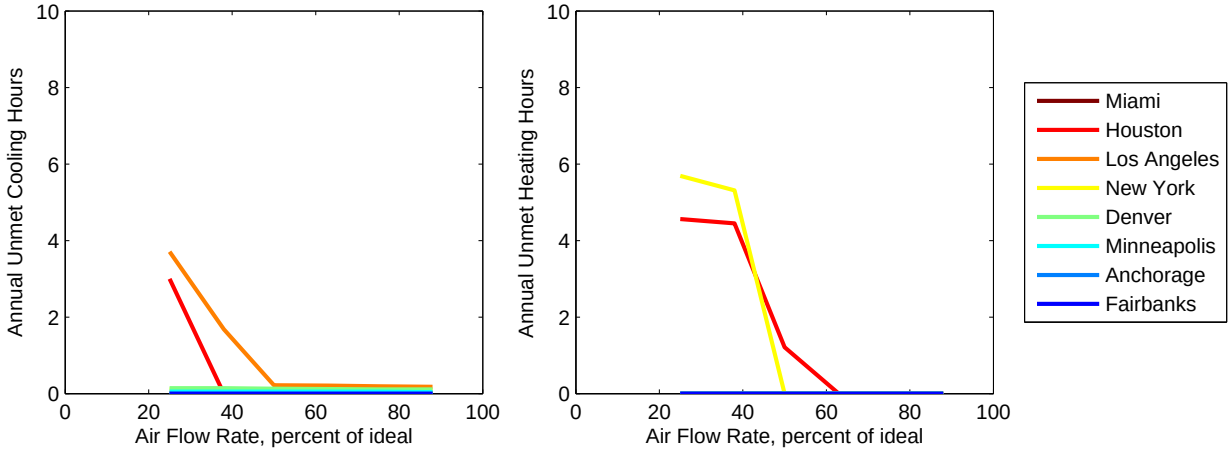

Figure 8.12: Unmet cooling and heating load hours vs. flow rate. Ducts in conditioned zone.

8.2.8 Comparison of results to literature

Although there is only one study in the literature that includes distribution losses and long-term performance (as opposed to instantaneous air conditioner performance), the results of this study can be compared to previous research in the literature. Figure 8.13 compares the results of the Stephens et al. field and lab experiment results (no change in daily HVAC energy consumption at 7-10% increase in flowrate) [16][17], which were conducted in Austin, Texas to our results for Houston, Texas, with two different duct locations. Although the Stephens et al. study only covers a small range of changes in flow rate (7-10%), in a single climate, the results are consistent with the findings of this thesis.

There have been several studies of the impact of degraded air flow rates on air conditioner performance (EER). The results of these studies can be compared with the air conditioner performance model used for this project (from ASHRAE Standard 152 [33]). Figure 8.14 shows this comparison. The two studies of coil fouling (Siegel et al. [8] and Yang et al. [12][13][14]) both had flow rate degradation of less than 10%. Their results are consistent with the air conditioner performance model in ASHRAE Standard 152. The Palani et al. [11] results cover a wide range of flow rates and is very close to the model. This is because the ASHRAE Standard 152 model is based on the experiments conducted by Palani et al. [33].

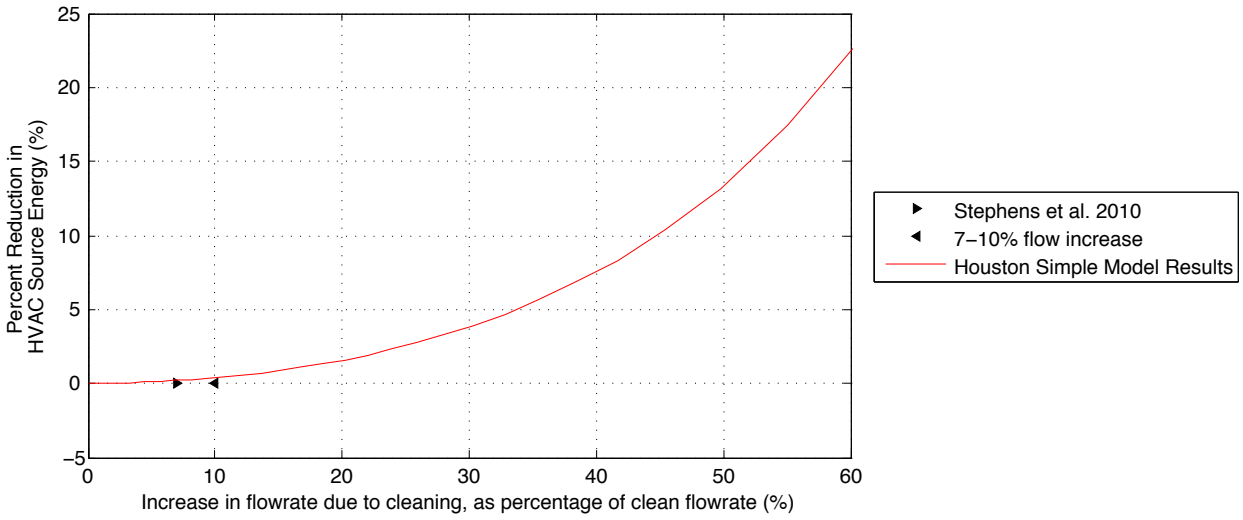

Figure 8.13: Comparison of results to field and lab experiments by Stephens et al. (2010)

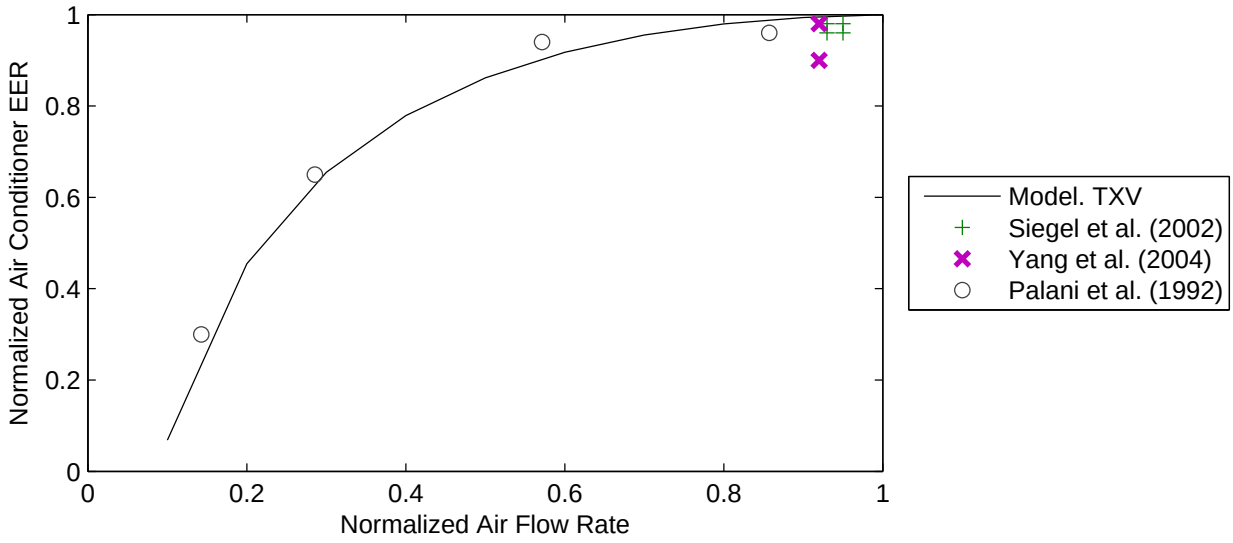

Figure 8.14: Comparison of A/C model to lab experiments in literature

Chapter 9

Conclusions and Future Work

9.1 Summary and Conclusions

9.1.1 Simulation Model

A simulation model was developed in order to evaluate the effect of system fouling on HVAC energy consumption. The model includes two custom components that were developed in order to model the complexities of a fan-duct system. Chapter 5 discusses how the model was verified through laboratory and field testing.

9.1.2 Field Testing

A field test experiment was conducted on two single-family detached houses in order to test the effect of system cleaning on heating energy use. The two houses only had light evaporator coil fouling, which was not ideal. The system cleaning, which included cleaning the evaporator coil, furnace, and blower, in addition to the ductwork, resulted in a 10% increase in air flow rate at house #1 and a 6% increase at house #2. In both cases, the filter pressure drop was the component that had the greatest decrease with cleaning. From this, we can conclude that if a system's evaporator coil has only a light accumulation of dust, a full system cleaning would not be worthwhile from an energy standpoint; simply changing the filter would have a similar impact.

In order to evaluate the energy impact of the system cleaning, energy consumption for the before and after cleaning periods was normalized with respect to degree days. However, because of weather differences,

thermal mass effects, and large jumps in the thermostat setpoint, the weather normalization comparison did not yield usable results. Thus, in order to evaluate the impact of cleaning, a detailed simulation model of house #1 was created. Through simulations of the before- and after- cleaning periods, it was determined that the system cleaning and the resulting 10% increase in flowrate had a negligible impact on the house's heating energy efficiency. The testing at house #2 did not yield usable energy results because there was only one day that required heating after the cleaning was done. We can conclude that for houses with ducts located within the conditioned zone, moderate improvements in flowrate (25% or less) will have a negligible impact on heating energy efficiency.

Other conclusions from the field testing include:

- Duct leakage does not uniformly increase or decrease with system cleaning; it depends on the characteristics of the duct system.
- Reducing the system flow rate dramatically (by 30% to 40%) is difficult to achieve; to do so for the field test, the return path had to be completely obstructed with sheet metal. Because of the great uncertainty when assuming a fan curve, An alternate method of determining system flow

Because the two field test houses were only lightly fouled, a NADCA technician took pressure measurement at a third house so that a real-world system with significant fouling could be evaluated. These house #3 measurements were used as a case study as a way to present the results of the parametric simulations.

9.1.3 Parametric Analysis

In order to expand upon the conclusions of the field testing, a parametric analysis was conducted. The parametric simulation analysis was divided into three sections for computational efficiency:

Pressure drop parametric Using a variety of pressure drop components from the literature, a "worst case scenario" was found that corresponds to the greatest change in flow rate possible: a 39% decrease with fouling. The largest change in duct pressurization, which drives duct leakage, was a 63% decrease with fouling.

Building and climate parametric The TRNSYS model was simulated over the range of flow rate changes determined in the pressure drop parametric, for eight different climate zones and two building types (residential and small commercial).

Duct system parametric Using the method of determining distribution system efficiency in ASHRAE Standard 152, a variety of duct system characteristics (location, insulation, and leakage) was applied to the results of the building parametric in order to determine the range of energy savings possible.

As mentioned above, the measurements from house #3 were used to present the results of the parametric analyses. The dimensionless fan curve model estimated the increase in flowrate due to cleaning as 19%, relative to normal. It was found that as this number increases, the sensitivity to fan curve uncertainty increases dramatically: an 85 rpm (9%) error in the rpm used in the fan curve model can translate into a 310% error in flowrate increase, which can translate into an order of magnitude of error in percent reduction in HVAC source energy, depending on the climate and duct characteristics.

Thus, it is concluded that when relying on a fan curve model to estimate the change in flow rate due to cleaning, such as when using the simplified tool presented in Chapter 7, the fan curve is a major source of uncertainty and the results should be interpreted with this uncertainty in mind. When the increase with flowrate is smaller (i.e., when on the flatter region of the curve presented in Figure 8.1), there can be more confidence in the results.

As part of the parametric analysis, the sensitivity of results to duct characteristics (location, leakage, and insulation) and the after-cleaning flowrate was explored. The following conclusions were drawn for the analysis of residential HVAC systems:

- In general, fan energy consumption increases with cleaning, but is only a small contributor to changes in HVAC source energy (less than 2%). This is what causes negative savings in certain instances. As will be explained later, fan energy is a much bigger factor for the small commercial building case.
- When the ducts are in a conditioned zone, distribution system efficiency is 100%, as calculated by ASHRAE Standard 152. This means that with a system cleaning, there is negligible change in heating system efficiency for all climates and all levels of fouling, and the only change in cooling

energy comes from improvement in air conditioner flowrate (heat pump performance would improve as well):

  - With 19% increase in flowrate, relative to clean, the HVAC source energy savings ranges from 0.90% in Miami to -1.4% in Anchorage.
  - With 39% increase in flowrate (the maximum from the pressure drop parametric), the savings ranges from -4% in Anchorage to 8% in Miami.

- When the ducts are outside of a conditioned zone, the reduced distribution system efficiency leads to greater savings:
  - With 19% increase in flowrate and uninsulated and leaky ducts located in an attic, the HVAC source energy savings ranges from 1% in the hotter climates, to 3-5% in the colder climates.
  - With 39% increase in flowrate and uninsulated and leaky ducts located in an attic, the savings ranges from 7% in Los Angeles, to 13% in Fairbanks, AK.
  - Typically, the greatest savings occurs with ducts (uninsulated and leaky) in a garage, followed closely by an attic location. Savings are less (50% to 75% less) for unconditioned basements and crawlspaces.
  - If a duct system is well insulated and sealed (R-5; leakage class 6 or less), the heating energy savings is reduced to less than 5% and the results become similar to when the ducts are in the conditioned zone; that is, the change in air conditioner (or heat pump) COP becomes dominant.
  - Cooling energy savings is more sensitive to duct leakage than it is to duct insulation.
  - For heating, the first inch (R-3) of insulation is most significant. After that, duct leakage becomes the dominant factor.
  - If uninsulated and leaky ducts are in an unconditioned space, a sure way to save energy is to insulate and seal them. However, ensuring proper system flow rate (e.g., through system cleaning) is still important for optimal air conditioner performance.

- Energy savings will be greater for systems that have a less-than-ideal clean flow rate. HVAC source energy savings from can reach up to 80% for some scenarios where clean airflow is severely restricted down to 20% of ideal by poor duct layout or other obstructions not removable by cleaning.

Other conclusions from the parametric simulations include:

- HVAC systems that have simple ductwork with low resistance to flow are more sensitive to changes in pressure drop than systems with more complex ductwork.
- The pressure drop of shallow evaporator coils (i.e., fewer rows) is more affected by fouling than deep coils.

9.1.4 Small Commercial Building Analysis

Results from the small office building simulations show that HVAC source energy almost always increases with an increase in flowrate due to cleaning. The exception is when the ducts are outside the thermal envelope and are uninsulated and leaky:

- At 20% increase in flowrate, savings with cleaning ranges from -8% in Miami to 5% in Minneapolis.
- At 40% increase in flowrate, savings with cleaning ranges from -13% in Miami to 30% in Minneapolis.

However, there is a non-energy benefit to a system cleaning: outside air ventilation rates are restored to their designed levels.

9.1.5 Savings Estimation Tool

A simplified method of estimating potential savings resulting from a system cleaning, based on correlations derived from the parametric simulations, was developed and incorporated into a savings estimation spreadsheet tool that can be used by field technicians. A paper data form that mirrored the input page of the spreadsheet tool was developed to facilitate collection of information in the field. The fan curve was identified as a major source of uncertainty because the tool takes pressure measurements as inputs and relies on the fan curve to determine the before and after cleaning flow rates. An uncertainty analysis was

conducted to determine the significance of this error. Measuring the temperature rise across the furnace to determine flow rate has less uncertainty and is the recommended method for use with the savings calculation tool. If greater accuracy for the tool is desired, it is recommended that flow rate is measured directly; a flow-plate type device that fits into the filter slot, such as the one described by Francisco and Palmiter [35], would be able to quickly and accurately take the necessary flow rate measurements. Despite the uncertainty associated with the fan curve, the tool is valuable in that it can be used to get an estimate of the range of possible energy and cost savings resulting from a system cleaning.

9.1.6 Prioritization of HVAC System Maintenance

This study showed that for some systems with low air flow rates and ducts outside the conditioned space, significant energy savings can be achieved through a system cleaning. How should system cleaning be prioritized vs. other HVAC system maintenance like duct sealing/insulating or checking refrigerant charge?

Palani et al. reviewed several surveys of HVAC systems showing abnormally high consumption. Of the 43 systems in the surveys, 77% had improper refrigerant charge, 37% had inadequate air flow, and 14% had a leak or kink in a refrigerant line [11]. From their laboratory tests, Palani et al. found that the most significant degradations in EER resulted from: a 50% or greater reduction in evaporator air flow rate, a restricted refrigerant line (before the expansion valve), and a 30% or greater undercharge of refrigerant. It is difficult to know exactly how common it is to find a 30% undercharge or a 50% degraded air flow rate, but these findings suggest that refrigerant charge may be more common and significant a problem than inadequate air flow rate.

The savings resulting from sealing and insulating ducts in an unconditioned attic can be compared to the savings resulting from a system cleaning. Several parametric runs were conducted to illustrate this comparison. The results from these runs are shown in Figure 9.1, which shows the energy cost savings resulting from duct sealing and insulating or increasing system flow rate to the ideal flow rate, for a range of flow rates. The lines marked "$>200^{o}$F" show theoretical savings for flowrates that are low enough to trigger the furnace temperature high limit switch. Realistically, the furnace would not continue to fire, and would continually short-cycle.

In all three of the climates (Miami, Denver, and Minneapolis), the energy cost savings resulting from duct sealing and insulating is always greater than that resulting from restoring the system flow rate to ideal. In the range of flow rates expected to be seen in the field (70%-100% of ideal), duct sealing and insulating results in significantly more savings than does a system cleaning. Therefore, for a system with uninsulated and unsealed ducts in an unconditioned space, improving the ducts should always be the highest priority. In summary, the prioritization of HVAC system maintenance should be:

(1) If ducts are in an un- or semi-conditioned space, and are leaky and/or uninsulated, they should be sealed and insulated.

(2) The HVAC system should be checked for proper refrigerant charge and evaporator flow rate. If either is found to be degraded by 30% or more, the problem should be remedied. For a degraded flow rate, this may involve cleaning the evaporator coil, changing out the filter, cleaning registers, opening dampers, or increasing blower motor speed.

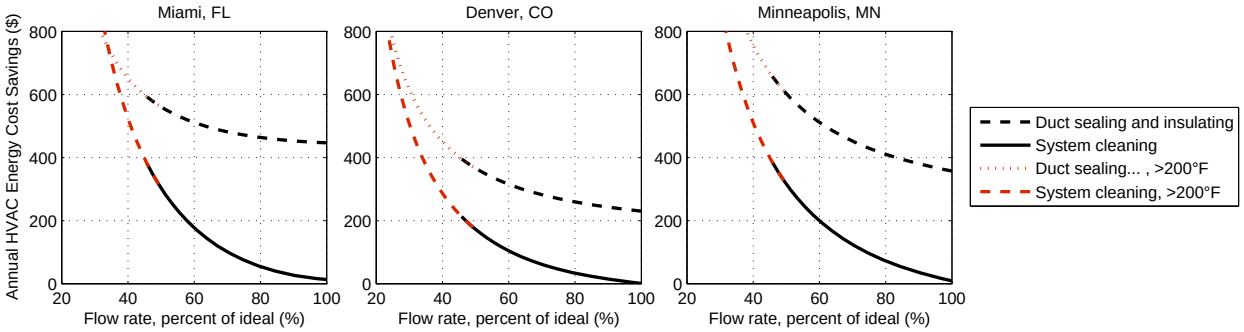

Figure 9.1: System Cleaning vs. Duct Sealing and Insulating - For almost all flowrates, duct sealing and insulating results in greater savings.

9.2 Future Work

9.2.1 Heavy Fouling Cases

The research conducted for this thesis has established the relationship between degraded flow rates and HVAC energy consumption. A worst-case fouling scenario (39% flowrate degradation) has been identified

based on pressure drop coefficients from the literature. The field testing conducted as part of this research was limited in that the houses only had light coil fouling and flow rates at 10% below normal. What remains to be seen is what the typical flow rate degradation is for systems with heavily fouled coils, which NADCA defines as when the upstream side of the coil is matted with dust. A field survey of buildings with heavy fouling, including actual flow rate measurements before and after coil cleaning, would be helpful in determining the typical impact of "heavy fouling" on flow rates. A flow-plate type device that fits into the filter slot, such as the one described by Francisco and Palmiter [35], would be a useful tool for such a field survey, as it can quickly and accurately take flow rate measurements.

9.2.2 Air Conditioning Field Study

This project originally sought to study the effect of system fouling on air conditioning energy consumption with a summer field test in addition to the winter field test. However, since buildings with heavy fouling and occupants willing to participate were not able to be found, a summer field test would not have been worthwhile. However, a field experiment that includes air conditioning may not be necessary because there have been many studies which have examined the effect of fouled coils and/or filters on air conditioner energy consumption [8][16][39][17].

9.2.3 Duct Leakage Measurements

The duct leakage class model used in this analysis is a simplification in that is uses a single value for duct pressure to estimate duct leakage, whereas in reality, the duct pressure changes throughout the duct system. In this analysis, the duct pressures at the supply plenum (i.e., immediately after the air handler) and return plenum (i.e., immediately before the air handler) are used to calculate supply and return leakage, respectively. This would be acceptable if 100% of the leakage areas were at the plenums, but this is not likely the case for many duct systems. Future research should measure the actual change in duct leakage due to changes in system pressure drops.

9.2.4 High-Efficiency and Variable Speed Fan Motors

New, higher efficiency types of fan motors are becoming more popular in the residential market. All of the fan motors used in this analysis were traditional AC induction motors. Future research should explore the implications of new motor types including permanent split capacitor (PSC) motors and DC brushless motors, also known as electrically-commutated motors (ECM). DC brushless motors would be particularly interesting because of their drastically differently shaped fan curves. Variable speed fan motors are being sold as a high-end option for some residential HVAC systems. The impact of this development should be explored as well.

Bibliography

[1] U.S. Department of Energy -Energy Information Administration. 2005 residential energy consumption survey. http://www.eia.doe.gov/emeu/recs/, 2008.

[2] Heat & cool efficiently : ENERGY STAR. http://www.energystar.gov/index.cfm?c=heat_cool.pr_hvac.

[3] W. J. Fisk, D. Faulkner, J. Palonen, and O. Seppanen. Performance and costs of particle air filtration technologies. Indoor Air, 12(4):223–234, 2002.

[4] Canada Mortgage, Housing Corporation. Research Division, D. Auger, and N. Inc. Efficiency of residential duct cleaning. The Division, 1994.

[5] U.S. Environmental Protection Agency. Should you have the air ducts in your home cleaned? Technical Report EPA 402-K-97-002, October 1997.

[6] B. C. Krafthefer and U. Bonne. Energy use implications of methods to maintain heat exchanger coil cleanliness. ASHRAE Transactions, 92(1B):420–434, 1986.

[7] B.C. Krafthefer, D.R. Rask, and U. Bonne. Air-Conditioning and heat pump operating cost savings by maintaining coil cleanliness. ASHRAE Transactions, pages 1458–1472, 1987.

[8] Jeffrey Siegel, Iain Walker, and Max Sherman. Dirty air conditioners: Energy implications of coil fouling. In ACEEE Summer Study on Energy Efficiency in Buildings, page vp. ; PDFN, Pacific Grove, CA, 2002.

[9] T. M Rossi and J. E Braun. Minimizing operating costs of vapor compression equipment with optimal service scheduling. INTERNATIONAL JOURNAL OF HEATING VENTILATION AIR CONDITIONING AND REFRIGERATING RESEARCH, 2:326, 1996.

[10] D. S Parker, J. R Sherwin, R. A Raustad, and D. B Shirey III. Impact of evaporator coil airflow in residential air-conditioning systems. ASHRAE Transactions, 103:395405, 1997.

[11] M. Palani, D. ONeal, and J. Haberl. The effect of reduced evaporator air flow on the performance of a residential central air conditioner. In the Proceedings of the 1992 Symposium on Building Systems in Hot-Humid Climates, page 2026, 1992.

[12] L. Yang, J.E. Braun, and E.A. Groll. The Role of Filtration in Maintaining Clean Heat Exchanger Coils. ARTI-21CR/611-40050-01. Air-Conditioning and Refrigeration Technology Institute, Arlington, 2004.

[13] Li Yang, James E. Braun, and Eckhard A. Groll. The impact of evaporator fouling and filtration on the performance of packaged air conditioners. International Journal of Refrigeration, 30(3):506–514, 2007.

[14] Li Yang, James E. Braun, and Eckhard A. Groll. The impact of fouling on the performance of filter-evaporator combinations. International Journal of Refrigeration, 30(3):489–498, 2007.

[15] ASHRAE. Fundamentals. 2009 ASHRAE Handbook. American Society of Heating, Refrigerating, and Air-Conditioning Engineers, Inc, Atlanta, 2009.

[16] B. Stephens, A. Novoselac, and J. A. Siegel. Energy implications of filters in residential and Light-Commercial buildings (RP-1299). submitted to. ASHRAE Transactions, 2009.

[17] B. Stephens, A. Novoselac, and J. A Siegel. The effects of filtration on pressure drop and energy consumption in residential HVAC systems (RP-1299). HVAC&R RESEARCH, 2010.

[18] J. Phelan, M. J Brandemuehl, and M. Krarti. In-situ performance testing of fans and pumps for energy analysis. ASHRAE Transactions., (332), 1997.

[19] LBNL and Navigant Consulting. Technical support document: Energy conservation standards for residential furnaces and boilers, September 2004.

[20] Michael J. Brandemuehl and Michael R. Wassmer. Final report ASHRAE 1197-RP updated energy calculation models for residential HVAC equipment. Technical Report ASHRAE 1197-RP.

[21] Mingsheng Liu, David E. Claridge, and Song Deng. An air filter pressure loss model for fan energy calculation in air handling units. International Journal of Energy Research, 27(6):589–600, 2003.

[22] R. D. Rivers and D. J. Murphy. Determination of air filter performance under variable air volume (VAV) conditions. Final Report of ASHRAE Research Project, 675, 1996.

[23] C. Wray. Duct thermal performance models. LBNL-53410. Technical report, Lawrence Berkeley National Laboratory, Berkeley, 2003.

[24] R. Hendron. Building america research benchmark definition, updated december 20, 2007. Technical report, NREL/TP-550-42662. Golden, CO: National Renewable Energy Laboratory, 2008.

[25] EIA. Square footage measurements and comparisons: Caveat emptor., volume 13. 2008.

[26] P. Torcellini, M. Deru, B. Griffith, K. Benne, M. Halverson, D. Winiarski, and D. B. Crawley. DOE commercial building benchmark models. 2008.

[27] ISO 3966:2008 - measurement of fluid flow in closed conduits – velocity area method using pitot static tubes. http://www.iso.org/iso/catalogue_detail.htm?csnumber=50626.

[28] M. Krarti. Energy audit of building systems: an engineering approach. CRC, 2000.

[29] M. H. Sherman and D. T. Grimsrud. Measurement of infiltration using fan pressurization and weather data. NASA STI/Recon Technical Report N, 81:32332, 1980.

[30] Donghyun Seo. Development of a universal model for predicting hourly solar radiation Application: Evaluation of an optimal daylighting controller. Ph.D. dissertation, University of Colorado-Boulder, Boulder, CO, 2010.

[31] Donghyun Seo. Solar model accuracy, July 2010.

[32] M. Palani, D. L. O'Neal, and J. S. Haberl. Monitoring the performance of a residential central air conditioner under degraded conditions on a test bench. 1992.

[33] ASHRAE. Method of Test for Determining Design and Seasonal Efficiencies of Residential Thermal Distribution Systems. ANSI/ASHRAE Standard 152-2004. American Society of Heating, Refrigerating, and Air-Conditioning Engineers, Inc, Atlanta, 2004.

[34] J. McWilliams. Review of air flow measurement techniques. LBNL-49747, Lawrence Berkeley National Laboratory, 2002.

[35] Paul W Francisco and Larry Palmiter. Field evaluation of a new device to measure air handler flow. ASHRAE Transactions, 109:403, 2003.

[36] ASHRAE. ASHRAE standard 152-2004a. method of test for determining the design and seasonal efficiencies of residential thermal distribution systems, 2004.

[37] Lawrence Berkeley National Laboratory. ASHRAE 152 spreadsheets. http://www1.eere.energy.gov/buildings/building_america/perf_analysis.html.

[38] J. Lstiburek, K. Pressnail, and J. Timusk. Air pressure and building envelopes. Journal of Building Physics, 26(1):53, 2002.

[39] B. Stephens, A. Novoselac, and J. A Siegel. Impacts of HVAC filtration on Air-Conditioner energy consumption in residences. In Proceedings of Healthy Buildings 2009, 2009.

Appendix A

House #3 Measurement Data Form

Building Information

State: Co City: Lakewood

Conditioned floor area: 1980 square feet Number of stories: 2 main/Basement

Does the building have?
☑ Both forced-air heating and central A/C ☐ Just forced-air heating ☐ Just central A/C

Electricity cost: ____ per kWh
Heating Fuel: ☑ Gas ☐ Propane ☐ Oil ☐ Electricity
Heating Fuel cost: ____ per *therm / gallon / kWh* (circle)

HVAC Information

Blower Wheel Diameter: 9" in. (measure to nearest inch)

Motor speed: Heating: 925 RPM ☑ Direct drive
3 speed
Cooling: 1050 RPM ☐ Belt: Motor sheave diameter: ____
Slip Factor (SF): ____ Fan sheave diam.: ____

Furnace Input Capacity: 90,000 Btu/hr ☐ Heat Pump: ____ tons HSPF: ____
Output Capacity: 72,000 Btu/hr

A/C Capacity: ____ Btu/hr *or* 3 tons SEER: ____ *or* EER: ____

Evaporator Coil Fouling (not for calculation purposes): ☐ None ☐ Light ☐ Medium ☑ Heavy

Ducts:	Supply Ducts	Return Ducts
Are the ducts in a space that is:	☑ conditioned ☐ unconditioned	☑ conditioned ☐ unconditioned
Where are the majority of the ducts located? (check multiple if half and half)	☐ attic ☐ garage ☑ basement ☐ crawlspace ☐ living area	☐ attic ☐ garage ☑ basement ☐ crawlspace ☐ living area

Number of return registers: 2

Duct Insulation thickness …on Supply duct: 0 in. …on Return duct: 0 in.

N/A Duct sealing: ☐ Transverse joints sealed ☐ Longitudinal seams sealed

Duct shape (trunk lines): ☑ Rectangular ☐ Round

Measurements (take all measurements in "Fan-On" thermostat mode)

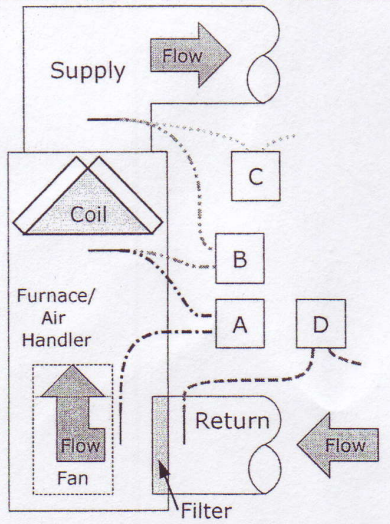

Measure static pressure differences to two decimal places.
Measure amps to one decimal place.
Measure watts or volts to nearest whole number.

	Before cleaning:	**After cleaning:**
A) ΔP across fan:	.68 in w.c.	.55 in w.c.
B) ΔP across coil:	.15 in w.c.	.07 in w.c.
C) Gauge P in supply plenum:	.25 in w.c.	.19 in w.c.
D) Gauge P in return plenum:	.27 in w.c.	.25 in w.c.
Fan: ____ watts or 3.2 amps (121 V)		3.8 W or A

Appendix B

Tables of Simulation Results

Table B.1: Reduction in HVAC Source Energy due to Cleaning vs. Duct Location - 19% flowrate increase

Duct Location	Climate Zone Location							
	Miami (%)	Houston (%)	LA (%)	NY (%)	Denver (%)	Minn. (%)	Anch. (%)	Fairbanks (%)
Unconditioned Garage	4	4	3	5	5	6	6	8
Unconditioned Attic	4	4	2	4	5	5	6	8
Unconditioned Crawlspace	2	2	1	2	2	2	2	3
Unconditioned Basement	2	2	1	2	2	2	2	3
Uncond. Attic sealed/ins.	1	1	0	0	0	0	0	0
Uncond. Crawlspace, sealed/ins.	0	0	0	0	0	0	-1	0
Conditioned Zone	1	1	-1	-1	-1	-1	-1	0

Table B.2: Reduction in HVAC Source Energy due to Cleaning - 19% flowrate increase - Ducts in Unconditioned Attic

Duct Insulation (ft^2 °F h/Btu)	Leakage Class (cfm/100 ft^2)	Climate Zone Location							
		Miami (%)	Houston (%)	LA (%)	NY (%)	Denver (%)	Minn. (%)	Anch. (%)	Fairbanks (%)
R-0	3	0	0	0	2	2	3	3	4
R-0	6	0	1	0	2	2	3	3	4
R-0	12	1	1	0	2	3	3	4	5
R-0	30	2	2	1	3	4	4	5	6
R-0	48	4	4	2	4	5	5	6	8
R-3	3	1	0	0	0	0	0	0	1
R-3	6	1	1	0	0	0	1	0	1
R-3	12	1	1	0	1	1	1	1	1
R-3	30	2	2	1	2	2	2	2	3
R-3	48	4	4	2	3	3	3	3	4
R-6	3	1	0	0	0	0	0	0	0
R-6	6	1	1	0	0	0	0	0	0
R-6	12	1	1	0	0	0	0	0	1
R-6	30	2	2	1	1	1	2	1	2
R-6	48	4	4	2	2	2	3	2	3
R-9	3	0	0	0	0	0	0	-1	0
R-9	6	1	0	0	0	0	0	-1	0
R-9	12	1	1	0	0	0	0	0	0
R-9	30	2	2	1	1	1	1	1	2
R-9	48	4	4	2	2	2	2	2	3
R-12	3	0	0	0	0	0	0	-1	0
R-12	6	1	0	0	0	0	0	-1	0
R-12	12	1	1	0	0	0	0	0	0
R-12	30	2	2	1	1	1	1	1	1
R-12	48	4	3	2	2	2	2	2	3
R-15	3	0	0	0	-1	-1	0	-1	0
R-15	6	1	0	0	0	0	0	-1	0
R-15	12	1	1	0	0	0	0	-1	0
R-15	30	2	2	1	1	1	1	0	1
R-15	48	4	3	2	2	2	2	2	3

Table B.3: Reduction in HVAC Source Energy due to Cleaning vs. Duct Location - 39% flowrate increase

Duct Location	Climate Zone Location							
	Miami (%)	Houston (%)	LA (%)	NY (%)	Denver (%)	Minn. (%)	Anch. (%)	Fairbanks (%)
Unconditioned Garage	16	16	14	17	17	18	19	21
Unconditioned Attic	15	15	14	16	16	17	17	19
Unconditioned Crawlspace	13	13	11	10	9	9	7	9
Unconditioned Basement	14	13	11	10	9	9	7	9
Uncond. Attic sealed/ins.	11	10	9	6	5	5	2	3
Uncond. Crawlspace, sealed/ins.	10	10	9	5	4	4	0	1
Conditioned Zone	11	10	8	5	3	3	-1	0

Table B.4: Reduction in HVAC Source Energy due to Cleaning - 39% flowrate increase - Ducts in Unconditioned Attic

Duct Insulation (ft^2 °F h/Btu)	Leakage Class (cfm/100 ft^2)	Climate Zone Location							
		Miami (%)	Houston (%)	LA (%)	NY (%)	Denver (%)	Minn. (%)	Anch. (%)	Fairbanks (%)
R-0	3	9	9	9	11	11	12	12	14
R-0	6	10	10	9	11	12	12	13	14
R-0	12	10	10	10	12	12	13	13	15
R-0	30	13	13	12	14	14	15	15	17
R-0	48	15	15	14	16	16	17	17	19
R-3	3	10	10	9	7	6	6	4	5
R-3	6	11	10	9	7	6	6	4	5
R-3	12	11	11	10	8	7	7	5	6
R-3	30	14	13	12	10	9	9	7	8
R-3	48	16	16	14	12	11	11	9	10
R-6	3	10	10	9	6	5	5	2	3
R-6	6	11	10	9	6	5	5	2	3
R-6	12	12	11	10	7	6	6	3	4
R-6	30	14	13	12	9	8	8	5	6
R-6	48	16	16	14	12	10	10	7	8
R-9	3	10	10	9	6	5	4	1	2
R-9	6	11	10	9	6	5	4	1	2
R-9	12	12	11	10	7	6	5	2	3
R-9	30	14	13	12	9	8	7	4	5
R-9	48	16	16	14	11	10	10	7	8
R-12	3	10	10	9	5	4	4	1	1
R-12	6	11	10	9	6	5	4	1	2
R-12	12	12	11	10	6	5	5	2	2
R-12	30	14	13	12	9	7	7	4	5
R-12	48	16	16	14	11	10	9	6	7
R-15	3	10	10	9	5	4	3	0	1
R-15	6	11	10	9	6	4	4	1	1
R-15	12	12	11	10	6	5	5	1	2
R-15	30	14	13	12	8	7	7	3	4
R-15	48	16	15	14	11	9	9	6	7

Table B.5: Reduction in HVAC Source Energy due to Cleaning - Sensitivity to RPM used in Fan Model - Ducts in Conditioned Zone

RPM used in Fan Curve Model (RPM)	Flow rate increase relative to clean (%)	Climate Zone Location							
		Miami (%)	Houston (%)	LA (%)	NY (%)	Denver (%)	Minn. (%)	Anch. (%)	Fairbanks (%)
1425	3	-9.1	-8.4	-10.0	-5.7	-4.6	-4.0	-2.6	-1.8
1175	6	-8.5	-8.2	-10.1	-6.5	-5.4	-4.5	-4.1	-2.3
1050	10	-7.9	-7.7	-9.8	-6.4	-5.3	-3.8	-4.2	-2.8
1025	11	-7.7	-7.5	-9.6	-6.3	-5.3	-4.0	-4.4	-3.0
1000	12	-7.4	-7.2	-9.3	-6.2	-5.3	-4.5	-4.6	-3.2
975	14	-7.0	-6.9	-8.9	-6.1	-5.4	-5.0	-4.9	-3.4
950	16	-6.3	-6.3	-8.3	-5.9	-5.2	-4.8	-5.0	-3.4
925	**19**	**-5.3**	**-5.4**	**-7.4**	**-5.4**	**-4.8**	**-4.6**	**-5.0**	**-3.5**
900	24	-3.5	-3.7	-5.8	-4.6	-4.2	-4.1	-5.1	-3.6
875	31	0.2	-0.3	-2.4	-2.7	-2.9	-3.1	-5.1	-3.7
859	39	5.3	4.3	2.1	-0.2	-1.1	-1.7	-5.1	-3.8
850	45	12.6	11.0	8.7	3.3	1.5	0.4	-5.2	-3.9
845	51	19.8	17.6	15.1	6.8	4.0	2.4	-5.2	-4.0
840	59	35.0	31.5	28.4	14.1	9.2	6.6	-5.2	-4.1

Table B.6: Reduction in HVAC Source Energy due to Cleaning - Sensitivity to RPM used in Fan Model - Ducts in Unconditioned Attic

RPM used in Fan Curve Model (RPM)	Flow rate increase relative to clean (%)	Climate Zone Location							
		Miami (%)	Houston (%)	LA (%)	NY (%)	Denver (%)	Minn. (%)	Anch. (%)	Fairbanks (%)
1425	3	-14.6	-13.4	-12.3	-7.3	-5.2	-5.0	-2.4	-2.8
1175	6	-13.3	-12.4	-12.0	-7.6	-5.4	-4.7	-3.3	-2.7
1050	10	-12.6	-11.8	-11.5	-6.8	-4.5	-2.7	-2.2	-2.0
1025	11	-12.3	-11.5	-11.2	-6.6	-4.2	-2.7	-2.0	-1.7
1000	12	-12.0	-11.2	-10.8	-6.3	-4.0	-3.1	-1.8	-1.3
975	14	-11.5	-10.8	-10.3	-5.8	-3.6	-3.4	-1.6	-0.7
950	16	-10.9	-10.1	-9.5	-5.0	-2.6	-2.4	-0.5	0.5
925	**19**	**-9.8**	**-8.9**	**-8.2**	**-3.6**	**-1.1**	**-0.9**	**1.0**	**2.4**
900	24	-7.7	-6.9	-6.0	-1.2	1.5	1.7	3.8	5.6
875	31	-3.3	-2.4	-1.3	3.9	7.0	7.4	9.6	12.5
859	39	2.8	3.8	5.0	10.7	14.2	14.9	17.2	21.7
850	45	11.9	12.9	14.2	20.5	24.5	25.7	28.0	35.0
845	51	21.1	22.1	23.3	30.1	34.5	36.2	38.5	48.1
840	59	40.7	41.6	42.4	50.1	55.3	58.1	60.0	75.5

Appendix C

Additional Lab Experiment Data

2 TEST FACILITY

Larson Laboratory

Experiments and data collection were conducted at the HVAC Larson Laboratory located in the Engineering Center on the campus of the University of Colorado at Boulder. This lab is dedicated to Karl Larson, a graduate of the University of Colorado, for his gracious donations to the lab. The Larson Lab, shown in Figure 3, has been designed to allow for various unique experiments. Outdoor air can be introduced into the system through an air handling unit. The air handling unit has been designed to condition the air to any typical climate zone. This air is then supplied to the main air handling unit. Return air can also be cycled through the main air handling unit or mixed with the outdoor conditioned air.

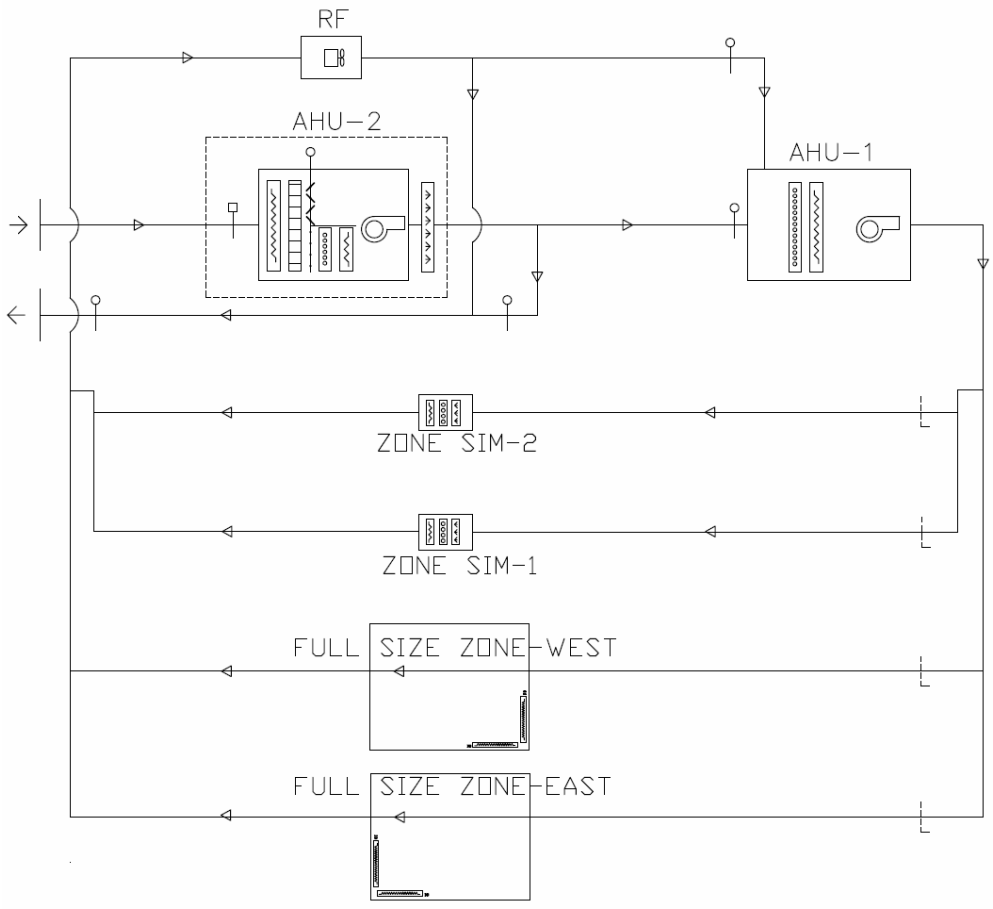

Figure 3: Air-Side Plan View of the Larson Laboratory

The main air handling unit supplies air to four potential zones, two simulated zones and two full size zones. The simulated zones have been fitted with cooling coils and electrical resistance to simulate building loads. The full size zones have been insulated (R-50) thoroughly to make them nearly isolated and have been fitted with baseboard heaters and the option to use a chilled wall heat exchanger.

The system's chilled water is supplied by a 75 ton Trane chiller that can also be used to charge a thermal ice storage unit, rated at 190 ton-hours. The main air handling unit's heating coil is supplied through a Weil-McLain electric boiler rated at 48 kW.

The experiments utilized the return air and a single zone. All other zones and connecting ducts were closed through the use of blast gates. The instantaneous verification experiment utilized one of the zone simulators to allow for less duct leakage. The short-term building load verification utilized one of the full size zones to allow for a more realistic building load and system design. Experiments conducted for energy savings also utilized one of the zone simulators to in order to eliminate variables in the testing. Figure 4 shows the basic diagram of the lab experiments and airflow through the system. Prior to the experiments ducts were also modified to remove the effectiveness of fan powered mixing boxes in the zone simulator as well and sealing the worst cracks in the ducts to reduce duct leakage.

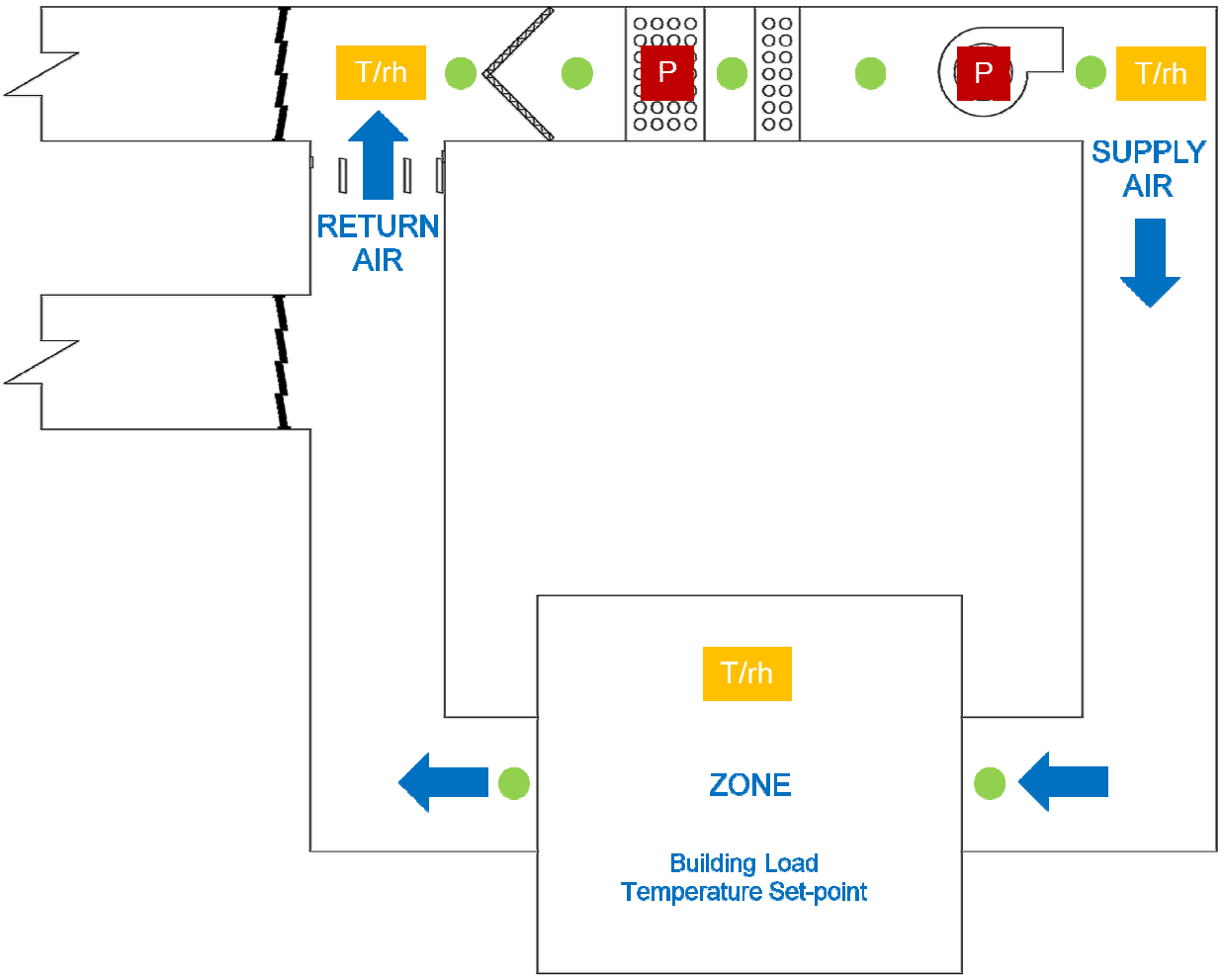

Figure 4: Diagram of Experiment

Sensor Equipment

The majority of the experiments focus on the measurements of pressure, power, and airflow. The short-term building load experiment also included measurements of temperature and humidity. The pressure sensors are Setra model 265's (Figure 5) with varying ranges dependent on their location in the HVAC system with an accuracy of ± 1.0% of full scale. These sensors have been installed using eight inch static pressure probes and are located before and after the HVAC components (filter, cooling coil, heating coil, fan, supply duct, and return duct). This installation can be seen in Figure 6.

The majority of the airflow sensors are also pressure sensors, manufactured by MKS (Figure 7), that are used to measure the dynamic pressure which is used to calculate the airflow. These

airflow sensors have varying ranges with an accuracy of ± 0.5% of full scale. Other airflow sensors, Ebtron, use thermal measurements to determine the air velocity which is then used to calculate airflow. These Ebtron sensors have of 0-5,000 feet per minute range with an accuracy of ± 0.1% of full scale. These airflow sensors collect data on the supply air from the fan, the air supplied to the zone, and the return airflow.

Figure 5: Setra Pressure Measurement Sensor

Figure 6: Installed Probe of Pressure Sensor

The supply fan power consumption sensor is manufactured by TransData (Figure 8) with a range of 50kW and an accuracy of ± 0.2% of full scale. The transformer and transducer for the power sensor are powered externally as to keep this rated accuracy. Lastly the temperature and relative humidity sensors used are HOBO® Temperature, Relative Humidity Data Loggers (Figure 9) , manufactured by Onset. The temperature measurement has a range from -20 to 70 °C with an accuracy of ± 0.4°C @ 25°C while the relative humidity measurement has a range of 25% to 95% with an accuracy of ± 3.5% from 25% - 85%. The HOBO® Data Loggers were placed in the supply duct, zone, return duct, and in the laboratory space.

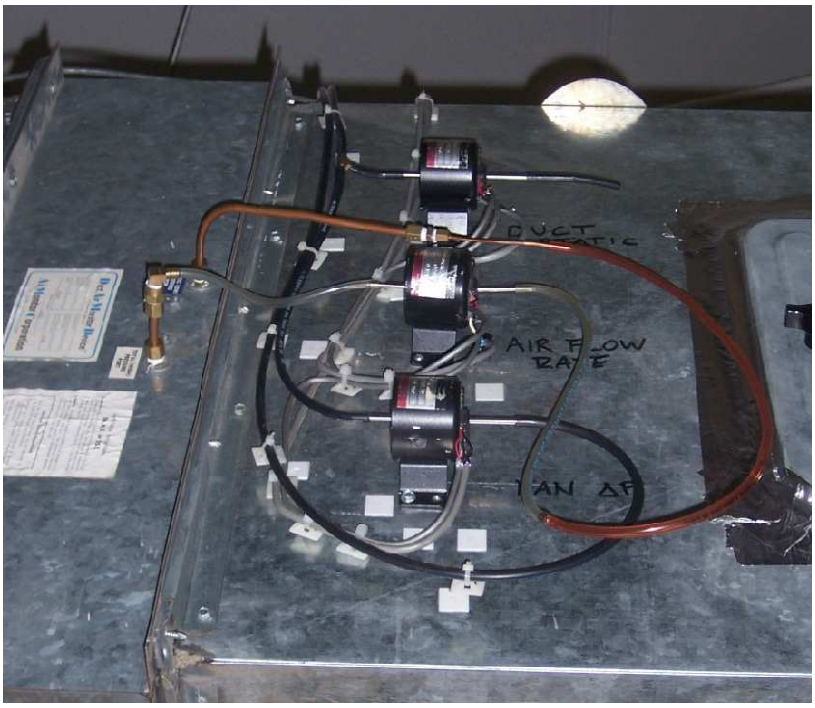

Figure 7: MKS Pressure Sensors for Airflow

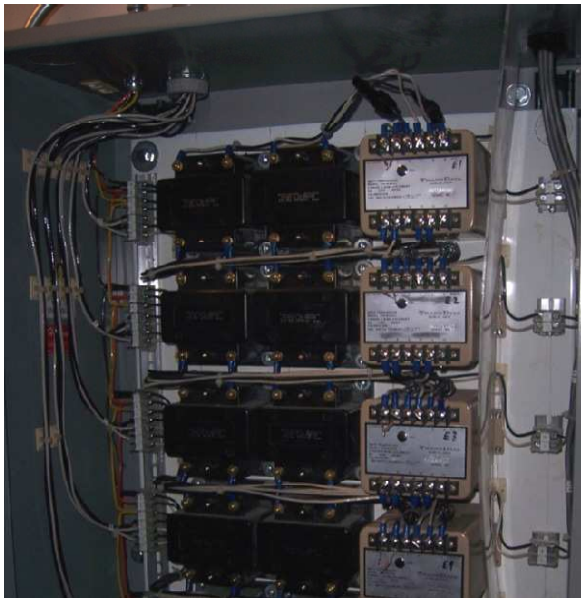

Figure 8: TransData Watt Transducers

Figure 9: HOBO Data Logger for Temperature and Relative Humidity

All of these sensors prior to data collection have been calibrated to be within their manufacturer's stated errors. Typical calibrations can be found in the Appendix: Calibration.

Table 1: Pressure Sensors

Unit	Location	Model Number (SETRA-265-)	Range (Pa)	Error
P-1	Filter	12R5WD2BT1C	0 to 623	± 1.0% of full scale
P-2	Cooling Coil	10R5WD2BT1C	0 to 125	± 1.0% of full scale
P-3	Heating Coil	10R5WD2BT1C	0 to 125	± 1.0% of full scale
P-4	Supply Fan	1010WD2BT1C	0 to 2491	± 1.0% of full scale
P-5	Supply Fan Gauge	1005WD2BT1C	0 to 1245	± 1.0% of full scale
P-6	Supply Duct	1005WD2BT1C	0 to 1245	± 1.0% of full scale
P-7	Simulated Zone	12R5WD2BT1C	0 to 623	± 1.0% of full scale
P-8	Return Duct	12R5WD2BT1C	0 to 623	± 1.0% of full scale

Table 2: Airflow Sensors

Unit	Location	Model Number	Range	Error
A-1	Supply Airflow	MKS 223BD-000.2AAUS	0 to 25 Pa	± 0.5% of full scale
A-2	Pre-Simulator Airflow	MKS 223BD-00001AAUS	0 to 125 Pa	± 0.5% of full scale
A-3	Zone Simulator Airflow	MKS 223BD-00001AAUS	0 to 125 Pa	± 0.5% of full scale
A-4	Return Airflow	MKS 223BD-00001AAUS	0 to 125 Pa	± 0.5% of full scale
A-5	Recirculation Airflow	Ebtron 2200	0 to 5,000 FPM	± 0.1% of full scale
A-6	West Zone Airflow	MKS 223BD-00001AAUS	0 to 125 Pa	± 0.5% of full scale
A-7	East Zone Airflow	Ebtron 2200	0 to 5,000 FPM	± 0.1% of full scale

Table 3: Power Consumption Sensor

Unit	Location	Sensor (TransData)	Range	Error
W-1	Supply Fan	20EWS501	0-50,000 W	± 0.2% of full scale

Table 4: Temperature Sensors

Unit	Location	Sensor (Onset)	Range	Error
T-1	HOBO® Temperature, Relative Humidity Data Logger	U10-003	-20 - 70 °C	± 0.4°C @ 25°C

Table 5: Relative Humidity Sensors

Unit	Location	Sensor (Onset)	Range	Error
RH-1	HOBO® Temperature, Relative Humidity Data Logger	U10-003	25% - 95%	± 3.5% from 25%-85%

Experiments and data collection were conducted using Automated Logic Corporation's Building Automation System (BAS) and WebCTRL software. The computer system is shown in Figure 10. Data was collected at five second intervals. Steady state measurements were averaged over at least two minutes of data after waiting at least 30 seconds for the system to arrive at a steady air flow.

Figure 10: Automated Logic Corporation's BAS Computer System

Appendix D

Description of Small Office Building Benchmark Model

Building Summary Small Office post-1980 construction

	Value
Program	
Building Name	Benchmark Small Office
Available Fuel Types	gas, electricity
Principal Building Activity	Office
Form	
Total Floor Area (m^2)	511
Building Shape	Rectangle
Aspect Ratio	1.5
Number of Floors	1
Window Fraction (Window to Wall Ratio)	
South	0.244
East	0.198
North	0.198
West	0.198
Total	0.212
Skylight/TDD Percentage	
Shading Geometry	None
Azimuth	0.0
Thermal Zoning	core zone with four perimeter zones
Floor to Ceiling Height (m)	3.1
Roof type	Attic
Fabric	
Exterior walls	
Construction Type	Mass wall
Gross Dimensions - Total Area (m^2)	281.5
Net Dimensions - Total Area (m^2)	222.0
Wall to Skin Ratio	0.32
Roof	
Construction Type	Attic
Gross Dimensions - Total Area (m^2)	598.8
Net Dimensions - Total Area (m^2)	598.8
Roof to Skin Ratio	0.68
Window Dimensions (m^2)	
South	16.7
East	11.2
North	16.7
West	11.2
Total Area (m^2)	55.8
Operable area (m^2)	0
Skylights/TDD	
Dimensions - Total Area (m^2)	
Operable area (m^2)	
Foundation	
Foundation Type	Mass Floor
Construction	4in slab w/carpet
Dimensions - Total Area (m^2)	511.0
Interior Partitions	
Construction	2x4 steel-frame with gypsum board
Dimensions - Total Area (m^2)	0
Internal Mass	

Construction	15 cm wood	
Dimensions - Total Area (m^2)		1,022.5
Thermal diffusivity (m^2/s)		1.84E-07
Air Barrier System		
Infiltration (ACH)		1.68
HVAC		
System Type	PSZ-AC	
Heating Type	Gas furnace	
Cooling Type	Unitary DX	
Fan Control	Constant volume	
Service Water Heating		
SWH Type	gas water heater	
Fuel	gas	
Thermal Efficiency (%)		78
Temperature Setpoint (ºC)		60
Water Consumption (m^3)		17.63

Zone Summary

Zone Name	Conditioned (Y/N)	Multiplier	Area (m^2)	Volume (m^3)	Floor-to-Ceiling Height (m)	Gross Wall Area (m^2)	Window Glass Area (m^2)	People (m^2/per)	People	Lights (W/m^2)	Elec Plug and Process (W/m^2)	Gas Plug and Process (W/m^2)	SWH (L/h)	Ventilation (L/s/Person)	Ventilation (L/s/m^2)	Ventilation Total (L/s)	Exhaust (L/s)	Infiltration (ACH)
Core_ZN	Yes	1	150	456	3.05	0	0	18.58	8.05	19.48	8.07		11.4	10.00		80.55		0.00
Perimeter_ZN_1	Yes	1	113	346	3.05	84	21	18.58	6.11	19.48	8.07			10.00		61.06		2.33
Perimeter_ZN_2	Yes	1	67	205	3.05	56	11	18.58	3.62	19.48	8.07			10.00		36.22		2.46
Perimeter_ZN_3	Yes	1	113	346	3.05	84	17	18.58	6.11	19.48	8.07			10.00		61.06		2.33
Perimeter_ZN_4	Yes	1	67	205	3.05	56	11	18.58	3.62	19.48	8.07			10.00		36.22		2.46
Attic	No	1	568	720	1.27	0	0									0.00		1.00
Total Conditioned Zones			**511**	**1,559**		**281.5**	**60**		**28**									
Data Source								1		2	4	4	4	3	3	3	4	4

Sources
[1] ASHRAE Standard 62.1-2004 Table 6-1, Atlanta, GA: American Society of Heating, Refrigerating and Air-Conditioning Engineers.
[2] ASHRAE Standard 90.1-1989, Atlanta, GA: American Society of Heating, Refrigerating and Air-Conditioning Engineers.
[3] ASHRAE Standard 62-1999 Table 6-1, Atlanta, GA: American Society of Heating, Refrigerating and Air-Conditioning Engineers.
[4] DOE Benchmark Report

Location Summary

	Miami	Houston	Phoenix	Atlanta	Los Angeles	Las Vegas
Program						
ASHRAE 90.1-2004 Climate Zone	1A	2A	2B	3A	3B-CA	3B
Available Fuel Types	gas, electricity	gas, electricity	gas, electricity	gas, electricity	gas, electricity	gas, electricity
Fabric						
Exterior walls						
Construction Type	Mass wall	Mass wall	Mass wall	Mass wall	Mass wall	Mass wall
R-value (m^2·K / W)	0.42	0.52	0.43	0.61	0.42	0.61
Roof						
Construction Type	Attic	Attic	Attic	Attic	Attic	Attic
R-value attic floor (m^2·K / W)	2.38	2.67	3.83	2.45	1.76	3.67
Window						
U-Factor (W / m^2·K)	5.84	5.84	5.84	4.09	5.84	5.84
SHGC	0.25	0.25	0.25	0.26	0.44	0.25
Visible transmittance	0.11	0.11	0.11	0.13	0.27	0.11
Skylights/TDD						
U-Factor (W / m^2·K)	n/a	n/a	n/a	n/a	n/a	n/a
SHGC	n/a	n/a	n/a	n/a	n/a	n/a
Visible transmittance	n/a	n/a	n/a	n/a	n/a	n/a
Foundation						
Foundation Type	Mass Floor	Mass Floor	Mass Floor	Mass Floor	Mass Floor	Mass Floor
Construction	4in slab w/carpet	4in slab w/carpet	4in slab w/carpet	4in slab w/carpet	4in slab w/carpet	4in slab w/carpet
R-value (m^2·K / W)	0.54	0.54	0.54	0.54	0.54	0.54
HVAC						
HVAC Sizing						
Air Conditioning (kW)						
PSZ-AC:1_COOLC DXCOIL	11.19	10.30	10.18	10.30	9.07	10.30
PSZ-AC:2_COOLC DXCOIL	11.54	12.69	10.33	14.05	8.90	10.02
PSZ-AC:3_COOLC DXCOIL	8.13	7.72	7.43	8.51	5.75	6.09
PSZ-AC:4_COOLC DXCOIL	11.82	12.04	10.19	13.52	7.87	9.50
PSZ-AC:5_COOLC DXCOIL	9.78	9.56	9.16	8.67	8.98	8.09
Heating (kW)						
PSZ-AC:1_HEATC	15.41	16.08	15.28	16.09	13.79	15.26
PSZ-AC:2_HEATC	13.21	15.06	13.06	17.39	12.76	13.72
PSZ-AC:3_HEATC	9.70	9.55	10.17	10.87	8.58	8.73
PSZ-AC:4_HEATC	13.83	14.80	13.39	17.17	11.18	13.54
PSZ-AC:5_HEATC	12.42	12.58	12.55	11.87	13.06	11.31
HVAC Efficiency						
Air Conditioning (COP)						
PSZ-AC:1_COOLC DXCOIL	3.12	3.16	3.19	3.17	3.18	3.19
PSZ-AC:2_COOLC DXCOIL	3.01	3.01	3.08	3.05	3.15	3.15
PSZ-AC:3_COOLC DXCOIL	3.04	3.04	3.15	3.07	3.19	3.19
PSZ-AC:4_COOLC DXCOIL	3.03	3.03	3.10	3.06	3.13	3.17
PSZ-AC:5_COOLC DXCOIL	3.09	3.09	3.16	3.12	3.19	3.19
Heating Efficiency (%)						
PSZ-AC:1_HEATC	0.80	0.80	0.80	0.80	0.80	0.80
PSZ-AC:2_HEATC	0.80	0.80	0.80	0.80	0.80	0.80
PSZ-AC:3_HEATC	0.80	0.80	0.80	0.80	0.80	0.80
PSZ-AC:4_HEATC	0.80	0.80	0.80	0.80	0.80	0.80
PSZ-AC:5_HEATC	0.80	0.80	0.80	0.80	0.80	0.80
HVAC Control - Economizer						
PSZ-AC:1_FAN	NoEconomizer	NoEconomizer	NoEconomizer	NoEconomizer	NoEconomizer	NoEconomizer
PSZ-AC:2_FAN	NoEconomizer	NoEconomizer	NoEconomizer	NoEconomizer	NoEconomizer	NoEconomizer
PSZ-AC:3_FAN	NoEconomizer	NoEconomizer	NoEconomizer	NoEconomizer	NoEconomizer	NoEconomizer
PSZ-AC:4_FAN	NoEconomizer	NoEconomizer	NoEconomizer	NoEconomizer	NoEconomizer	NoEconomizer
PSZ-AC:5_FAN	NoEconomizer	NoEconomizer	NoEconomizer	NoEconomizer	NoEconomizer	NoEconomizer
Fan Max Flow Rate (m^3/s)						
PSZ-AC:1_FAN	0.62	0.60	0.61	0.61	0.54	0.62
PSZ-AC:2_FAN	0.53	0.58	0.53	0.69	0.51	0.57
PSZ-AC:3_FAN	0.40	0.37	0.43	0.44	0.35	0.37
PSZ-AC:4_FAN	0.56	0.57	0.55	0.68	0.44	0.56
PSZ-AC:5_FAN	0.52	0.50	0.53	0.48	0.54	0.49

Location Summary

	San Francisco	Baltimore	Albuquerque	Seattle	Chicago
Program					
ASHRAE 90.1-2004 Climate Zone	3C	4A	4B	4C	5A
Available Fuel Types	gas, electricity	gas, electricity	gas, electricity	gas, electricity	gas, electricity
Fabric					
Exterior walls					
Construction Type	Mass wall	Mass wall	Mass wall	Mass wall	Mass wall
R-value (m^2·K / W)	0.42	1.47	0.93	1.76	1.76
Roof					
Construction Type	Attic	Attic	Attic	Attic	Attic
R-value attic floor (m^2·K / W)	2.00	3.04	2.99	2.75	3.32
Window					
U-Factor (W / m^2·K)	4.09	3.35	4.09	4.09	3.35
SHGC	0.39	0.36	0.36	0.39	0.39
Visible transmittance	0.25	0.27	0.23	0.25	0.31
Skylights/TDD					
U-Factor (W / m^2·K)	n/a	n/a	n/a	n/a	n/a
SHGC	n/a	n/a	n/a	n/a	n/a
Visible transmittance	n/a	n/a	n/a	n/a	n/a
Foundation					
Foundation Type	Mass Floor	Mass Floor	Mass Floor	Mass Floor	Mass Floor
Construction	4in slab w/carpet	4in slab w/carpet	4in slab w/carpet	4in slab w/carpet	4in slab w/carpet
R-value (m^2·K / W)	0.54	0.54	0.54	0.54	0.54
HVAC					
HVAC Sizing					
Air Conditioning (kW)					
0.00	6.72	10.97	9.63	7.08	10.66
0.00	9.03	14.95	12.18	9.15	19.68
0.00	4.79	8.38	7.60	5.67	10.72
0.00	7.54	14.84	11.96	8.97	19.59
0.00	6.47	8.18	7.99	6.81	10.58
Heating (kW)					
0.00	11.06	18.13	13.40	12.15	18.44
0.00	13.85	18.18	15.75	14.40	23.40
0.00	7.44	11.26	9.77	8.87	14.48
0.00	11.79	17.94	15.49	14.14	23.07
0.00	9.77	11.29	10.22	10.44	14.47
HVAC Efficiency					
Air Conditioning (COP)					
0.00	3.19	3.18	3.19	3.19	3.19
0.00	3.19	3.01	3.19	3.19	3.04
0.00	3.19	3.07	3.19	3.19	3.09
0.00	3.19	3.01	3.19	3.19	3.03
0.00	3.19	3.09	3.19	3.19	3.10
Heating Efficiency (%)					
0.00	0.80	0.80	0.80	0.80	0.80
0.00	0.80	0.80	0.80	0.80	0.80
0.00	0.80	0.80	0.80	0.80	0.80
0.00	0.80	0.80	0.80	0.80	0.80
0.00	0.80	0.80	0.80	0.80	0.80
HVAC Control - Economizer					
0.00	NoEconomizer	NoEconomizer	NoEconomizer	NoEconomizer	NoEconomizer
0.00	NoEconomizer	NoEconomizer	NoEconomizer	NoEconomizer	NoEconomizer
0.00	NoEconomizer	NoEconomizer	NoEconomizer	NoEconomizer	NoEconomizer
0.00	NoEconomizer	NoEconomizer	NoEconomizer	NoEconomizer	NoEconomizer
0.00	NoEconomizer	NoEconomizer	NoEconomizer	NoEconomizer	NoEconomizer
Fan Max Flow Rate (m^3/s)					
0.00	0.41	0.66	0.58	0.43	0.64
0.00	0.55	0.69	0.74	0.55	0.91
0.00	0.29	0.43	0.46	0.34	0.56
0.00	0.46	0.68	0.72	0.54	0.89
0.00	0.39	0.43	0.48	0.41	0.56

Location Summary

	Boulder	Minneapolis	Helena	Duluth	Fairbanks
Program					
ASHRAE 90.1-2004 Climate Zone	5B	6A	6B	7	8
Available Fuel Types	gas, electricity	gas, electricity	gas, electricity	gas, electricity	gas, electricity
Fabric					
Exterior walls					
Construction Type	Mass wall	Mass wall	Mass wall	Mass wall	Mass wall
R-value (m^2·K / W)	1.26	2.48	2.23	2.89	3.75
Roof					
Construction Type	Attic	Attic	Attic	Attic	Attic
R-value attic floor (m^2·K / W)	3.45	3.91	3.59	4.40	5.68
Window					
U-Factor (W / m^2·K)	3.35	2.96	2.96	2.96	2.96
SHGC	0.39	0.39	0.39	0.49	0.62
Visible transmittance	0.31	0.31	0.31	0.41	0.54
Skylights/TDD					
U-Factor (W / m^2·K)	n/a	n/a	n/a	n/a	n/a
SHGC	n/a	n/a	n/a	n/a	n/a
Visible transmittance	n/a	n/a	n/a	n/a	n/a
Foundation					
Foundation Type	Mass Floor	Mass Floor	Mass Floor	Mass Floor	Mass Floor
Construction	4in slab w/carpet	4in slab w/carpet	4in slab w/carpet	4in slab w/carpet	4in slab w/carpet
R-value (m^2·K / W)	0.54	0.54	0.54	0.54	0.54
HVAC					
HVAC Sizing					
Air Conditioning (kW)					
0.00	9.54	11.04	8.06	9.03	7.36
0.00	15.32	21.52	17.79	20.57	22.85
0.00	9.56	11.56	11.06	11.26	14.18
0.00	15.10	19.37	17.50	21.34	22.49
0.00	9.57	11.50	11.05	11.14	14.18
Heating (kW)					
0.00	14.04	19.32	13.78	16.55	16.14
0.00	19.88	25.76	24.54	26.87	35.88
0.00	12.33	15.91	15.16	16.59	22.14
0.00	19.63	25.40	24.19	26.48	35.39
0.00	12.35	15.90	15.15	16.58	22.14
HVAC Efficiency					
Air Conditioning (COP)					
0.00	3.19	3.19	3.19	3.19	3.19
0.00	3.17	3.05	3.17	3.11	3.22
0.00	3.19	3.10	3.19	3.17	3.19
0.00	3.17	3.10	3.17	3.08	3.22
0.00	3.19	3.11	3.19	3.18	3.19
Heating Efficiency (%)					
0.00	0.80	0.80	0.80	0.80	0.80
0.00	0.80	0.80	0.80	0.80	0.80
0.00	0.80	0.80	0.80	0.80	0.80
0.00	0.80	0.80	0.80	0.80	0.80
0.00	0.80	0.80	0.80	0.80	0.80
HVAC Control - Economizer					
0.00	NoEconomizer	NoEconomizer	NoEconomizer	NoEconomizer	NoEconomizer
0.00	NoEconomizer	NoEconomizer	NoEconomizer	NoEconomizer	NoEconomizer
0.00	NoEconomizer	NoEconomizer	NoEconomizer	NoEconomizer	NoEconomizer
0.00	NoEconomizer	NoEconomizer	NoEconomizer	NoEconomizer	NoEconomizer
0.00	NoEconomizer	NoEconomizer	NoEconomizer	NoEconomizer	NoEconomizer
Fan Max Flow Rate (m^3/s)					
0.00	0.58	0.67	0.49	0.55	0.44
0.00	0.93	1.00	1.07	1.07	1.38
0.00	0.58	0.62	0.67	0.66	0.86
0.00	0.91	0.99	1.06	1.05	1.36
0.00	0.58	0.62	0.67	0.66	0.86

DOE Commercial Building Benchmark - Small Office

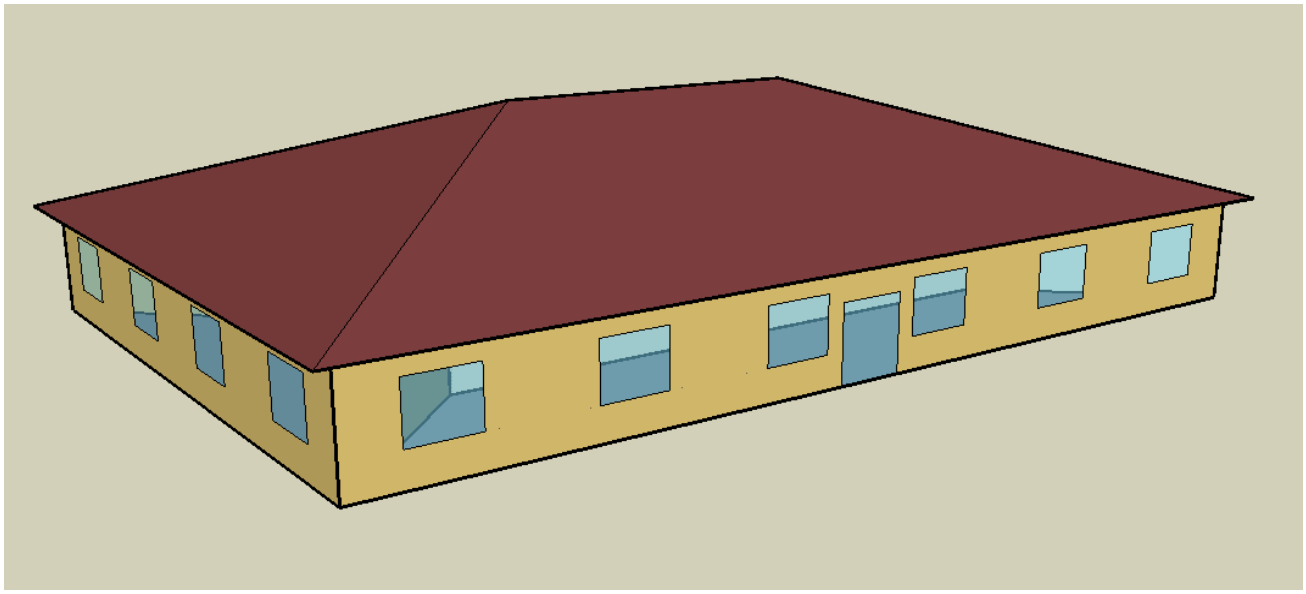

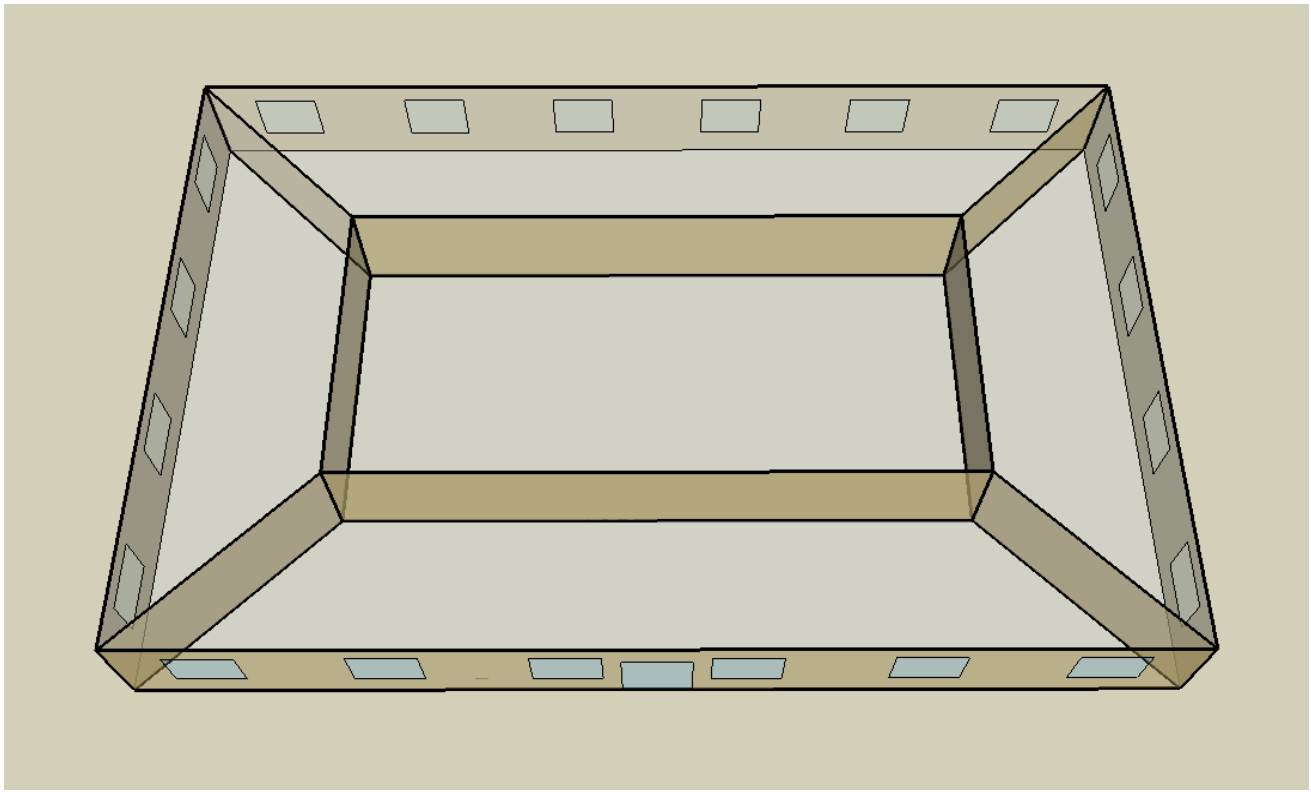

Schedule	Type	Through	Day of Week	1	2	3	4	5	6	7	8	9	10	11	12	13	14	15	16
BLDG_LIGHT_SCH	Fraction	Through 12/31	WD	0.1	0.1	0.1	0.1	0.1	0.1	0.1	0.3	0.9	0.9	0.9	0.9	0.9	0.9	0.9	0.9
			SummerDesign	1	1	1	1	1	1	1	1	1	1	1	1	1	1	1	1
			Sat	0.1	0.1	0.1	0.1	0.1	0.1	0.1	0.1	0.3	0.3	0.3	0.3	0.2	0.2	0.2	0.2
			WinterDesign	0	0	0	0	0	0	0	0	0	0	0	0	0	0	0	0
			Sun, Hol, Other	0.1	0.1	0.1	0.1	0.1	0.1	0.1	0.1	0.1	0.1	0.1	0.1	0.1	0.1	0.1	0.1
BLDG_EQUIP_SCH	Fraction	Through 12/31	WD	0.4	0.4	0.4	0.4	0.4	0.4	0.4	0.4	0.9	0.9	0.9	0.9	0.8	0.9	0.9	0.9
			SummerDesign	1	1	1	1	1	1	1	1	1	1	1	1	1	1	1	1
			Sat	0.3	0.3	0.3	0.3	0.3	0.3	0.4	0.4	0.5	0.5	0.5	0.5	0.4	0.4	0.4	0.4
			WinterDesign	0	0	0	0	0	0	0	0	0	0	0	0	0	0	0	0
			Sun, Hol, Other	0.3	0.3	0.3	0.3	0.3	0.3	0.3	0.3	0.3	0.3	0.3	0.3	0.3	0.3	0.3	0.3
BLDG_OCC_SCH	Fraction	Through 12/31	WD	0	0	0	0	0	0	0.1	0.2	1	1	1	1	0.5	1	1	1
			SummerDesign	0	0	0	0	0	0	1	1	1	1	1	1	1	1	1	1
			Sat	0	0	0	0	0	0	0.1	0.1	0.3	0.3	0.3	0.3	0.1	0.1	0.1	0.1
			WinterDesign	0	0	0	0	0	0	0	0	0	0	0	0	0	0	0	0
			Sun, Hol, Other	0	0	0	0	0	0	0	0	0	0	0	0	0	0	0	0
BLDG_ELEVATORS	Fraction	Through 12/31	WD, SummerDesign	0	0	0	0	0	0	0	0.4	0.7	0.4	0.4	0.4	0.6	0.5	0.4	0.4
			Sat, WinterDesign	0	0	0	0	0	0	0	0.2	0.1	0.2	0.2	0.3	0.2	0.1	0.1	0
			Sun, Hol, Other	0	0	0	0	0	0	0	0	0	0	0	0	0	0	0	0
INFIL_SCH	Fraction	Through 12/31	WD, SummerDesign	1	1	1	1	1	1	0	0	0	0	0	0	0	0	0	0
			Sat, WinterDesign	1	1	1	1	1	1	0	0	0	0	0	0	0	0	0	0
			Sun, Hol, Other	1	1	1	1	1	1	1	1	1	1	1	1	1	1	1	1
INFIL_HALF_ON_SCH	Fraction	Through 12/31	WD, SummerDesign	1	1	1	1	1	1	0.5	0.5	0.5	0.5	0.5	0.5	0.5	0.5	0.5	0.5
			Sat, WinterDesign	1	1	1	1	1	1	0.5	0.5	0.5	0.5	0.5	0.5	0.5	0.5	0.5	0.5
			Sun, Hol, Other	1	1	1	1	1	1	1	1	1	1	1	1	1	1	1	1
INFIL_QUARTER_ON_SCH	Fraction	Through 12/31	WD, SummerDesign	1	1	1	1	1	1	0.3	0.3	0.3	0.3	0.3	0.3	0.3	0.3	0.3	0.3
			Sat, WinterDesign	1	1	1	1	1	1	0.3	0.3	0.3	0.3	0.3	0.3	0.3	0.3	0.3	0.3
			Sun, Hol, Other	1	1	1	1	1	1	1	1	1	1	1	1	1	1	1	1
BLDG_SWH_SCH	Fraction	Through 12/31	WD, SummerDesign	0.1	0.1	0.1	0.1	0.1	0.1	0.1	0.2	0.4	0.4	0.4	0.5	0.6	0.5	0.3	0.3
			Sat, WinterDesign	0.1	0.1	0.1	0.1	0.1	0.1	0.1	0.1	0.2	0.2	0.2	0.2	0.2	0.2	0.2	0.1
			Sun, Hol, Other	0	0	0	0	0	0.1	0	0	0	0	0	0.1	0.1	0.1	0.1	0
Hours_of_operation	On/Off	Through 12/31	WD, SummerDesign	0	0	0	0	0	0	1	1	1	1	1	1	1	1	1	1
			Sat, WinterDesign	0	0	0	0	0	0	1	1	1	1	1	1	1	1	1	1
			Sun, Hol, Other	0	0	0	0	0	0	0	0	0	0	0	0	0	0	0	0
ALWAYS_ON	Fraction	Through 12/31	All	1	1	1	1	1	1	1	1	1	1	1	1	1	1	1	1
ALWAYS_OFF	Fraction	Through 12/31	All	0	0	0	0	0	0	0	0	0	0	0	0	0	0	0	0
HVACOperationSchd	On/Off	Through 12/31	WD, SummerDesign	0	0	0	0	0	0	1	1	1	1	1	1	1	1	1	1
			Sat, WinterDesign	0	0	0	0	0	0	1	1	1	1	1	1	1	1	1	1
			Sun, Hol, Other	0	0	0	0	0	0	0	0	0	0	0	0	0	0	0	0
PlantOnSched	On/Off	Through 12/31	All	1	1	1	1	1	1	1	1	1	1	1	1	1	1	1	1
FAN_SCH	Fraction	Through 12/31	All	1	1	1	1	1	1	1	1	1	1	1	1	1	1	1	1

ReheatCoilAvailSched	Fraction	Through 12/31	All	1	1	1	1	1	1	1	1	1	1	1	1	1	1	1	1
CoolingCoilAvailSched	Fraction	Through 12/31	All	1	1	1	1	1	1	1	1	1	1	1	1	1	1	1	1
HTGSETP_SCH	Temperature	Through 12/31	WD	16	16	16	16	16	21	21	21	21	21	21	21	21	21	21	21
			SummerDesign	16	16	16	16	16	16	16	16	16	16	16	16	16	16	16	16
			Sat	16	16	16	16	16	16	21	21	21	21	21	21	21	21	21	21
			WinterDesign	21	21	21	21	21	21	21	21	21	21	21	21	21	21	21	21
			Sun, Hol, Other	16	16	16	16	16	16	16	16	16	16	16	16	16	16	16	16
CLGSETP_SCH	Temperature	Through 12/31	WD, SummerDesign	30	30	30	30	30	30	24	24	24	24	24	24	24	24	24	24
			Sat	30	30	30	30	30	30	24	24	24	24	24	24	24	24	24	24
			WinterDesign	30	30	30	30	30	30	30	30	30	30	30	30	30	30	30	30
			Sun, Hol, Other	30	30	30	30	30	30	30	30	30	30	30	30	30	30	30	30
Humidity Setpoint Schedule	Humidity	Through 12/31	WD, SummerDesign	50	50	50	50	50	50	50	50	50	50	50	50	50	50	50	50
			Sat, WinterDesign	50	50	50	50	50	50	50	50	50	50	50	50	50	50	50	50
			Sun, Hol, Other	50	50	50	50	50	50	50	50	50	50	50	50	50	50	50	50
MinRelHumSetSch	Humidity	Through 12/31	All	30	30	30	30	30	30	30	30	30	30	30	30	30	30	30	30
MaxRelHumSetSch	Humidity	Through 12/31	All	60	60	60	60	60	60	60	60	60	60	60	60	60	60	60	60
MinOA_MotorizedDamper_Sche	Fraction	Through 12/31	WD, SummerDesign	0	0	0	0	0	0	0	1	1	1	1	1	1	1	1	1
			Sat, WinterDesign	0	0	0	0	0	0	0	1	1	1	1	1	1	1	1	1
			Sun, Hol, Other	0	0	0	0	0	0	0	0	0	0	0	0	0	0	0	0
MinOA_Sched	Fraction	Through 12/31	All	1	1	1	1	1	1	1	1	1	1	1	1	1	1	1	1
Dual Zone Control Type Sched	Control Type	Through 12/31	All	4	4	4	4	4	4	4	4	4	4	4	4	4	4	4	4
Seasonal-Reset-Supply-Air-Tem	Temperature	Through 3/31	All	13	13	13	13	13	13	13	13	13	13	13	13	13	13	13	13
		Through 9/30	All	13	13	13	13	13	13	13	13	13	13	13	13	13	13	13	13
		Through 12/31	All	13	13	13	13	13	13	13	13	13	13	13	13	13	13	13	13
CW-Loop-Temp-Schedule	Temperature	Through 12/31	All	6.7	6.7	6.7	6.7	6.7	6.7	6.7	6.7	6.7	6.7	6.7	6.7	6.7	6.7	6.7	6.7
HW-Loop-Temp-Schedule	Temperature	Through 12/31	All	60	60	60	60	60	60	60	60	60	60	60	60	60	60	60	60
Heating-Supply-Air-Temp-Sch	Temperature	Through 12/31	All	16	16	16	16	16	16	16	16	16	16	16	16	16	16	16	16
ACTIVITY_SCH	Any Number	Through 12/31	All	120	120	120	120	120	120	120	120	120	120	120	120	120	120	120	120
WORK_EFF_SCH	Fraction	Through 12/31	All	0	0	0	0	0	0	0	0	0	0	0	0	0	0	0	0
AIR_VELO_SCH	Any Number	Through 12/31	All	0.2	0.2	0.2	0.2	0.2	0.2	0.2	0.2	0.2	0.2	0.2	0.2	0.2	0.2	0.2	0.2
CLOTHING_SCH	Any Number	Through 04/30	All	1	1	1	1	1	1	1	1	1	1	1	1	1	1	1	1
		Through 09/30	All	0.5	0.5	0.5	0.5	0.5	0.5	0.5	0.5	0.5	0.5	0.5	0.5	0.5	0.5	0.5	0.5
		Through 12/31	All	1	1	1	1	1	1	1	1	1	1	1	1	1	1	1	1
SHADING_SCH	Any Number	Through 12/31	All	0	0	0	0	0	0	0	0	0	0	0	0	0	0	0	0
Core_ZN Water Equipment Late	Fraction	Through 12/31	All	0	0	0	0	0	0	0	0	0	0	0	0	0	0	0	0
Core_ZN Water Equipment Sens	Fraction	Through 12/31	All	0	0	0	0	0	0	0	0	0	0	0	0	0	0	0	0
Core_ZN Water Equipment Tem	Temperature	Through 12/31	All	49	49	49	49	49	49	49	49	49	49	49	49	49	49	49	49
Core_ZN Water Equipment Hot	Temperature	Through 12/31	All	55	55	55	55	55	55	55	55	55	55	55	55	55	55	55	55
SWHSys1-Loop-Temp-Schedule	Temperature	Through 12/31	All	60	60	60	60	60	60	60	60	60	60	60	60	60	60	60	60
SWHSys1 Water Heater Setpoint	Temperature	Through 12/31	All	60	60	60	60	60	60	60	60	60	60	60	60	60	60	60	60
SWHSys1 Water Heater Ambien	Temperature	Through 12/31	All	22	22	22	22	22	22	22	22	22	22	22	22	22	22	22	22

17	18	19	20	21	22	23	24	Hours Per Day	Hours Per Week	Hours Per Year
0.9	0.5	0.3	0.3	0.2	0.2	0.1	0.1	10.5	56.5	2946.07
1	1	1	1	1	1	1	1	24		
0.2	0.1	0.1	0.1	0.1	0.1	0.1	0.1	2.8		
0	0	0	0	0	0	0	0	0		
0.1	0.1	0.1	0.1	0.1	0.1	0.1	0.1	1.2		
0.9	0.5	0.4	0.4	0.4	0.4	0.4	0.4	14.1	86.15	4492.11
1	1	1	1	1	1	1	1	24		
0.4	0.3	0.3	0.3	0.3	0.3	0.3	0.3	8.45		
0	0	0	0	0	0	0	0	0		
0.3	0.3	0.3	0.3	0.3	0.3	0.3	0.3	7.2		
1	0.3	0.1	0.1	0.1	0.1	0.1	0.1	9.1	47.4	2471.57
1	1	1	1	1	1	0.1	0.1	16.1		
0.1	0	0	0	0	0	0	0	1.9		
0	0	0	0	0	0	0	0	0		
0	0	0	0	0	0	0	0	0		
0.5	0.6	0.1	0	0	0	0	0	5.35	28.26	1473.56
0.1	0.1	0	0	0	0	0	0	1.51		
0	0	0	0	0	0	0	0	0		
0	0	0	0	0	0	1	1	8	76	3962.86
0	0	1	1	1	1	1	1	12		
1	1	1	1	1	1	1	1	24		
0.5	0.5	0.5	0.5	0.5	0.5	1	1	16	122	6361.43
0.5	0.5	1	1	1	1	1	1	18		
1	1	1	1	1	1	1	1	24		
0.3	0.3	0.3	0.3	0.3	0.3	1	1	12	99	5162.14
0.3	0.3	1	1	1	1	1	1	15		
1	1	1	1	1	1	1	1	24		
0.4	0.3	0.2	0.2	0.2	0.1	0.1	0.1	5.37	30.55	1592.96
0.1	0.1	0.1	0.1	0.1	0.1	0.1	0.1	2.57		
0	0	0	0	0	0.1	0	0	1.13		
1	1	1	1	1	1	0	0	16	92	4797.14
1	1	0	0	0	0	0	0	12		
0	0	0	0	0	0	0	0	0		
1	1	1	1	1	1	1	1	24	168	8760
0	0	0	0	0	0	0	0	0	0	0
1	1	1	1	1	1	0	0	16	92	4797.14
1	1	0	0	0	0	0	0	12		
0	0	0	0	0	0	0	0	0		
1	1	1	1	1	1	1	1	24	168	8760
1	1	1	1	1	1	1	1	24	168	8760

1	1	1	1	1	1	1	1	24	168	8760
1	1	1	1	1	1	1	1	24	168	8760
21	21	21	16	16	16	16	16	450	3058.2	159463.3
16	16	16	16	16	16	16	16	374.4		
21	16	16	16	16	16	16	16	433.8		
21	21	21	21	21	21	21	21	504		
16	16	16	16	16	16	16	16	374.4		
24	24	24	24	24	24	30	30	624	4488	234017.1
24	24	30	30	30	30	30	30	648		
30	30	30	30	30	30	30	30	720		
30	30	30	30	30	30	30	30	720		
50	50	50	50	50	50	50	50	1200	8400	438000
50	50	50	50	50	50	50	50	1200		
50	50	50	50	50	50	50	50	1200		
30	30	30	30	30	30	30	30	720	5040	262800
60	60	60	60	60	60	60	60	1440	10080	525600
1	1	1	1	1	1	0	0	15	86	4484.29
1	1	0	0	0	0	0	0	11		
0	0	0	0	0	0	0	0	0		
1	1	1	1	1	1	1	1	24	168	8760
4	4	4	4	4	4	4	4	96	672	35040
13	13	13	13	13	13	13	13	312	2184	113880
13	13	13	13	13	13	13	13	312	2184	
13	13	13	13	13	13	13	13	312	2184	
6.7	6.7	6.7	6.7	6.7	6.7	6.7	6.7	160.8	1125.6	58692
60	60	60	60	60	60	60	60	1440	10080	525600
16	16	16	16	16	16	16	16	384	2688	140160
120	120	120	120	120	120	120	120	2880	20160	1051200
0	0	0	0	0	0	0	0	0	0	0
0.2	0.2	0.2	0.2	0.2	0.2	0.2	0.2	4.8	33.6	1752
1	1	1	1	1	1	1	1	24	168	6924
0.5	0.5	0.5	0.5	0.5	0.5	0.5	0.5	12	84	
1	1	1	1	1	1	1	1	24	168	
0	0	0	0	0	0	0	0	0	0	0
0	0	0	0	0	0	0	0	1.2	8.4	438
0	0	0	0	0	0	0	0	4.8	33.6	1752
49	49	49	49	49	49	49	49	1171.2	8198.4	427488
55	55	55	55	55	55	55	55	1320	9240	481800
60	60	60	60	60	60	60	60	1440	10080	525600
60	60	60	60	60	60	60	60	1440	10080	525600
22	22	22	22	22	22	22	22	528	3696	192720